NISTIR 6659

Thermodynamic, Transport, and Chemical Properties of "Reference" JP-8

Thomas J. Bruno
Marcia Huber
Arno Laesecke
Eric Lemmon
Mark McLinden
Stephanie L. Outcalt
Richard Perkins
Beverly L. Smith
Jason A. Widegren

NIST
National Institute of Standards and Technology
United States Department of Commerce

NISTIR 6659

Thermodynamic, Transport, and Chemical Properties of "Reference" JP-8

Thomas J. Bruno
Marcia Huber
Arno Laesecke
Eric Lemmon
Mark McLinden
Stephanie L. Outcalt
Richard Perkins
Beverly L. Smith
Jason A. Widegren

Physical and Chemical Properties Division
National Institute of Standards and Technology
325 Broadway
Boulder, CO 80305-3337

July 2010

U.S. DEPARTMENT OF COMMERCE
Gary Locke, Secretary

NATIONAL INSTITUTE OF STANDARDS AND TECHNOLOGY
Patrick D. Gallagher, Director

Table of Contents

Accomplishments and New Findings:

This report will not necessarily be presented in the order in which work was performed, but rather we will progress from the general topics to the more specific topics. Thus, the chemical analysis and the thermal decomposition measurements that were made, which necessarily affect all conclusions that can be drawn from all subsequent measurements, will be presented first. Then, we will present the property measurement work on the pure fluids that were needed to support model development. Subsequent to this section, we present the measurements on the actual aviation fuels, and then finally the thermodynamic and transport modeling results.

Chemical Analyses of JP-8 and Jet-A samples:

A total of five individual samples of representative aviation fuels (one JP-8, three Jet-A, one Fischer Tropsch synthetic fuel, S-8) were obtained from the Air Force Research Laboratory for this work. The sample of JP-8 was POSF-3773, directly from the Wright Patterson Air Force Base flight line. The three samples of Jet-A were POSF -3602, -3638 and -4658, the latter being a composite mixture prepared by AFRL. The synthetic Fischer Tropsch fuel was POSF-4734.

A chemical analysis was done on each of the fluid samples by gas chromatography mass spectrometry (30 m capillary column of 5% phenyl polydimethyl siloxane having a thickness of 1 μm, temperature program from 90 to 250 °C, 10 °C per minute). Mass spectra were collected for each peak from 15 to 550 RMM (relative molecular mass) units[1, 2]. Chromatographic peaks made up of individual mass spectra were examined for peak purity, then the mass spectra were used for qualitative identification. Components in excess of 0.5 mole percent were selected for identification and tabulated for each fluid. In addition to this detailed analysis, the hydrocarbon type classification based on ASTM D-2789 was performed. These results figure in the overall mixture characterization, and are also used for comparisons with the chemical analyses of individual distillate fractions (discussed in the section on distillation curves). In addition, this approach to characterizing the mixtures allows the development of fluid mixture files for equation of state development, which will be described later.

The chemical analysis typically allows the identification of between 40 and 60 percent (by mass) of the fluid components. There are usually numerous minor components that cannot be identified because of their low concentrations, and other cases in which chromatographic peak overlap prevents reliable identification of even the more abundant components. An example of the summary of a chemical analysis for Jet-A (the results for Jet-A-4658) is provided in Table 1. Since this fluid represents a composite of samples of Jet-A, additional information is provided for this fluid. In this table, peaks are labeled by numbers or letters. Lettered peaks are relatively minor but are included for a specific reason, such as to provide a budget for the highly volatile components. The peak profile describes how the peak was handled for mass spectral determination. This is typically a single (S) point, an average (A) or both. The correlation coefficient is a numerical figure of merit describing the match of the analyte peak with a library entry. It is important to understand that this number is not necessarily the best measure of the "goodness of fit". The confidence indicator, ranging from high (H), moderate (M) to uncertain (U) is a more reliable indicator, since it is based on more factors, including chromatographic behavior. The area percentages provided are uncalibrated, raw area counts on the total ion chromatogram.

For comparison, the summary analyses for S-8-4734 is provided in Table 2, and for JP-8-3773 is provided in Table 3. For these fluids we provide a synopsis only, without the chromatographic details. We note that occasionally, it is not possible to determine the isomerization of a branched hydrocarbon on the basis of the mass spectrum of the chromatographic peak. In these cases, we have used the variable "x" to note the uncertainty. For example, x-methyl dodecane simply indicates uncertainty in the position of the methyl group on the hydrocarbon backbone.

Table 1: A chemical analysis for Jet-A-4658 performed with gas chromatography – mass spectrometry, used for fuel characterization, and for the development of mixture equations of state.

Peak No.	Retention Time, min	Peak Profile	Correlation Coefficient	Confidence	Name	CAS No.	Area Percentage
a	1.726	S	72.9	H	n-heptane	142-82-5	0.125
b	1.878	S	76.9	H	methyl cyclohexane	108-87-2	0.198
c	2.084	S	71.6	H	2-methyl heptane	592-27-8	0.202
1	2.144	S	29.2	H	Toluene	108-88-3	0.320
d	2.223	S	41.9	H	cis-1,3-dimethyl cyclohexane	638-04-0	0.161
2	2.351	S	44.0	H	n-octane	111-65-9	0.386
e	2.945	S	31.1	H	1,2,4-trimethyl cyclohexane	2234-75-5	0.189
3	3.036	S	12.4	H	4-methyl octane	2216-34-4	0.318
4	3.169	S	37.6	H	1,2-dimethyl benzene	95-47-6	0.575
5	3.527	S	33.9	H	n-nonane	111-84-2	1.030
6	3.921	S	NA	U	?		0.321
7	4.066	S & A	NA	H	x-methyl nonane	NA	0.597
8	4.576	S & A	7.97	M[1]	4-methyl nonane	17301-94-9	0.754
9	4.655	S	35.8	H	1-ethyl-3-methyl benzene	620-14-4	1.296
10	4.764	S	10.7	H	2,6-dimethyl octane	2051-30-1	0.749
11	4.836	A	5.27	U[2]	1-methyl-3-(2-methylpropyl) cyclopentane	29053-04-1	0.285
12	5.012	S	27.8	M[2]	1-ethyl-4-methyl benzene	622-96-8	0.359
13	5.049	A	13.7	M[2]	1-methyl-2-propyl cyclohexane	4291-79-6	0.370

14	5.291	S	26.3	H	1,2,4-trimethyl benzene	95-63-6	1.115
15	5.325	S	37.7	H	n-decane	124-18-5	1.67
16	5.637	S	36	H	1-methyl-2-propyl benzene	1074-17-5	0.367
17	5.825	S	36	H	4-methyl decane	2847-72-5	0.657
18	5.910	S	26.9	H	1,3,5-trimethyl benzene	108-67-8	0.949
19	6.073	S & A	NA	M	x-methyl decane	NA	0.613
20	6.176	S	5.01	M[2]	2,3-dimethyl decane	17312-44-6	0.681
21	6.364	S & A	25.7	M[2]	1-ethyl-2,2,6-trimethyl cyclohexane	71186-27-1	0.364
22	6.516	S & A	35.6	H	1-methyl-3-propyl benzene	1074-43-7	0.569
f	6.662	S & A	NA	U[2]	aromatic	NA	0.625
23	6.589	S	20.4	M[3]	5-methyl decane	13151-35-4	0.795
24	6.728	S	22.9	H	2-methyl decane	6975-98-0	0.686
25	6.862	A	23.2	H	3-methyl decane	13151-34-3	0.969
26	7.110	S	NA	U	Aromatic	NA	0.540
27	7.159	S	NA	U	Aromatic	NA	0.599
28	7.310	S	17.9	M	1-methyl-(4-methylethyl) benzene	99-87-6	0.650
29	7.626	A	22.0	H	n-undecane	1120-21-4	2.560
29	7.971	A	NA	M	x-methyl undecane	NA	1.086
30	8.875	A	22.3	M	1-ethyl-2,3-dimethyl benzene	933-98-2	1.694
31	9.948	A	19.6	H	n-dodecane	112-40-3	3.336
32	10.324	S	19.0	H	2,6-dimethyl undecane	17301-23-4	1.257
33	12.377	S & A	10.8	H	n-tridecane	629-50-5	3.998
33a	12.901	S	24.1`	M	1,2,3,4-tetrahydro-2,7-dimethyl naphthalene	13065-07-1	0.850
33b	13.707	S	3.5	M	2,3-dimethyl dodecane	6117-98-2	0.657
33c	14.138	S	14.5	M	2,6,10-trimethyl dodecane	3891-98-3	0.821
33d	13.834	S	NA	M	x-methyl tridecane	NA	0.919
33e	13.998	S	NA	M	x-methyl tridecane	NA	0.756
34	14.663	S	29.8	H	n-tetradecane	629-59-4	1.905
35	16.86	S	24.7	H	n-pentadecane	629-62-9	1.345

1 trailing impurity
2 highly impure composite peak
3 there is evidence of an aromatic impurity in this peak

The meaning of the confidence and profile indicators (H, M,U, S, A) are discussed in the text.

Table 2: A listing of the major components found in the sample of S-8-4734. The area percentages provided are from raw uncorrected areas resulting from the integration of the GC-MS total ion chromatogram. When ambiguity exists regarding isomerization, the substituent position is indicated as a general variable, x.

Name	CAS No.	Area Percentage	Name	CAS No.	Area Percentage
2-methyl heptane	592-27-8	0.323	n-undecane	1120-21-4	2.420
3-methyl heptane	589-81-1	0.437	x-methyl undecane	NA	1.590
1,2,3-trimethyl cyclopentane	15890-40-1	0.965	3-methyl undecane	1002-43-3	1.15
2,5-dimethyl heptane	2216-30-0	1.131	5-methyl undecane	1632-70-8	1.696
4-methyl octane	2216-34-4	2.506	4-methyl undecane	2980-69-0	1.045
3-methyl octane	2216-33-3	1.323	2-methyl undecane	7045-71-8	1.072
n-nonane	111-84-2	1.623	2,3-dimethyl undecane	17312-77-5	1.213
3,5-dimethyl octane	15869-96-9	1.035	n-dodecane	112-40-3	2.595
2,6-dimethyl octane	2051-30-1	0.756	4-methyl dodecane	6117-97-1	0.929
4-ethyl octane	15869-86-0	1.032	x-methyl dodecane	NA	0.744
4-methyl nonane	17301-94-9	1.904	2-methyl dodecane	1560-97-0	1.293
2-methyl nonane	871-83-0	1.019	x-methyl dodecane	NA	1.281
3-methyl nonane	5911-04-6	1.385	n-tridecane	629-50-5	1.739
n-decane	124-18-5	2.050	4-methyl tridecane	26730-12-1	0.836
2-5-dimethyl nonane	17302-27-1	1.175	6-propyl tridecane	55045-10-8	1.052
5-ethyl-2-methyl octane	62016-18-6	1.015	x-methyl tridecane	NA	1.066
5-methyl decane	13151-35-4	1.315	n-tetradecane	629-59-4	1.562
4-methyl decane	2847-72-5	1.134	x-methyl tetradecane	NA	1.198
2-methyl	6975-98-0	1.529	5-methyl	25117-32-2	0.720

decane			tetradecane		
3-methyl decane	13151-34-3	1.583	n-pentadecane	629-62-9	1.032
			x-methyl tetradecane	NA	0.727

Table 3: A listing of the major components found in the sample of JP-8-3773. The area percentages provided are from raw uncorrected areas resulting from the integration of the GC-MS total ion chromatogram. When ambiguity exists regarding isomerization, the substituent position is indicated as a general variable, x.

Compound	CAS No.	Area %	Compound	CAS No.	Area %
n-heptane	142-82-5	0.125	2,3-dimethyl decane	17312-44-6	0.681
methyl cyclohexane	108-87-2	0.198	1-ethyl-2,2,6-trimethyl cyclohexane	71186-27-1	0.364
2-methylheptane	592-27-8	0.202	1-methyl-3-propyl benzene	1074-43-7	0.569
toluene	108-88-3	0.320	aromatic unknown	NA	0.625
cis-1,3-dimethyl cyclohexane	638-04-0	0.161	5-methyldecane	13151-35-4	0.795
n-octane	111-65-9	0.386	2-methyldecane	6975-98-0	0.686
1,2,4-trimethyl cyclohexane	2234-75-5	0.189	3-methyldecane	13151-34-3	0.969
4-methyl octane	2216-34-4	0.318	aromatic unknown	NA	0.540
1,2-dimethyl benzene	95-47-6	0.575	aromatic unknown	NA	0.599
n-nonane	111-84-2	1.030	1-methyl-(4-methylethyl) benzene	99-87-6	0.650
x-methylnonane	NA	0.597	n-undecane	1120-21-4	2.560
4-methylnonane	17301-94-9	0.754	x-methyl undecane	NA	1.086
1-ethyl-3-methyl benzene	620-14-4	1.296	1-ethyl-2,3-dimethyl benzene	933-98-2	1.694

2,6-dimethyl octane	2051-30-1	0.749	n-dodecane	112-40-3	3.336
1-methyl-3-(2-methylpropyl) cyclopentane	29053-04-1	0.285	2,6-dimethyl undecane	17301-23-4	1.257
1-ethyl-4-methyl benzene	622-96-8	0.359	n-tridecane	629-50-5	3.998
1-methyl-2-propyl cyclohexane	4291-79-6	0.370	1,2,3,4-tetrahydro-2,7-dimethyl naphthalene	13065-07-1	0.850
1,2,4-trimethyl benzene	95-63-6	1.115	2,3-dimethyl dodecane	6117-98-2	0.657
n-decane	124-18-5	1.67	2,6,10-trimethyl dodecane	3891-98-3	0.821
1-methyl-2-propyl benzene	1074-17-5	0.367	x-methyl tridecane	NA	0.919
4-methyl decane	2847-72-5	0.657	x-methyl tridecane	NA	0.756
1,3,5-trimethyl benzene	108-67-8	0.949	n-tetradecane	629-59-4	1.905
x-methyl decane	NA	0.613	n-pentadecane	629-62-9	1.345

Thermal Decomposition:

Thermal Decomposition of Jet-A-4658:

The thermal decomposition of the aviation fuels has been assessed with an ampoule testing instrument and approach that has been developed at NIST[3, 4]. We note that this work is meant strictly to support the physical property measurement work, and not to delineate reaction mechanisms. The instrument, shown schematically in Figure 1, consists of a 304L stainless steel thermal block that is heated to the desired experimental temperature (here, between 250 and 450 °C, although our rate constants were measured between 375 and 450 °C). The block is supported in an insulated box with carbon rods; the temperature is maintained and controlled (by a PID controller) to within 0.1 °C in response to a platinum resistance sensor embedded in the thermal block. The ampoule cells consist of 6.4 cm lengths of ultrahigh pressure 316L stainless steel tubing (0.64 cm external diameter, 0.18 cm internal diameter) that are sealed on one end with a TIG welded stainless steel plug. Each cell is connected to a high-pressure high-temperature

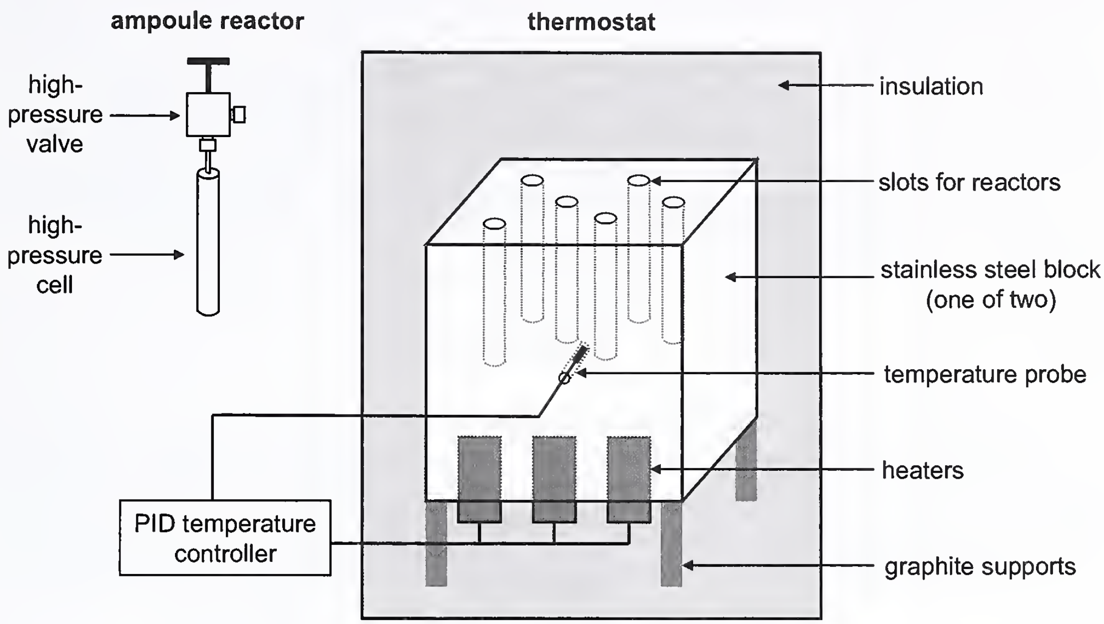

Figure 1: A schematic diagram showing the ampoule thermal decomposition apparatus that was developed at NIST to assess the thermal stability of the aviation fuels studied in this work.

valve at the other end with a short length of 0.16 cm diameter 316 stainless steel tubing with an internal diameter of 0.02 cm, also TIG welded to the cell. Each cell and valve is capable of withstanding a pressure in excess of 105 MPa at the desired temperature. The internal volume of each cell is known and remains constant at a given temperature. Fluid is added to the individual cell by mass (as determined by an approximate equation of state calculation) to give a total pressure of 34 MPa at the final fluid temperature. Measurements are done by measuring the integrated area of an emergent chromatographic peak suite that results from the decomposition. This is illustrated in Figure 2, in which a representative chromatogram of Jet-A is shown along with magnified insets of the emergent peak zone. In the "as received" sample, there are no peaks in the emergent zone, while after thermal stress, the suite develops and is seen to grow into the chromatogram as a function of increasing exposure time and temperature.

During the course of this work, we performed kinetic studies on two samples that are relevant to the development of the surrogate model for JP-8. First, we measured Jet-A-4658, which is the composite Jet-A sample[5]. Next, in order to facilitate the modeling process, we found it necessary to measure propylcyclohexane[6]. This became important because of the need to represent this class of cycloalkane. Before doing any property measurements, we needed to assess the thermal stability.

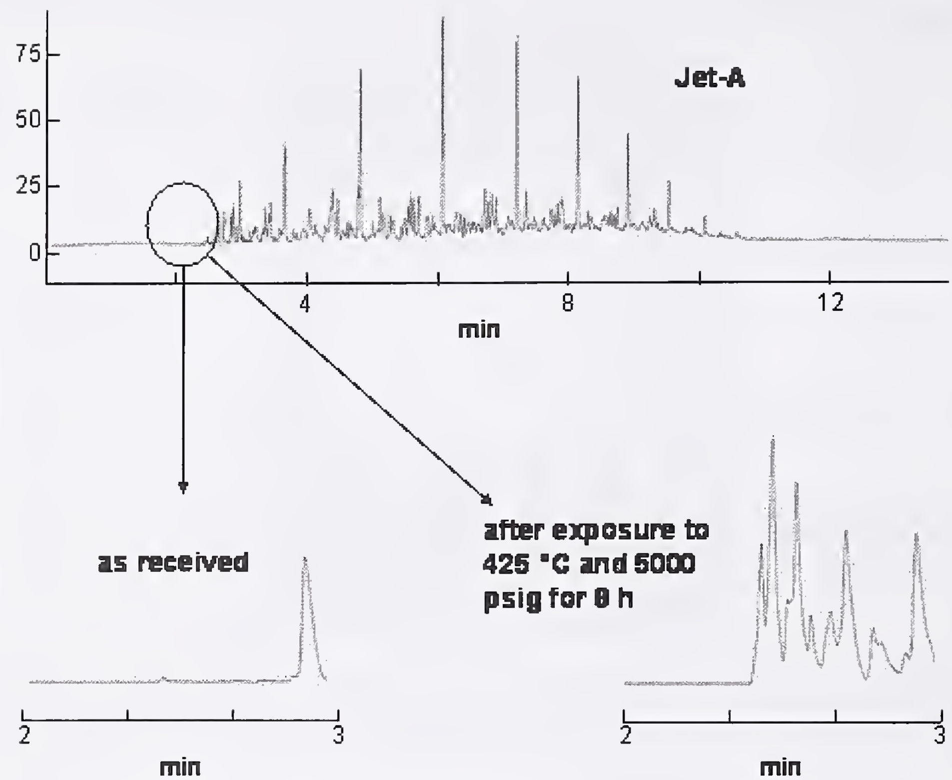

Figure 2: Representative chromatograms showing the usual kerosene component distribution, with the insets showing the very early eluting region. Upon thermal stress, one notes the development of emergent decomposition peaks.

The simplest type of decomposition is a first-order reaction in which a reactant (A) thermally decomposes into a product (B), equation 1. The rate law for such a reaction can be written in terms of the reactant or the product, equation 2, where [A] is the concentration of A, [B] is the concentration of B, k is the reaction rate constant, and t is the time. Equation 3 shows the integrated expression in terms of the reactant, where $[A]_t$ is the concentration of reactant at time t and $[A]_0$ is the initial reactant concentration:

$$A \rightarrow B, \tag{1}$$

$$-d[A]/dt = d[B]/dt = kt, \tag{2}$$

$$\ln[A]_t = \ln[A]_0 - kt. \tag{3}$$

Specifically, for a first-order reaction, a plot of ln[A] as a function of t should result in a straight line. Additionally, an Arrhenius plot should also yield a straight line.

The half-life, $t_{0.5}$, of a decomposition reaction is the time required for half of the reactants to become products. For a first-order reaction such as the one shown in equation 1, the half-life can be calculated directly from the rate constant, equation 4. A related quantity is the time it takes for 1% of the reactants to become products, $t_{0.01}$. For first-order reactions, $t_{0.01}$ also can be calculated directly from the rate constant, equation 5. The $t_{0.5}$ and $t_{0.01}$ of thermal decomposition are useful because they give a direct measure of the time period over which the concentration of thermal decomposition products will reach an unacceptable level. Hence, they are useful when deciding what conditions and protocols are to be used for property measurements. These quantities are given by:

$$t_{0.5} = 0.6931/k, \tag{4}$$

$$t_{0.01} = 0.01005/k. \tag{5}$$

In addition to calculating values for $t_{0.5}$ and $t_{0.01}$, rate constants determined over a temperature range can be used to evaluate the parameters of the Arrhenius equation, equation 6, where A is the pre-exponential factor, E_a is the activation energy, R is the gas constant, and T is the temperature. The Arrhenius parameters can then be used to predict rate constants at temperatures other than those examined experimentally:

$$k = A \exp(-E_a/RT). \tag{6}$$

Samples of Jet-A-4658 were decomposed in the stainless steel ampoule reactors at 375, 400, 425 and 450 °C. This temperature range was chosen because it allowed for reaction times of a convenient length. At 375 °C the reaction is relatively slow, so reaction times ranged from 4 to 24 h. At 450 °C the reaction is much faster, so reaction times ranged from 10 to 120 min. The unreacted Jet A was clear and nearly colorless. Mild thermal stress (i.e., the shortest reaction times at the lower temperatures) caused the liquid to become pale yellow. Severe thermal stress (i.e., the longest reaction times at the higher temperatures) caused the liquid to become very dark brown, opaque, and viscous. A small amount of dark particulate was regularly seen in the more thermally stressed samples. Additionally, low-molecular-weight decomposition products caused a pressurized vapor phase to develop inside the reactors. For the more severely stressed samples, it was common for the entire liquid sample to be expelled under pressure when the reactor valve was opened.

A separate analysis of this vapor phase was desired, and to accomplish this a gas-liquid separator designed at NIST for such work was employed[7]. This device is shown in Figure 3. The gas phase was then analyzed using a gas chromatograph with MS detection. Over 30 compounds were identified in the gas phase, with light alkanes being the most abundant. Table 4 shows the 10 most abundant compounds, based on total ion current in the MS detector. Note that the MS method employed precludes observation of methane. The apparent lack of alkene decomposition products is somewhat surprising, although it is known that high pressures and long reaction times decrease the yield of alkenes from the decomposition of alkanes. The rate of decomposition from alkanes

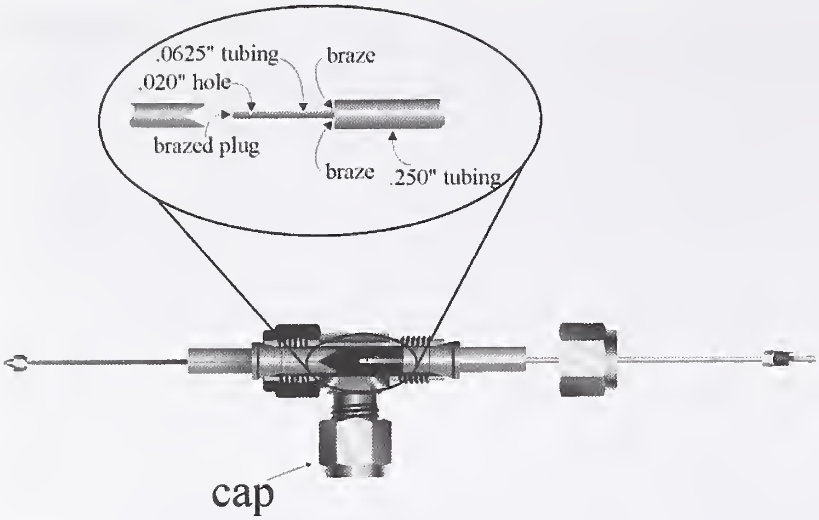

Figure 3: A schematic diagram of the gas-liquid separator that was used to examine the vapor phase of the thermally stressed Jet-A-4658. More details regarding this device can be found in ref 5.

Table 4: A listing of the most abundant compounds found in the vapor phase of thermally stressed Jet-A-4658, maintained for 2 hrs. at 450 °C.

Compound	% of Total Ion Current
butane	13.0
pentane	10.6
propane	10.4
2-methylpropane	8.6
2-methylbutane	8.1
ethane	6.6
hexane	6.4
2-methylpentane	5.9
methylcyclopentane	3.3
3-methylpentane	3.2

are also known to depend on the material used to construct the reactor.

The thermally stressed liquid phase of each sample was analyzed by a gas chromatograph equipped with a flame ionization detector. An easily identifiable suite of decomposition products had retention times between 2.3 and 2.8 min, Figure 4. The kinetic analysis was done based on this suite of peaks. We did not identify all of the individual compounds responsible for these peaks, but it is worth noting that pentane and hexane had retention times of 2.4 min and 2.5 min under these conditions, which suggests that most of these decomposition products had 5-7 carbon atoms. The observed product suite was essentially the same at all temperatures, with retention times that were constant to within 0.01 min. Undoubtedly, there were peaks for decomposition products in the broad kerosene "hump" that began around 2.9 min, but use of them for the kinetic analysis was impractical because of peak overlap and the lack of baseline resolution. Additionally, we did not routinely monitor compounds that were not retained in the liquid phase, including vapor-phase products and potential coke deposits.

As mentioned above, the kinetic analysis was done using the emergent suite of decomposition products in the liquid phase with retention times between 2.3 and 2.8 min. The rate constant, k, at each temperature was determined from data collected at four different reaction times, with 3 to 6 replicate decomposition reactions run at each reaction time. The value of k was obtained from a nonlinear least-squares fit of these data to equation 3. For example, Figure 4 is a plot of the data and curve-fit for 425 °C. Note that data were collected at seven time points, but only the first four data points in Figure 4 were used to determine k. The reason for excluding the later time points was to limit the influence of any secondary decomposition reactions on the kinetics. Even though it is unlikely that measurements would intentionally be carried out with instrumental residence times in excess of the first four time points, this area of the plot is still useful in that it represents the chemical decomposition regime that is possible if an instrument or engine enters an upset condition resulting in long residence times. Values for $t_{0.5}$ and $t_{0.01}$ are calculated from k by use of equations 4 and 5. The decomposition rate constants at all four temperatures, along with values of $t_{0.5}$ and $t_{0.01}$, are presented in Table 5. The standard uncertainties given were calculated from the standard deviation of replicate measurements and from the standard error in the nonlinear fit. The values of $t_{0.01}$ show that physical property measurements at ≥400 °C would require apparatus residence times on the order of 5 min or less. On the other hand, at 375 °C a residence time of about half an hour may be acceptable. First order rate constants reported for the decomposition of n-tetradecane are $k = 1.78 \times 10^{-5}\ s^{-1}$ at 400 °C, $k = 1.01 \times 10^{-4}\ s^{-1}$ at 425 °C, and $k = 4.64 \times 10^{-4}\ s^{-1}$ at 450 °C. Within our experimental uncertainty, these are the same as the values in Table 5 for Jet A.

An Arrhenius plot of the rate constants is shown in Figure 5. The Arrhenius parameters determined from a linear regression of the data are $A = 4.1 \times 10^{12}\ s^{-1}$ and $E_a = 220$ kJ·mol^{-1}. The standard uncertainty in Ea, calculated from the standard error in the slope of the regression, is 10 kJ·mol−1. The linearity of the Arrhenius plot ($r^2 > 0.9978$) over the 75 °C temperature range is an important validation that the assumption of first-order kinetics is reasonable. Note that the activation energy for the decomposition of Jet A is slightly lower than the values reported for pure C10–C14 n-alkanes; for example, for n-dodecane Ea is 260 kJ·mol^{-1} (with a reported uncertainty of 8 kJ·mol^{-1}).

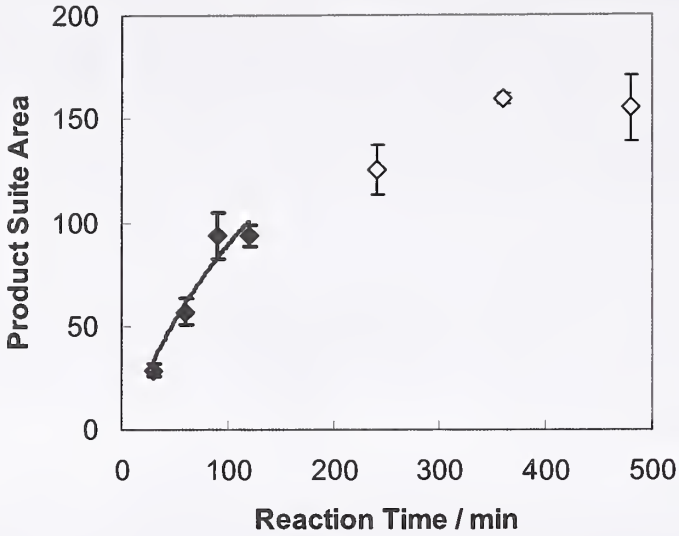

Figure 4: Plot of the corrected area counts of the decomposition product suite as a function of time at 425 °C. Only the data at short reaction times (solid symbols) were used to determine the rate constant. The error bars represent the standard deviation for replicate decomposition reactions at each time point.

Table 5: Kinetic data for the thermal decomposition of Jet-A-4658.

T / °C	k / s^{-1}	Uncertainty in k / s^{-1}	$t_{0.5}$ / h	$t_{0.01}$ / min
375	5.9×10^{-6}	3.9×10^{-6}	33	28
400	3.3×10^{-5}	1.8×10^{-5}	5.8	5.0
425	1.2×10^{-4}	0.6×10^{-4}	1.7	1.4
450	4.4×10^{-4}	2.3×10^{-4}	0.44	0.38

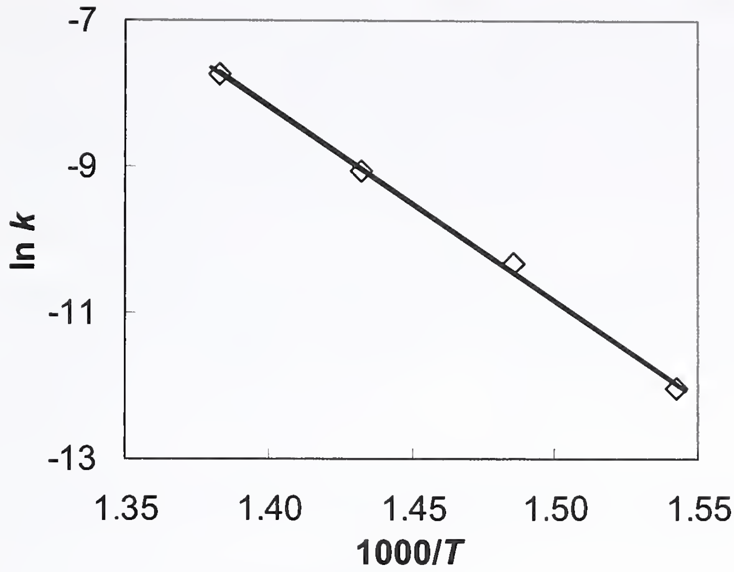

Figure 5: Arrhenius plot for the decomposition of Jet-A-4658. The Arrhenius parameters determined from the fit to the data are $A = 4.1 \times 10^{12}\ s^{-1}$ and $E_a = 220\ kJ \cdot mol^{-1}$.

Thermal Decomposition of Propylcyclohexane:

As mentioned above, we also found it necessary to incorporate some pure component property measurements into the model development. Two fluids were chosen to represent cyclic branched alkanes: methylcyclohexane and propylcyclohexane. Because adequate thermal stability data could be found for methyl cyclohexane, no additional measurements were done on this fluid. Propylcyclohexane required measurements, however, since no thermal decomposition data could be found.

The ampoule reactors were filled with propylcyclohexane by use of a procedure designed to achieve an initial pressure of 34.5 MPa (5000 psi) for all of the decomposition reactions. This is important because it mimics the high-pressure conditions during some physical property measurements, and it helps ensure that differences in observed decomposition rates are not due to differences in pressure. It also allows comparability with the jet-A-4658 measurements described above. After filling, air in the void space of the reactor was removed by one freeze-pump-thaw cycle. The loaded reactors were then inserted into the thermostatted stainless steel block and maintained at the reaction temperature for a period of time ranging from 10 min to 32 h. After decomposition, the reactors were removed from the thermostatted block and immediately cooled in room-temperature water. The thermally stressed propylcyclohexane was recovered and analyzed as described below. After each run, the cells and valves were carefully cleaned and dried. Blank experiments, in which the cell was loaded as described above but not heated, confirmed the effectiveness of the cleaning protocol.

The products of a 40 min decomposition reaction at 450 °C were identified by GC-MS. To accomplish this, a short length of glass capillary tubing was connected to the outlet on the reactor valve. The valve on the reactor was opened just enough to allow the pressurized mixture of gas and liquid in the reactor to escape slowly. Then the end of the capillary was briefly pushed through the inlet septum of the split/splitless injection port of the GC-MS, directly introducing the decomposed sample by flowing capillary injection. The components of the sample were then separated on a 30 m capillary column coated with a 0.25 μm film of (5%-phenyl)-methylpolysiloxane. The temperature program for the separation started with an initial isothermal separation at 35 °C for 6 min, followed by a 20 °C/min ramp to 175 °C. The most abundant decomposition products identified in this manner are listed in Table 6.

Table 6. Summary of the most abundant decomposition products after 40 min at 450 °C.

Compound	**% of Total Ion Abundance**
ethane + propane (not resolved)	2.3
pentane	0.7
methylcyclopentane	1.1
cyclohexane	5.5
cyclohexene	3.8
methylcyclohexane	2.1
methylenecyclohexane	3.4
1-methylcyclohexene	4.7
ethylcyclohexane	0.7
1-methyl-2-propylcyclopentane	6.9
propylcyclohexene (all isomers)	2.1
butylcyclohexane	1.1
1,3-diisopropylcyclohexane	2.8

In order to determine the kinetics of decomposition, the thermally stressed liquid phase of every decomposition reaction was analyzed by a gas chromatograph equipped with a flame ionization detector (GC-FID). Evaporative losses were minimized by transferring the liquid phase into a chilled (7 °C) glass vial and immediately diluting it with a known amount of n-dodecane. The resulting *n*-dodecane solution was typically 5% reacted propylcyclohexane (mass/mass). The sample was then analyzed by GC-FID using a 30 m capillary column coated with a 0.1 μm film of (5 %-phenyl)-methylpolysiloxane. The temperature program for the chromatographic separation consisted of an initial isothermal separation at 80 °C for 4 min, followed by a 30 °C/min gradient to 250 °C, with an additional minute at the final temperature. Figure 6 shows the suite of decomposition products that was seen in the chromatograms. The decomposition products were essentially the same at all temperatures, with retention times that were constant to within

0.01 min. Although we did not attempt to identify the individual peaks, the product suite observed by GC-FID is consistent with the product suite identified by GC-MS. These routine GC-FID analyses allowed us to track the extent of decomposition for each reaction. For example, about 20% of the propylcyclohexane had decomposed after 40 min at 450 °C, but only about 4% of the propylcyclohexane had decomposed after 32 h at 375 °C.

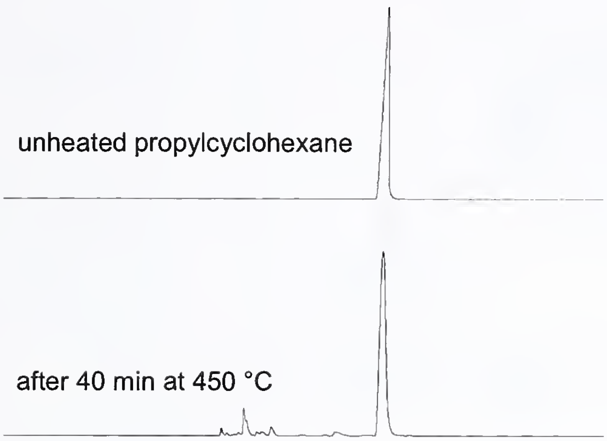

Figure 6: Chromatograms obtained by gas chromatography for unheated propylcyclohexane and for decomposed propylcyclohexane. The decomposed sample had been maintained at 450 °C for 40 min, which caused about 20 % of the propylcyclohexane to decompose.

The kinetic analysis was done by monitoring the relative decrease in the chromatographic signal of propylcyclohexane compared to the chromatographic signals for decomposition products. At each temperature data were collected at four or five different reaction times, with 3 to 5 replicate decomposition reactions at each reaction time. Following equation 3, the value of k at each temperature was obtained from the slope of a linear fit of ln(propylcyclohexane peak area %) as a function of t. Figure 7 shows such a plot obtained from the data at 450 °C. The linearity of the data justifies the assumption of first-order kinetics. The first-order rate constant obtained from the plot is 8.63×10^{-5} s^{-1}, with a standard uncertainty of 0.18×10^{-5} s^{-1}. The rate constants measured for all temperatures are provided in Table 7. An Arrhenius plot of the rate constants is shown in Figure 8. The Arrhenius parameters determined from a linear regression of the data are A = 2.56×10^{16} s^{-1} and $E_a = 283$ kJ·mol^{-1}. The standard uncertainty in E_a, calculated from the standard error in the slope of the regression, is 6 kJ·mol^{-1}. The linearity of the Arrhenius plot ($r^2 = 0.9999$) over the 75 °C temperature range is an important validation that the assumption of first-order kinetics is reasonable. Note that the activation energy for the decomposition of propylcyclohexane is slightly higher than the values reported for C_{10}–C_{14} *n*-alkanes; for example, for n-dodecane E_a is 260 kJ·mol^{-1} (with a reported uncertainty of 8 kJ·mol^{-1})[6].

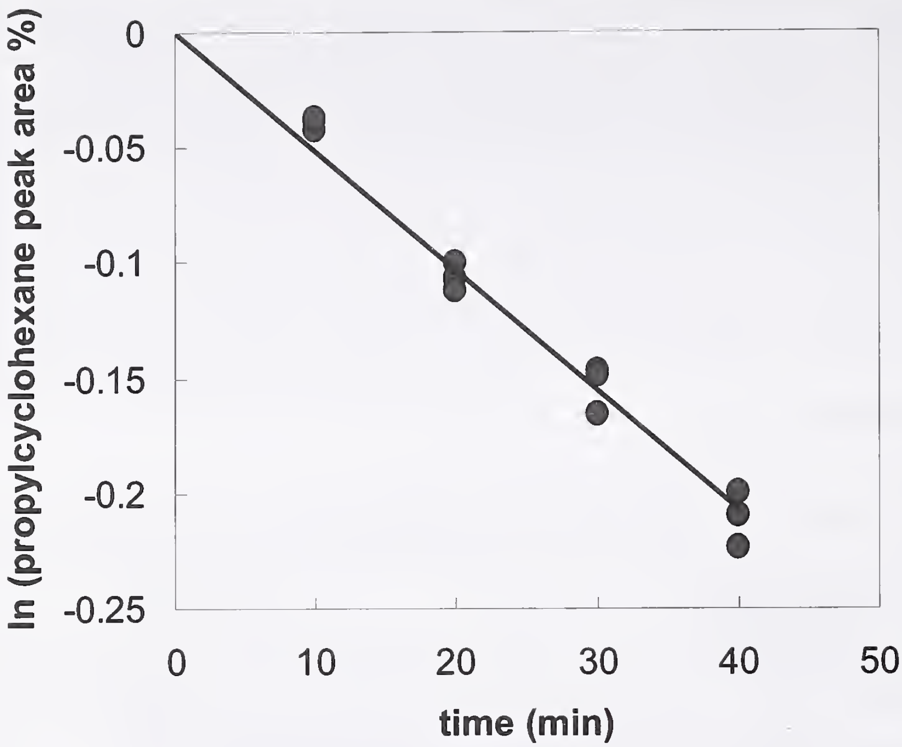

Figure 7: A plot of the ln(propylcyclohexane peak area %) as a function of time at 450 °C. The first-order rate constant for the decomposition reaction was determined from the slope of the linear fit to the data.

Table 7: Kinetic data for the thermal decomposition of propylcyclohexane.

T / °C	k / s^{-1}	Uncertainty in k / s^{-1}	$t_{0.5}$ / h	$t_{0.01}$ / min
375	3.66×10^{-7}	0.12×10^{-7}	526	458
400	2.67×10^{-6}	0.09×10^{-6}	72.2	62.8
425	1.59×10^{-5}	0.04×10^{-5}	12.1	10.5
450	8.63×10^{-5}	0.18×10^{-5}	2.23	1.94

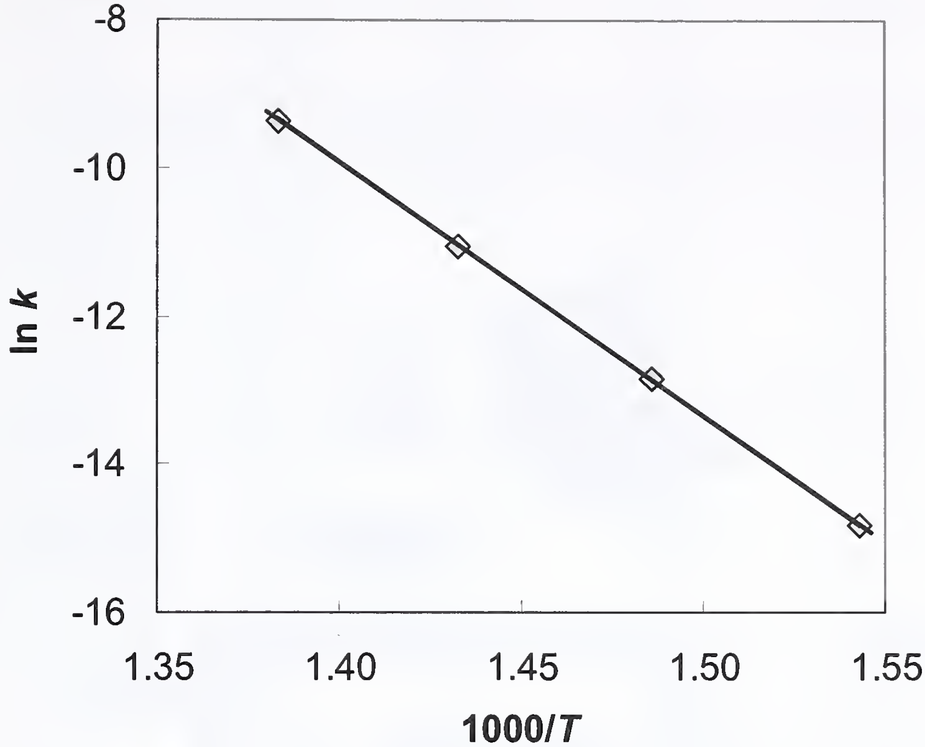

Figure 8: The Arrhenius plot for the decomposition of propylcyclohexane. The Arrhenius parameters determined from the linear fit are A = 2.56×10^{16} s^{-1} and E_a = 283 kJ·mol^{-1}.

<u>Thermophysical Property Measurements on Methylcyclohexane and Propylcyclohexane:</u>

Compressed Liquid Density Measurements for Methyl- and Propylcyclohexane:

A schematic of the apparatus used to measure compressed liquid densities over the temperature range of 270 K to 470 K and to pressures of 50 MPa is illustrated in Figure 9.[8] The heart of the apparatus is a commercial vibrating tube densimeter, however, several physical and procedural improvements have been implemented beyond that of the commercial instrument operated in a stand-alone mode. The densimeter is housed in a specially designed two-stage thermostat for improved temperature control. The uncertainty in the temperature is 0.02 K with short-term stability of 0.005 K. Pressures are measured with an oscillating quartz crystal pressure transducer with an uncertainty of 10 kPa. The densimeter is calibrated with measurements of vacuum, propane and toluene, over the temperature and pressure range of the apparatus to achieve an uncertainty in density of 1 kg/m^3.

The apparatus has been designed, and software has been written so that the operation and data acquisition are fully automated. Data are taken along isotherms over a temperature/pressure matrix programmed by the operator prior to the start of measurements. Electronically actuated pneumatic valves, and a programmable syringe pump are used to move from one pressure to the next and/or flush fresh sample through the system. Operation of the densimeter in this manner allows for measurements to be made 24 hours a day.

Compressed liquid densities of methylcyclohexane have been measured along eleven isotherms from 270 K to 470 K at pressures from 0.5 MPa to 40 MPa. A total of 140 points are reported in Table 8 and shown graphically in Figure 10.[9]

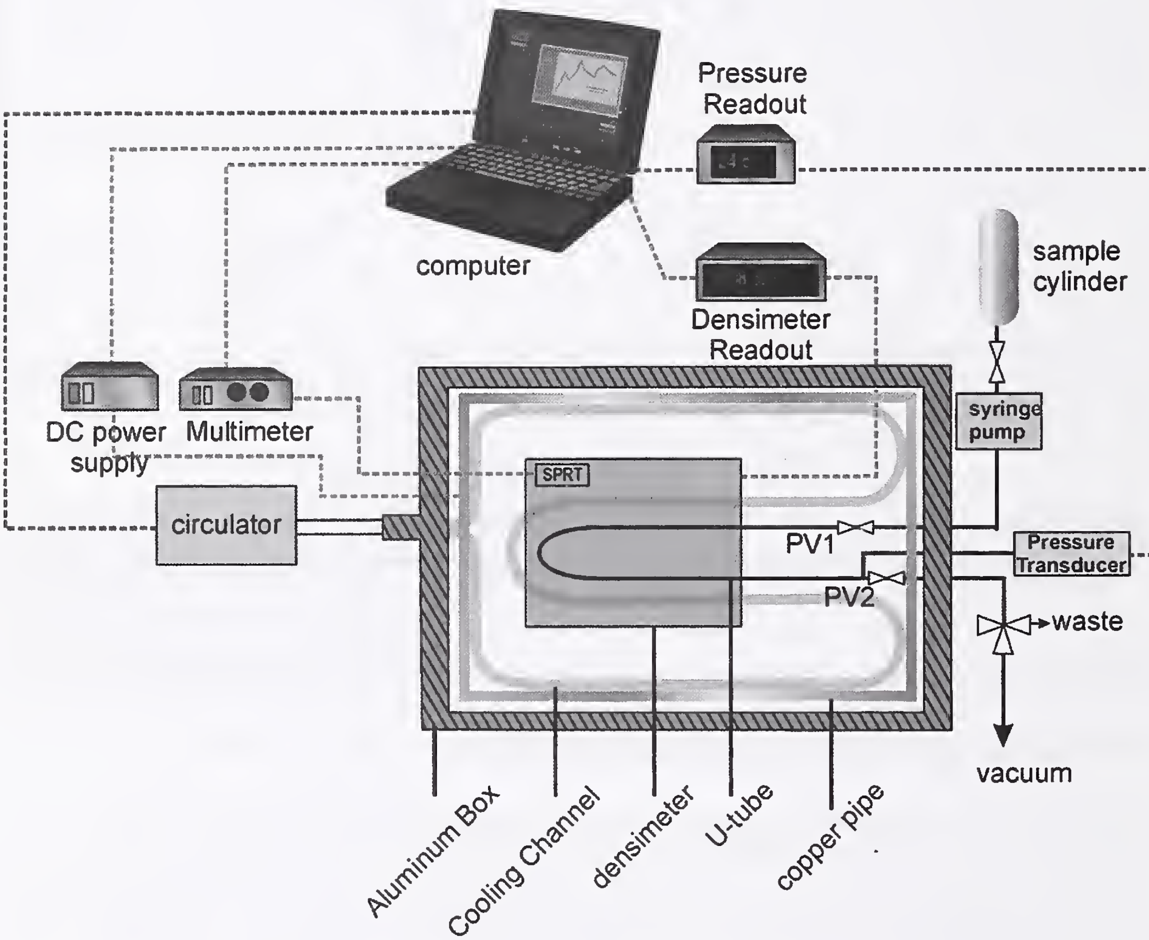

Figure 9. Schematic of the Compressed Liquid Density Apparatus.

Table 8. Compressed liquid densities of methylcyclohexane

Temperature (K)	Pressure (MPa)	Density (kg/m3)	Temperature (K)	Pressure (MPa)	Density (kg/m3)
270.00	40.007	814.61	390.00	40.003	731.07
270.00	35.009	811.80	390.00	35.004	726.33
270.00	30.008	808.90	390.00	29.996	721.31

270.00	25.004	805.91	390.00	25.009	715.97
270.00	20.008	802.83	390.00	20.007	710.24
270.00	15.006	799.63	390.00	15.001	704.06
270.00	10.005	796.31	390.00	10.003	697.32
270.00	5.007	792.85	390.00	5.011	689.86
270.00	4.004	792.13	390.00	4.003	688.24
270.00	2.998	791.41	390.00	3.004	686.61
270.00	2.005	790.68	390.00	2.008	684.95
270.00	1.003	789.96	390.00	0.999	683.2
270.00	0.502	789.59	390.00	0.502	682.32
290.00	39.998	800.66	410.00	39.999	717.45
290.00	34.996	797.59	410.00	35.003	712.28
290.00	29.996	794.41	410.00	30.002	706.79
290.00	24.995	791.12	410.00	25.002	700.89
290.00	20.007	787.71	410.00	19.997	694.5
290.00	14.995	784.14	410.00	15.004	687.54
290.00	9.999	780.43	410.00	10.006	679.84
290.00	5.004	776.54	410.00	5.002	671.17
290.00	3.994	775.73	410.00	4.003	669.29
290.00	3.007	774.91	410.00	3.000	667.35
290.00	2.000	774.08	410.00	2.003	665.35
290.00	1.003	773.25	410.00	1.000	663.27
290.00	0.497	772.82	410.00	0.507	662.23
310.00	40.034	786.33	430.00	40.017	703.89
310.00	34.999	782.89	430.00	34.998	698.25
310.00	30.014	779.38	430.00	30.000	692.21
310.00	25.007	775.73	430.00	25.005	685.69
310.00	20.006	771.95	430.00	19.999	678.55
310.00	15.009	767.98	430.00	14.997	670.67
310.00	10.007	763.81	430.00	10.006	661.83
310.00	5.016	759.43	430.00	4.999	651.64
310.00	3.997	758.50	430.00	3.997	649.38
310.00	2.999	757.59	430.00	3.003	647.06
310.00	2.005	756.66	430.00	2.002	644.62
310.00	1.009	755.72	430.00	0.493	640.64
310.00	0.500	755.22	450.00	39.991	690.35
330.00	40.011	772.18	450.00	34.996	684.22
330.00	35.006	768.48	450.00	29.995	677.59
330.00	30.003	764.63	450.00	24.995	670.36
330.00	25.001	760.61	450.00	20.003	662.4
330.00	20.006	756.40	450.00	15.001	653.46
330.00	15.009	752.00	450.00	10.004	643.22
330.00	10.001	747.31	450.00	4.999	631.1
330.00	5.003	742.35	450.00	4.000	628.37
330.00	4.000	741.29	450.00	3.001	625.51
330.00	3.012	740.25	450.00	1.999	622.5

330.00	2.002	739.17	450.00	1.000	619.32
330.00	1.000	738.08	470.00	39.994	676.99
330.00	0.501	737.54	470.00	35.000	670.31
350.00	40.000	758.41	470.00	30.009	663.05
350.00	35.003	754.41	470.00	25.005	655.04
350.00	30.011	750.22	470.00	19.995	646.07
350.00	25.004	745.82	470.00	14.995	635.87
350.00	20.001	741.17	470.00	9.995	623.93
350.00	15.005	736.24	470.00	5.001	609.33
350.00	10.006	730.97	470.00	4.003	605.94
350.00	5.000	725.31	470.00	2.999	602.32
350.00	4.007	724.13	470.00	1.999	598.46
350.00	3.009	722.92	470.00	1.002	594.33
350.00	2.003	721.69			
350.00	1.004	720.45			
350.00	0.500	719.79			
370.00	39.999	744.71			
370.00	34.994	740.36			
370.00	29.997	735.78			
370.00	25.005	730.95			
370.00	19.994	725.79			
370.00	15.007	720.28			
370.00	10.006	714.34			
370.00	5.000	707.86			
370.00	3.995	706.48			
370.00	3.000	705.08			
370.00	2.001	703.65			
370.00	0.994	702.17			
370.00	0.499	701.44			

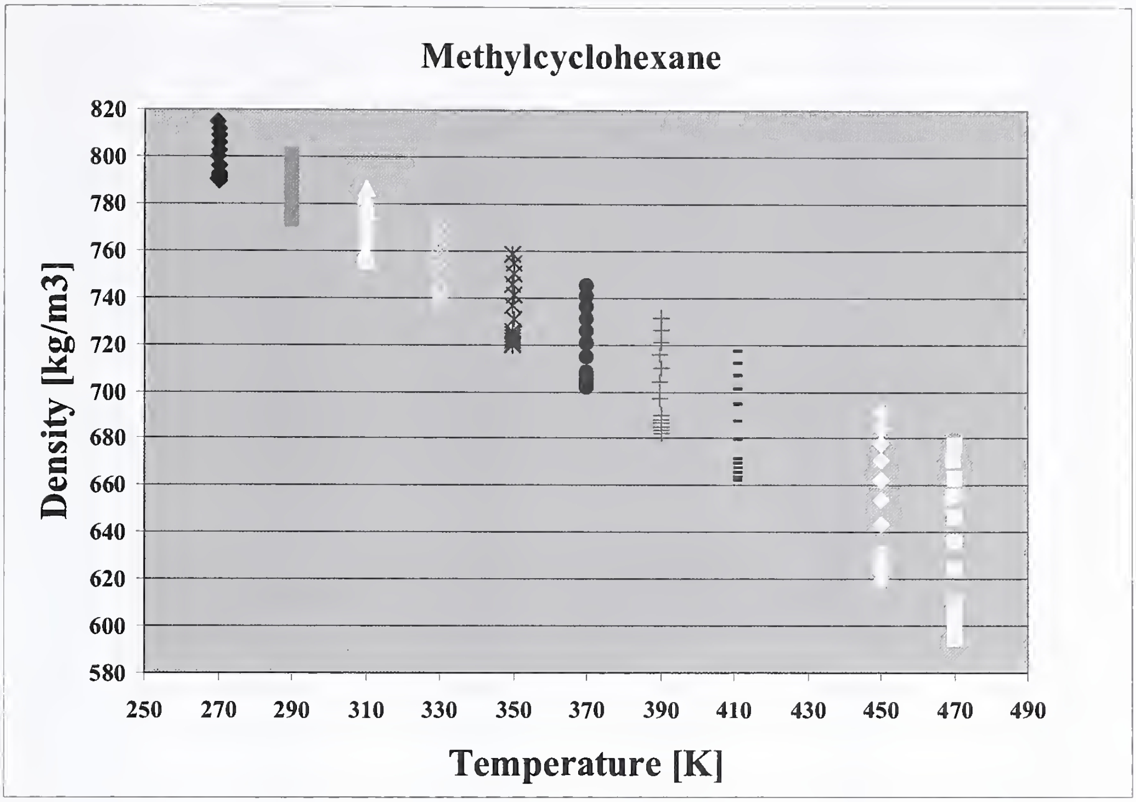

Figure 10. Compressed liquid densities of methylcyclohexane as a function of temperature.

Compressed liquid densities of propylcyclohexane have been measured along eleven isotherms from 270 K to 470 K at pressures from 0.5 MPa to 40 MPa. A total of 143 points are reported in Table 9 and are shown graphically in Figure 11.

Table 9. Compressed liquid densities of propylcyclohexane.

Temperature (K)	Pressure (MPa)	Density (kg/m3)	Temperature (K)	Pressure (MPa)	Density (kg/m3)
270.00	39.959	834.41	390.00	39.989	756.91
270.00	35.005	831.91	390.00	35.002	752.82
270.00	30.003	829.32	390.00	29.998	748.51
270.00	25.001	826.66	390.00	25.002	743.97
270.00	19.995	823.91	390.00	20.002	739.14
270.00	15.004	821.08	390.00	15.000	734.00
270.00	10.003	818.11	390.00	10.005	728.48
270.00	5.009	815.01	390.00	5.003	722.49
270.00	4.004	814.35	390.00	4.003	721.22
270.00	2.987	813.68	390.00	3.003	719.93
270.00	2.001	813.03	390.00	2.009	718.64
270.00	1.001	812.37	390.00	1.002	717.29
270.00	0.497	812.02	390.00	0.504	716.61

290.00	40.005	821.46	410.00	39.998	744.41
290.00	35.005	818.73	410.00	35.005	739.97
290.00	29.995	815.90	410.00	30.003	735.27
290.00	25.004	812.98	410.00	25.002	730.28
290.00	19.998	809.96	410.00	19.998	724.97
290.00	15.011	806.81	410.00	14.998	719.26
290.00	10.002	803.50	410.00	10.008	713.07
290.00	5.002	800.04	410.00	5.008	706.29
290.00	4.007	799.31	410.00	4.003	704.83
290.00	3.003	798.58	410.00	2.994	703.34
290.00	2.013	797.84	410.00	2.005	701.86
290.00	1.000	797.09	410.00	0.994	700.28
290.00	0.506	796.73	410.00	0.506	699.52
310.00	39.979	807.65	430.00	39.996	731.95
310.00	35.008	804.71	430.00	35.004	727.15
310.00	29.997	801.64	430.00	30.006	722.05
310.00	24.999	798.47	430.00	24.999	716.59
310.00	20.004	795.18	430.00	19.996	710.74
310.00	14.996	791.73	430.00	15.011	704.40
310.00	10.004	788.15	430.00	10.005	697.42
310.00	5.013	784.41	430.00	4.999	689.66
310.00	3.999	783.61	430.00	3.993	687.98
310.00	3.004	782.83	430.00	3.002	686.29
310.00	2.007	782.04	430.00	1.988	684.51
310.00	0.999	781.23	430.00	0.998	682.73
310.00	0.505	780.83	430.00	0.516	681.83
330.00	39.988	794.75	450.00	39.992	719.57
330.00	35.002	791.53	450.00	35.009	714.38
330.00	30.000	788.17	450.00	30.007	708.83
330.00	25.001	784.69	450.00	25.013	702.87
330.00	20.004	781.06	450.00	19.999	696.38
330.00	15.009	777.27	450.00	15.008	689.31
330.00	10.001	773.27	450.00	9.999	681.42
330.00	5.001	769.08	450.00	4.999	672.53
330.00	3.994	768.20	450.00	3.995	670.59
330.00	3.000	767.32	450.00	3.001	668.60
330.00	2.004	766.43	450.00	1.993	666.53
330.00	0.999	765.52	450.00	0.999	664.39
330.00	0.498	765.06	450.00	0.506	663.31
350.00	40.001	782.15	470.00	40.004	707.37
350.00	35.003	778.64	470.00	35.004	701.75
350.00	30.001	774.98	470.00	30.002	695.70
350.00	25.007	771.17	470.00	25.001	689.15
350.00	20.005	767.18	470.00	20.004	682.01
350.00	15.006	762.98	470.00	14.994	674.08
350.00	10.006	758.54	470.00	10.006	665.17

350.00	4.999	753.83	470.00	5.003	654.87
350.00	4.003	752.86	470.00	4.003	652.59
350.00	2.996	751.85	470.00	3.000	650.21
350.00	1.992	750.83	470.00	2.002	647.76
350.00	1.000	749.82	470.00	0.991	645.18
350.00	0.500	749.30	470.00	0.496	643.86
370.00	39.998	769.44			
370.00	34.998	765.65			
370.00	30.001	761.68			
370.00	25.001	757.53			
370.00	20.007	753.15			
370.00	15.011	748.51			
370.00	10.006	743.56			
370.00	5.003	738.27			
370.00	4.003	737.16			
370.00	3.002	736.02			
370.00	2.005	734.87			
370.00	1.006	733.71			
370.00	0.496	733.11			

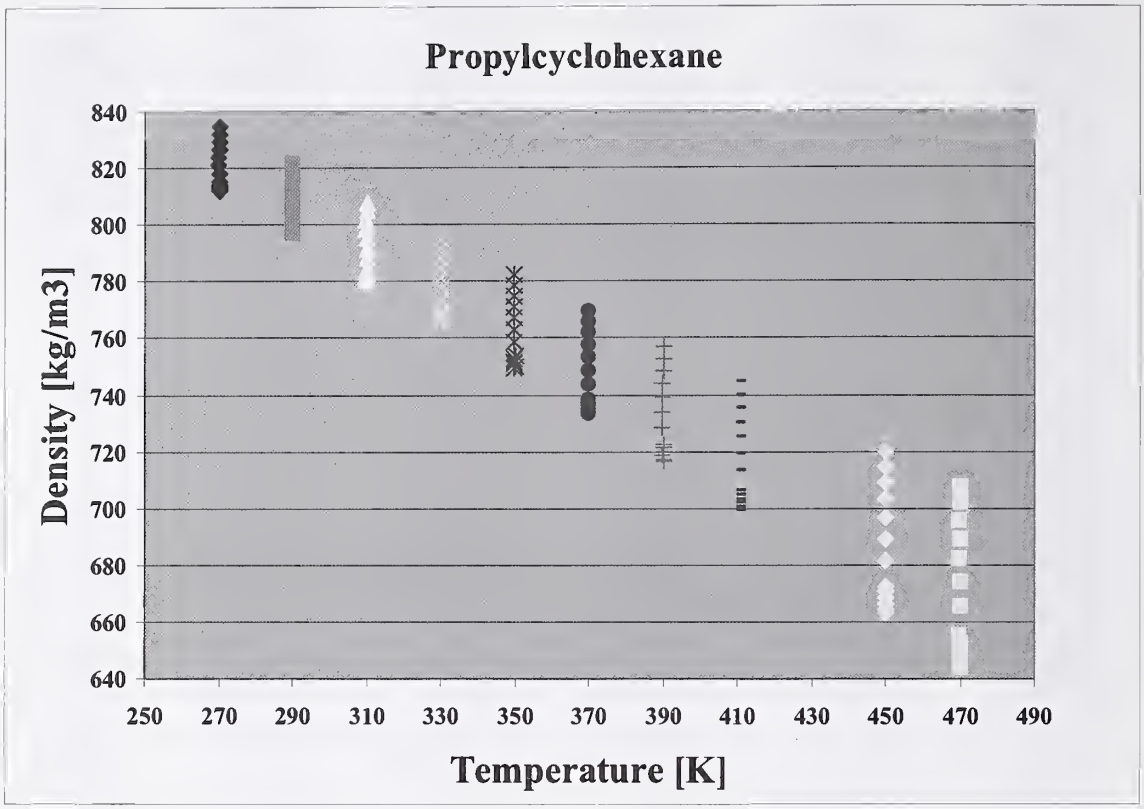

Figure 11. Compressed liquid densities of propylcyclohexane as a function of temperature.

Viscosity Measurements of Methyl- and Propylcyclohexane:

Viscosity measurements of methyl- and propylcyclohexane were carried out at ambient pressure in the temperature range 293.15 K to 373.15 K. These measurements are presented in Table 10. The instrument used was a commercial device consisting of an automated open gravitational flow viscometer with a suspended-level Ubbelohde glass capillary of 200 mm length with upper reservoir bulbs for a kinematic viscosity range from 0.3 $mm^2 \cdot s^{-1}$ to 30 $mm^2 \cdot s^{-1}$. As shown in the photograph of Figure 12, the glass capillary is mounted in a thermostatting bath filled with silicone oil. The thermostat includes a stirrer, a heat pipe to a thermoelectric Peltier cooler at the top of the instrument (not visible), and a platinum 100 Ω resistance temperature probe (PRT). The bath temperature is set with the operating software that is an integral part of the viscosity measurement system and it is controlled within 0.02 K between 293.15 K and 373.15 K. The resistance of the PRT is measured with an ac bridge. The calibration of the PRT on the International Temperature Scale of 1990 was checked by comparison with a water triple point cell. The estimated uncertainty of the temperature measurement system is 0.02 K.

Figure 12: A photograph of the viscometer used for the measurement of methyl- and propylcyclohexane.

The instrument allows viscosity measurements relative to liquids with well known viscosities. Calibrations were performed with certified viscosity standards to determine the constants C and E of the working equation:

$$\nu = C \cdot t - E / t^2. \qquad (7)$$

The first term on the right hand side of this equation is the reformulated Hagen-Poiseuille expression for laminar flow in a circular tube whereas the second term is the Hagenbach correction for kinetic energy losses. Symbol ν denotes the kinematic viscosity in $mm^2 \cdot s^{-1}$ and t the efflux time in seconds of a known volume of liquid through the capillary. Efflux times are measured with three thermistor sensors on the outside of the capillary above and below the two measuring bulbs. The thermistors detect the passing of the liquid meniscus at their locations and trigger an internal stopwatch. Depending on the viscosity range the two upper or the two lower thermistors are used to time the efflux of the test liquid through the respective measuring bulb of known volume.

The viscosity measurement system includes components to pump the test liquid into the upper measuring bulbs for repetitive efflux timings and to flush the capillary tube with two different solvents when the test liquid is changed. The operating software was set to perform five measurement runs at the most of which the three that agreed within 0.5% repeatability were averaged to calculate the viscosity. The uncertainty of the viscosity measurements reported here is estimated at 1.5 % to account for variations in the constants C and E that occurred for calibrations with different viscosity standards and to a lesser degree for calibrations at different temperatures.

The ambient pressure during the measurements was 83 kPa. Due to this, methyl cyclohexane could not be measured at 373.15 K because it evaporated at that temperature.

The design of the instrument, its calibration, and operation conform to the following standards:

- ASTM D 445 Standard Test Method for Kinematic Viscosity of Transparent and Opaque Liquids (and the Calculation of Dynamic Viscosity),

- ASTM D 446 Standard Specifications and Operating Instructions for Glass Capillary Kinematic Viscometers,

- D 2162 Test Method for Basic Calibration of Master Viscometers and Viscosity Oil Standards,

and the corresponding ISO standards 3104 and 3105.

Table 10: Kinematic viscosity of methyl- and propylcyclohexane measured in the open gravitational capillary viscometer system.

Methylcyclohexane		Propylcyclohexane	
Temperature T	Kinematic viscosity ν	Temperature T	Kinematic viscosity ν
K	$mm^2 \cdot s^{-1}$	K	$mm^2 \cdot s^{-1}$
363.15	0.4707	303.15	1.112
353.16	0.5113	293.15	1.277
343.15	0.5568	313.15	0.9830
333.15	0.6107	373.15	0.5500
323.15	0.6736	363.15	0.5966
313.15	0.7488	353.15	0.6499
303.21	0.8387	343.15	0.7140
293.23	0.9480	333.15	0.7877
		323.15	0.8759

Sound Speed Measurements of Methyl- and Propylcyclohexane:

A commercial density and sound speed analyzer was used to determine the sound speed of methyl- and propylcyclohexane at ambient pressure.[9] Temperature scans were programmed from 70 °C to 10 °C in decrements of 10 °C followed by a single measurement at 5 °C. The device contains a sound speed cell and a vibrating quartz tube densimeter in series. Temperature is measured with an integrated Pt-100 thermometer with an estimated uncertainty of 0.01 K. The sound speed cell has a circular cylindrical cavity of 8 mm diameter and 5 mm thickness that is sandwiched between the transmitter and receiver. The speed of sound is determined by measuring the time of flight of signals between the transmitter and receiver. The instrument was calibrated with air and deionized water at 20 °C. The reproducibility of the sound speed of water at 20 °C to within 0.01 % was checked before and after measurements of the test liquids. Careful cleaning of the sound speed cell with suitable solvents was found critical to avoid contaminations and to ensure this level of performance. For the same reason, fresh samples of test liquids were injected for each temperature scan instead of performing repetitive measurements on the same sample. At least four temperature scans were performed for each test liquid. The relative standard deviation of these repeated sound speed measurements was lower than 0.013 %. The manufacturer quoted uncertainty of sound speed measurements with this instrument is 0.1 %. The speeds of sound measured in this work (along with the density) are provided in Table 11, and shown graphically in Figure 13.

Table 11: Density, speed of sound, and adiabatic compressibility of methyl- and propylcyclohexane measured in the commercial density and sound speed analyzer. The ambient pressure during the measurements was 83 kPa.

	Methylcyclohexane			**Propylcyclohexane**		
Temperature T	**Density ρ**	**Speed of sound w**	**Adiab. compressibility κ_S**	**Density ρ**	**Speed of sound w**	**Adiab. compressibility κ_S**
K	**$kg \cdot m^{-3}$**	**$m \cdot s^{-1}$**	**TPa^{-1}**	**$kg \cdot m^{-3}$**	**$m \cdot s^{-1}$**	**TPa^{-1}**
278.15	782.3	1304.7	750.94	805.4	1371.3	660.26
283.15	778.0	1281.9	782.27	801.5	1349.6	685.01
293.15	769.3	1236.9	849.67	793.7	1307.1	737.38
303.15	760.7	1192.9	923.93	785.9	1265.5	794.47
313.15	751.9	1149.7	1006.1	778.1	1224.7	856.81
323.15	743.1	1107.4	1097.4	770.2	1184.7	925.02
333.15	734.3	1065.6	1199.3	762.3	1145.4	999.94
343.15	725.3	1024.5	1313.6	754.4	1106.9	1081.9

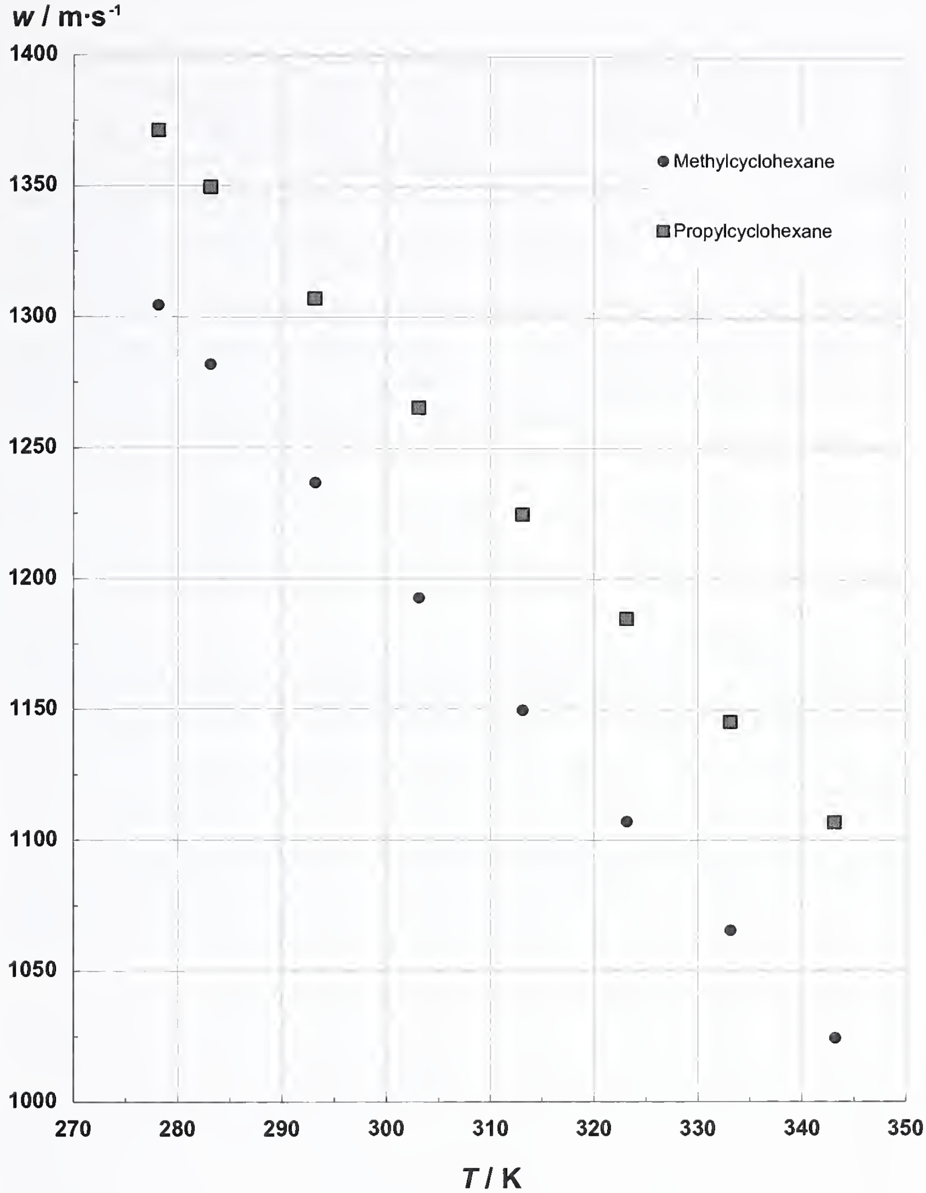

Figure 13: Measured speed of sound data for methyl- and propylcyclohexane

Adiabatic compressibilities at ambient pressure were obtained from the measured densities and speeds of sound via the thermodynamic relation $\kappa_s = -(\partial V/\partial p)_s/V = 1 / (\rho w^2)$, where V denotes volume, p is pressure, ρ is the density, and w the speed of sound. Subscript s indicates "at constant entropy s." For convenience, the calculated adiabatic compressibilities are included in Table 11.

The speed of sound and adiabatic compressibility data of the two liquids at ambient pressure are plotted in Figure 14 as a function of temperature. Comparing the plots illustrates how changing the molecular structure of methylcyclohexane by adding an ethyl-group $-CH_2-CH_2-$ to the aliphatic side chain to form propylcyclohexane influences the macroscopic properties of the two compounds. The speed of sound increases between

5.1 % at 273.15 K and 8.1 % at 343.15 K whereas the adiabatic compressibility increases between 13.8 % and 21.4 %. The densities of the test liquids at these two state points differ only by 3 % and 4 %, respectively. Thus, the adiabatic compressibility appears to reflect structural changes on the molecular scale with higher resolution than the other two properties.

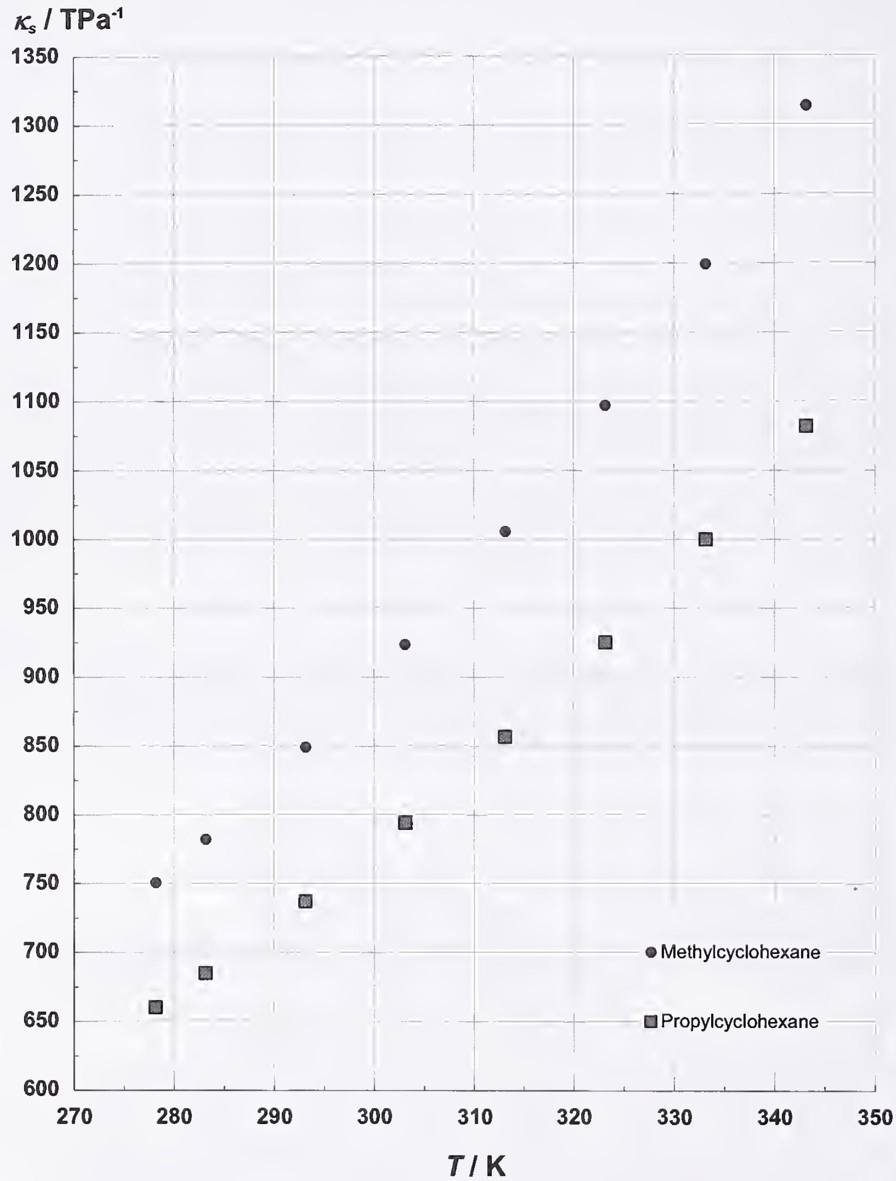

Figure 14: Measured adiabatic compressibility of methyl- and propylcyclohexane as a function of temperature at ambient pressure

Thermal Conductivity of Methyl- and Propylcyclohexane:

Transient hot-wire measurements of the thermal conductivity of the samples of methylcyclohexane and propylcyclohexane were made in the liquid and vapor phases; up to 600 K for propylcyclohexane. In addition, a supercritical isotherm at 593 K was measured for methylcyclohexane. Measurements for both fluids cover temperatures from 300 to 600 K with pressures up to 70 MPa. The transient hot-wire instrument has been described in detail elsewhere.[10, 11] The measurement cell is designed to closely approximate transient heating from a line source into an infinite fluid medium. The ideal (line source) temperature rise ΔT_{id} is given by:

$$\Delta T_{id} = \frac{q}{4\pi\lambda}\left[\ln(t) + \ln\left(\frac{4a}{r_0^2 C}\right)\right] = \Delta T_w + \sum_{i=1}^{10} \delta T_i, \qquad (8)$$

where q is the power applied per unit length, λ is the thermal conductivity of the fluid, t is the elapsed time, $a = \lambda/\rho C_p$ is the thermal diffusivity of the fluid, ρ is the density of the fluid, C_p is the isobaric specific heat capacity of the fluid, r_0 is the radius of the hot wire, $C = 1.781...$ is the exponential of Euler's constant, ΔT_w is the measured temperature rise of the wire, and δT_i are corrections to account for deviations from ideal line-source conduction. The only significant correction for the measurements is for the finite wire dimensions. A plot of ideal temperature rise versus logarithm of elapsed time should be linear, such that thermal conductivity can be found from the slope and thermal diffusivity can be found from the intercept of a line fit to the data.

At time zero, a fixed voltage is applied to heat the small diameter wire that is immersed in the fluid of interest. The wire is used as an electrical heat source while its resistance increase allows determination of the transient temperature rise as a function of elapsed time. Two platinum wires of 12.7 μm diameter were used for most of the measurements. The two wires, one about 18 cm long and one about 4 cm long, were used with a differential technique to eliminate axial conduction errors. A similar cell with anodized tantalum hot wires of 25 μm diameter was used for some measurements on liquid methylcyclohexane at temperatures from 300 K to 400 K. Short experiment times (nominally 1 s) and small temperature rises (nominally 1 to 4 K) were selected to eliminate heat transfer by free convection. Experiments at several different heating powers (and temperature rises) provide verification that free convection is not significant. Heat transfer due to thermal radiation is more difficult to detect and correct when the fluid can absorb and re-emit infrared radiation as these hydrocarbons do. Thermal radiation heat transfer will increase roughly in proportion to the absolute temperature cubed and can be characterized from an increase in the apparent thermal conductivity as experiment time increases since radiation emission from the fluid increases as the thermal wave diffuses outward.

At very low pressures, the steady-state hot-wire technique has the advantage of not requiring significant corrections. The working equation for the steady-state mode is based on a different solution of Fourier's law but the geometry is still that of concentric cylinders. This equation can be solved for the thermal conductivity of the fluid, λ,

$$\lambda = \frac{q \ln\left(\frac{r_2}{r_1}\right)}{2\pi(T_1 - T_2)}, \tag{9}$$

where q is the applied power per unit length, r_2 is the internal radius of the outer cylinder, r_1 is the external radius of the inner cylinder (hot wire), and $\Delta T = (T_1 - T_2)$ is the measured temperature difference between the hot wire and its surrounding cavity.

A total of 1389 points are reported in Appendix I (the lengths of these tables preclude inclusion within the body of the report) for the thermal conductivity of methylcyclohexane in the liquid, vapor and supercritical regions at pressures to 60 MPa. These data for methylcyclohexane are shown in Figure 15. A total of 668 points are reported in appendix I for the thermal conductivity of propylcyclohexane in the liquid and vapor regions at pressures to 60 MPa. Note that within the appendix, the thermal conductivity tables are divided into vapor and liquid, and by wire material. These data for propylcyclohexane are shown in Figure 16. Each experiment is characterized by the initial cell temperature T_0 and the mean experiment temperature T_e. There are generally 5 experiments at each initial cell temperature to verify that convection was not significant, since convection depends strongly on the temperature rise ($\Delta T = T_e - T_0$). The conditions of the fluid during each measurement are given by the experimental temperature T_e, pressure P_e, and density ρ_e. The thermal conductivity without correction for thermal radiation is given by λ_e..

The thermal conductivity data for these fluids have an uncertainty of less than 1 % for measurements removed from the critical point and for gas at pressures above 1 MPa, increasing to 3 % at the highest temperatures (near 600 K) and for gas at low pressures (<1 MPa) at a 95 % confidence level. A significant critical enhancement is observed in the thermal conductivity data near the critical point. There is likely a residual contribution due to emission of thermal radiation by the fluid that increases in proportion to temperature cubed up to 2 % to 3 % near 600 K.

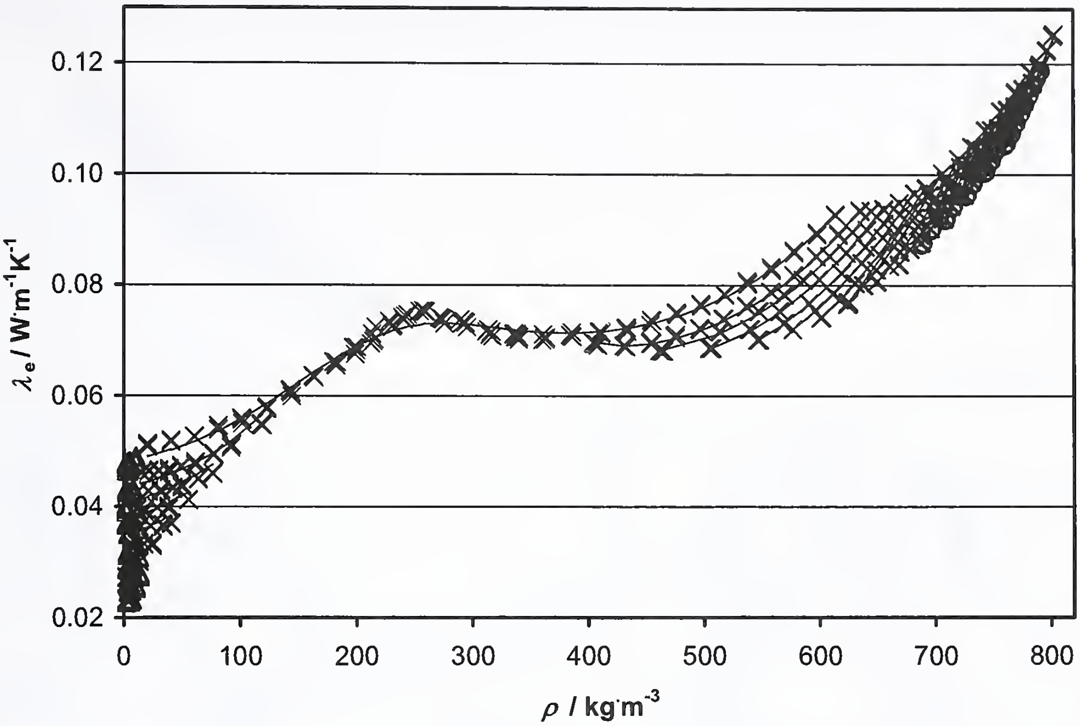

Figure 15: Thermal conductivity of methylcyclohexane at temperatures from 300 K to 595 K and pressures up to 60 MPa: ×, transient (Pt); O, transient (Ta); △, steady state (Pt); solid line given by the correlation developed in this work.

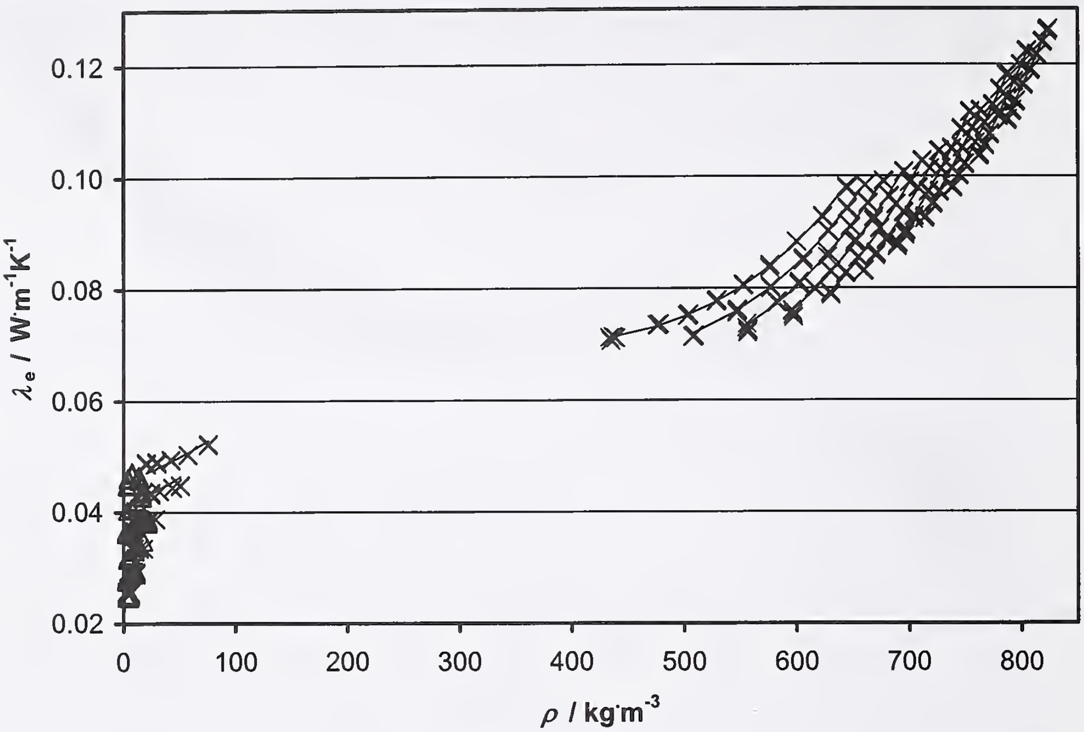

Figure 16: Thermal conductivity of propylcyclohexane at temperatures from 300 K to 600 K and pressures up to 60 MPa: ×, transient (Pt); △, steady state (Pt); solid line given by the correlation developed in this work.

Thermophysical Property Measurements on Jet-A, JP-8 and S-8:

Distillation Curves of Jet-A, JP-8 and S-8:

A new advanced method for the measurement of distillation curves of complex fluids has recently been introduced. The modifications to the classical measurement provide for (1) temperature and volume measurements of low uncertainty, (2) temperature control based upon fluid behavior, and most important, (3) a composition-explicit data channel in addition to the usual temperature-volume relationship[12-14]. This latter modification is achieved with a new sampling approach that allows precise qualitative as well as quantitative analyses of each fraction, on the fly. Any composition dependent property can be enhanced by combining it with the distillation curve information. For example, and especially relevant to fuels, we have shown that it is possible to obtain heat of combustion data for each distillate fraction[15]. In the advanced method, the temperature is logged in two locations. First, the temperature is measured directly in the fluid, which provides a true thermodynamic state point and true initial boiling temperature. This temperature is referred to as T_k. Second, the temperature is also measured in the distillation head, referred to at T_h. This temperature is directly comparable to historical data. We have applied this method to a wide variety of fuels and complex fluids[16-31]. A schematic diagram of the advanced apparatus is provided in Figures 17 - 19.

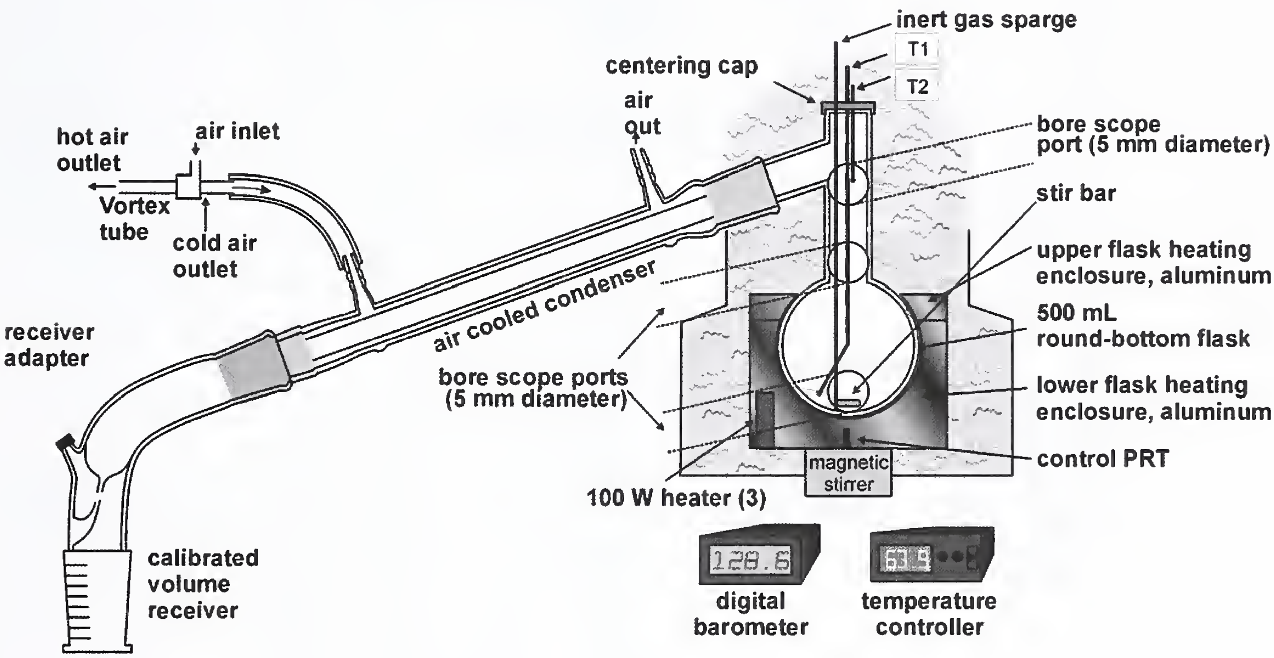

Figure 17: Schematic diagram of the overall apparatus used for the measurement of distillation curves.

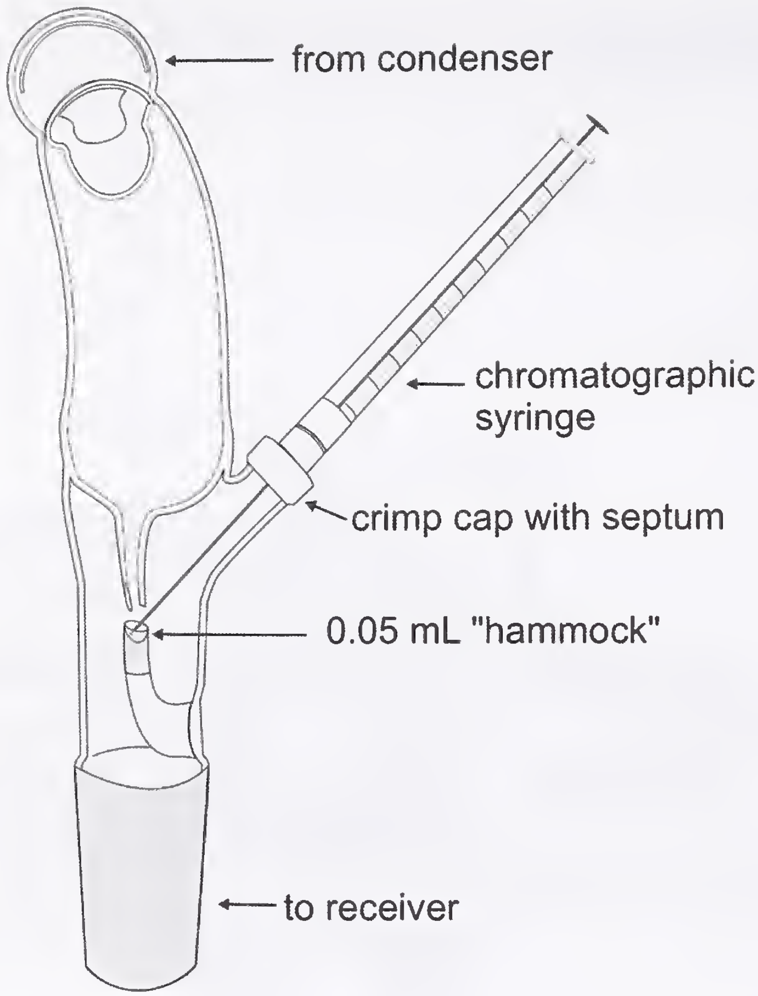

Figure 18: Schematic diagram of the receiver adapter to provide on-the-fly sampling of distillate cuts for subsequent analysis.

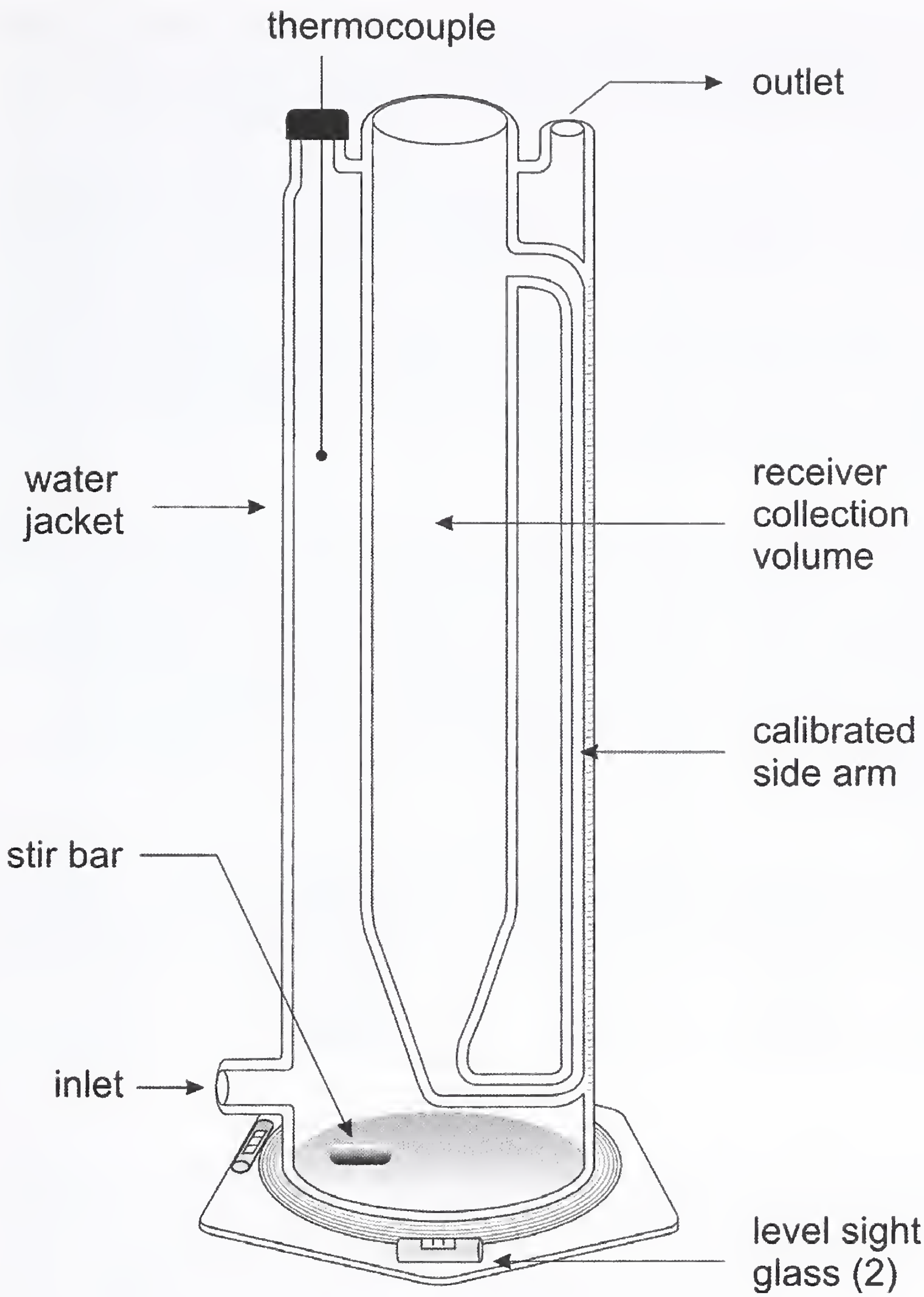

Figure 19: Schematic diagram of the level-stabilized receiver for distillation curve measurement.

During the initial heating of each sample in the distillation instrument, the behavior of the fluid was observed. Direct observation through the flask window or through the illuminated bore scope allowed measurement of the onset of boiling for each of the mixtures. Typically, during the early stages of a measurement the first bubbles will appear intermittently, and this action will quell if the stirrer is stopped momentarily. Sustained vapor bubbling is then observed. In the context of the advanced distillation curve measurement, sustained bubbling is also somewhat intermittent, but it is observable even when the stirrer is momentarily stopped. Finally, the temperature at which vapor is first observed to rise into the distillation head is observed. This is termed the vapor rise temperature. These observations are important because they are the initial boiling temperatures (IBT) of each fluid. The initial behaviors of three samples of Jet-A and the synthetic S-8 are provided in Table 12. These temperatures have been corrected to 1 atm. with the modified Sydney Young equation.[32]

Table 12: A summary of the initial behavior of the three individual samples of Jet-A, and the sample of S-8. In keeping with our advanced distillation curve protocol, the onset temperature is the temperature at which the first bubbles are observed. The sustained bubbling temperature is that at which the bubbling persists. The vapor rise temperature is that at which vapor is observed to rise into the distillation head, considered to be the initial boiling temperature of the fluid (highlighted in bold print). The temperatures have been adjusted to 1 atm with the modified Sydney Young equation; uncertainties are discussed in the text.

Observed Temperature	**Jet-A-3602, °C, 82.82 kPa**	**Jet-A-3638, °C, 82.11 kPa**	**Jet-A-4658, °C, 83.63 kPa**	**S-8, °C, 83.27 kPa**
onset	150.9	148.4	139.9	163.0
sustained	183.6	176.9	185.6	168.6
vapor rising	**191.0**	**184.2**	**190.5**	**181.9**

Representative distillation curve data for the three samples of Jet-A, presented in both T_k and T_h, are provided in Table 13. In this table, the estimated uncertainty (with a coverage factor k=2) in the temperatures is 0.1 °C. Note that the experimental uncertainty of T_k is somewhat lower than that of T_h, but as a conservative position, we use the higher value for both temperatures. The uncertainty in the volume measurement that is used to obtain the distillate volume fraction is 0.05 mL in each case. The same data are provided graphically in Figure 20.

Table 13: Representative distillation curve data for the three individual samples of Jet-A and the sample of S-8 measured in this work. The temperatures have been adjusted to 1 atm. with the modified Sydney Young equation; uncertainties are discussed in the text. These data are plotted in Figure 20.

Distillate Volume Fraction, %	**Jet-A-3602 82.82 kPa**		**Jet-A-3638 82.11 kPa**		**Jet-A-4658 83.63 kPa**		**S-8 83.27 kPa**	
	T_k, °C	T_h, °C	T_k, °C	T_h, °C	T_k, °C	T_h, °C	T_k, °C	T_h, °C
5	194.8	179.3	186.8	179.9	195.4	174.7	183.6	169.2
10	197.7	186.7	188.7	184.2	198.5	183.3	185.0	173.9
15	200.7	189.9	191.1	187.0	201.5	187.0	187.7	179.1
20	203.5	194.7	192.9	185.8	204.7	189.1	190.2	173.6
25	206.4	196.9	194.9	189.5	208.1	190.6	193.0	175.5
30	209.7	198.7	196.6	191.6	211.3	192.8	196.2	181.9
35	212.1	199.2	198.5	193.9	214.3	194.6	199.5	187.7
40	214.8	201.5	200.3	196.0	217.6	199.1	202.9	192.0
45	217.3	204.5	202.1	197.9	220.7	202.6	207.1	196.2
50	220.1	206.4	204.0	199.8	224.2	205.4	211.0	200.3
55	222.5	208.8	205.9	202.4	227.6	208.6	215.3	205.2
60	225.1	213.6	208.0	204.0	231.2	212.4	219.6	209.3
65	227.9	213.7	210.5	205.1	234.7	214.9	224.2	213.6
70	230.7	218.4	213.6	207.6	239.4	216.6	229.4	219.1
75	233.9	223.2	216.2	210.6	243.3	218.7	235.2	224.3
80	237.9	226.4	219.4	210.2	247.9	220.8	240.1	231.4
85	242.7	225.6	222.9	215.3	253.6	224.1	246.8	236.8

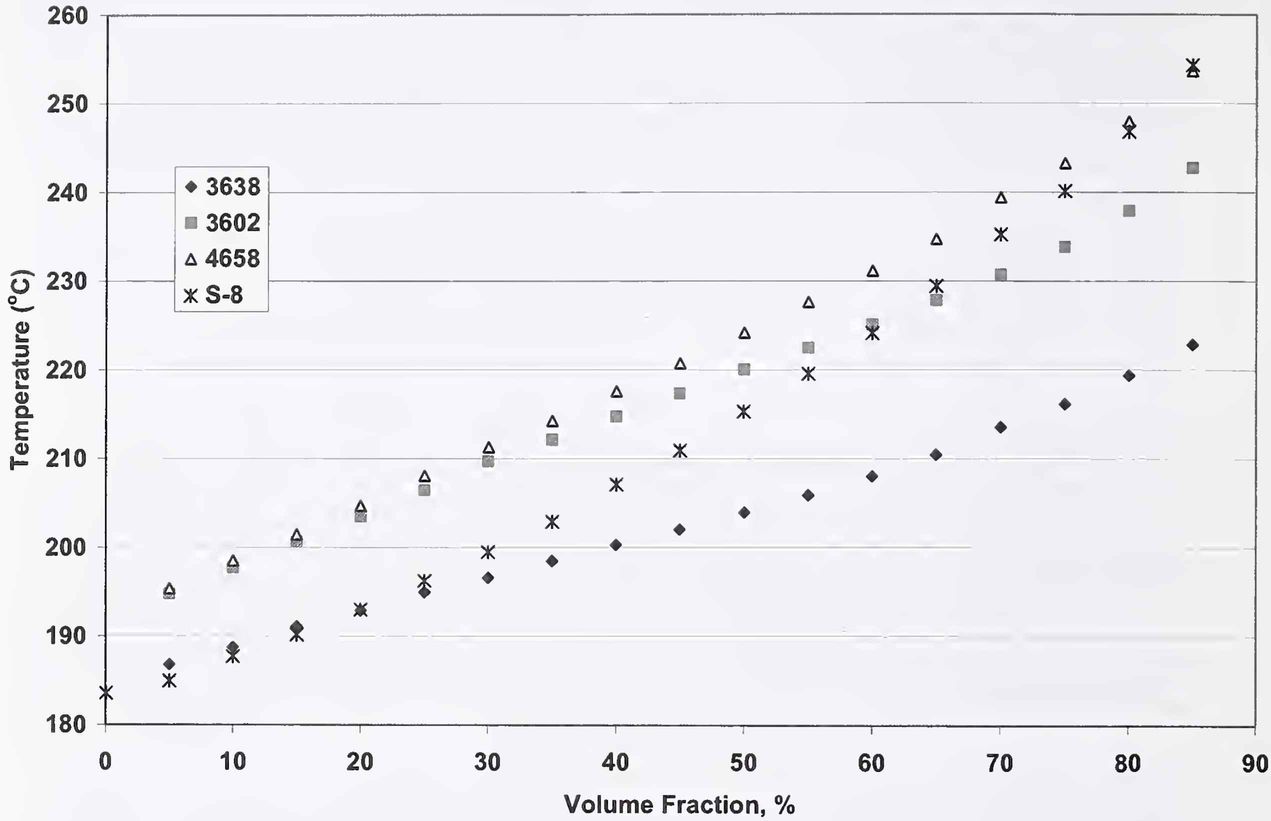

Figure 20: Representative distillation curves for each of the three samples of Jet-A and the sample of S-8 that have been measured as part of this work. The temperatures have been adjusted to 1 atm with the modified Sydney Young equation; uncertainties are discussed in the text.

The shapes of all of the curves are of the subtle sigmoid or growth curve type that one would expect for a highly complex fluid with many components, distributed over a large range of relative molecular mass. There is no indication of the presence of azeotropic constituents, since there is an absence of multiple inflections and curve flattening. As an example of typical repeatability of these curves, we show in Figure 21 six curves measured for Jet-A-4658. We note that in the latter stages of the distillations, the repeatability suffers slightly.

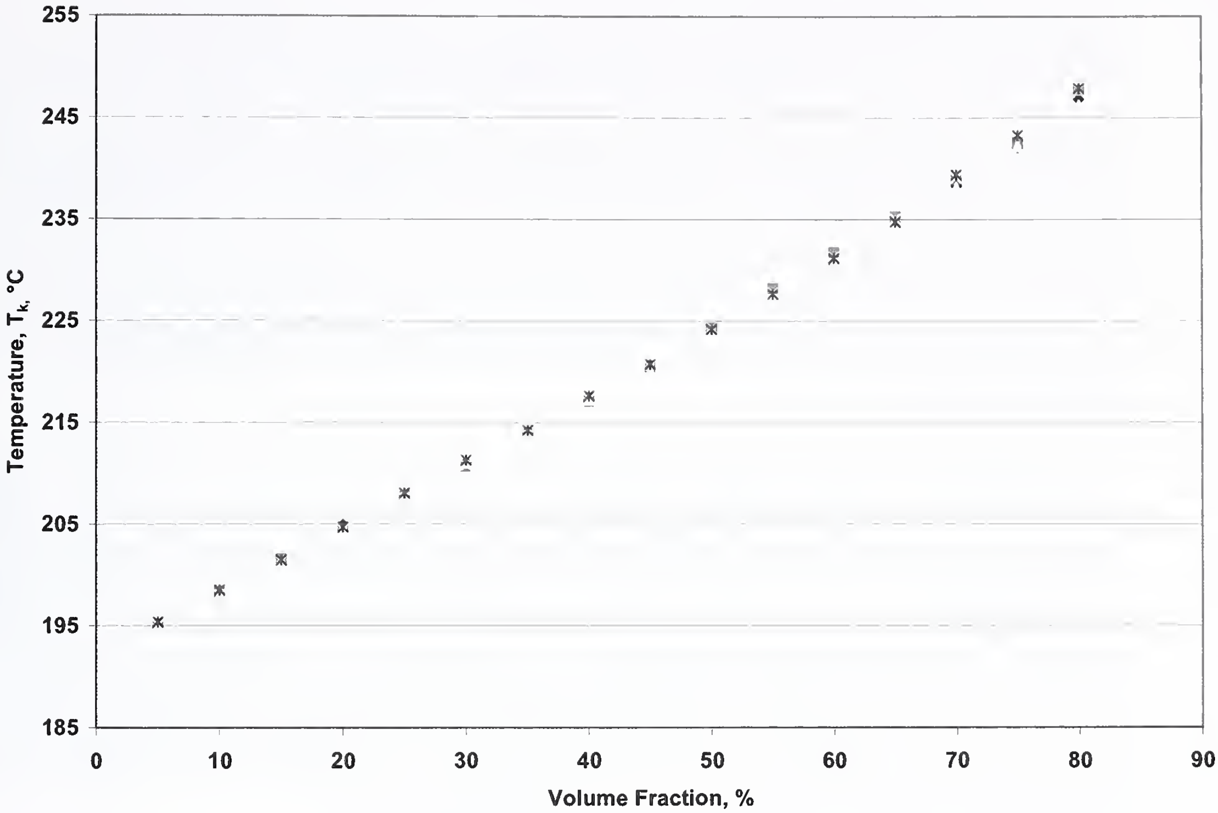

Figure 21: Plot showing the repeatability of the distillation curve measurement. Here, six measurements of the curve for Jet-A-4658 are provided. The uncertainty bars of the individual temperatures are of the same size as the plotting symbols.

The plotted curves are particularly instructive since the difference presented by Jet-A-3838 with respect to Jet-A-3602 and Jet-A-4658 is clearly shown. It is also clear from the curves that the differences are not merely in the early parts of the curves, but rather the difference persists throughout the curve and is in fact magnified at higher distillate volume fraction values. This behavior is indicative of fluids that differ in overall composition or chemical family throughout the entire composition range of the fluid. This is in contrast to differences that result from one fluid merely having somewhat more volatile constituents that boil off in the early stages of the distillation curve measurement, and is often caused by the presence of a different distribution of components within a chemical family. Indeed, this observation was found to be consistent with a gas chromatographic analysis of the three fuel samples (the procedure for which was described in the experimental section), since Jet-A-3602 and Jet-A-4658 appear to contain much higher concentrations of heavier components. This can be shown by examining the total area of chromatographic peaks that elute subsequent to the emergence of n-tetradecane, for each sample. For Jet-A-3638, this comprises 2.47 % of the total peak areas, while for Jet-A-3602 and Jet-A-4658, this comprises 12.07 and 17.57 %, respectively. Note that these peak areas are the raw, uncalibrated values, and are used only for comparison among the three fluids.

The rather consistent difference in the distillation curves of Jet-A-3638 and the other two Jet-A fluids is not seen when one examines the behavior of S-8. With this fluid, the curve rises much more sharply than do the Jet-A curves. This is typically observed when a fluid has somewhat more volatile constituents that boil off in the early stages of the distillation curve measurement. While the fluid initially begins to vaporize at a relatively lower temperature (especially when compared to Jet-A-3602 and Jet-A-4658), by a distillate volume fraction of 45 %, the curve of this fluid is approaching those of Jet-A-3602 and Jet-A-4658. By a distillate volume fraction of 60 %, the curve of S-8 and those of Jet-A-3602 and Jet-A-4658 have essentially merged. Note that this is consistent with the onset behaviors and chromatographic analyses presented in the discussion of the initial temperatures.

The relationship between T_k and T_h is presented in Figure 22, in which both temperatures are presented for the data shown in Table 13. We note that T_k always leads T_h. This behavior is consistent with a complex mixture with a continually changing composition. Note that when these two temperatures converge, it is evidence of either a single component being generated (by vaporization) in the kettle, or the presence of an azeotrope that controls the composition of both phases. The absence of such a convergence can be interpreted as further evidence of the absence of azeotropic behavior. It is clear that an examination of the initial temperatures and the detailed structures of the distillation curves (presented in T_k and T_h) can serve as method to evaluate the loose specifications that can sometimes characterize gas turbine fuels.

For comparison, the distillation curve was measured for JP-8-3773, a sample of which was obtained directly from the flight line at Wright Patterson Air Force Base. The distillation curve was measured for six aliquots of this fluid. The initial temperatures for this fluid are provided in Table 14, while representative distillation curve measurements presented in T_k and T_h are provided in Table 15. A graphical depiction of the distillation curve is provided in Figure 23. Since this fluid has all the additives typically present in JP-8 relative to Jet-A, the very minor differences between JP-8 and Jet-A reflected in these distillation curves may be indicative of these additives. Additional work would be needed to confirm this, especially considering the wide specifications allowable for Jet-A and JP-8.

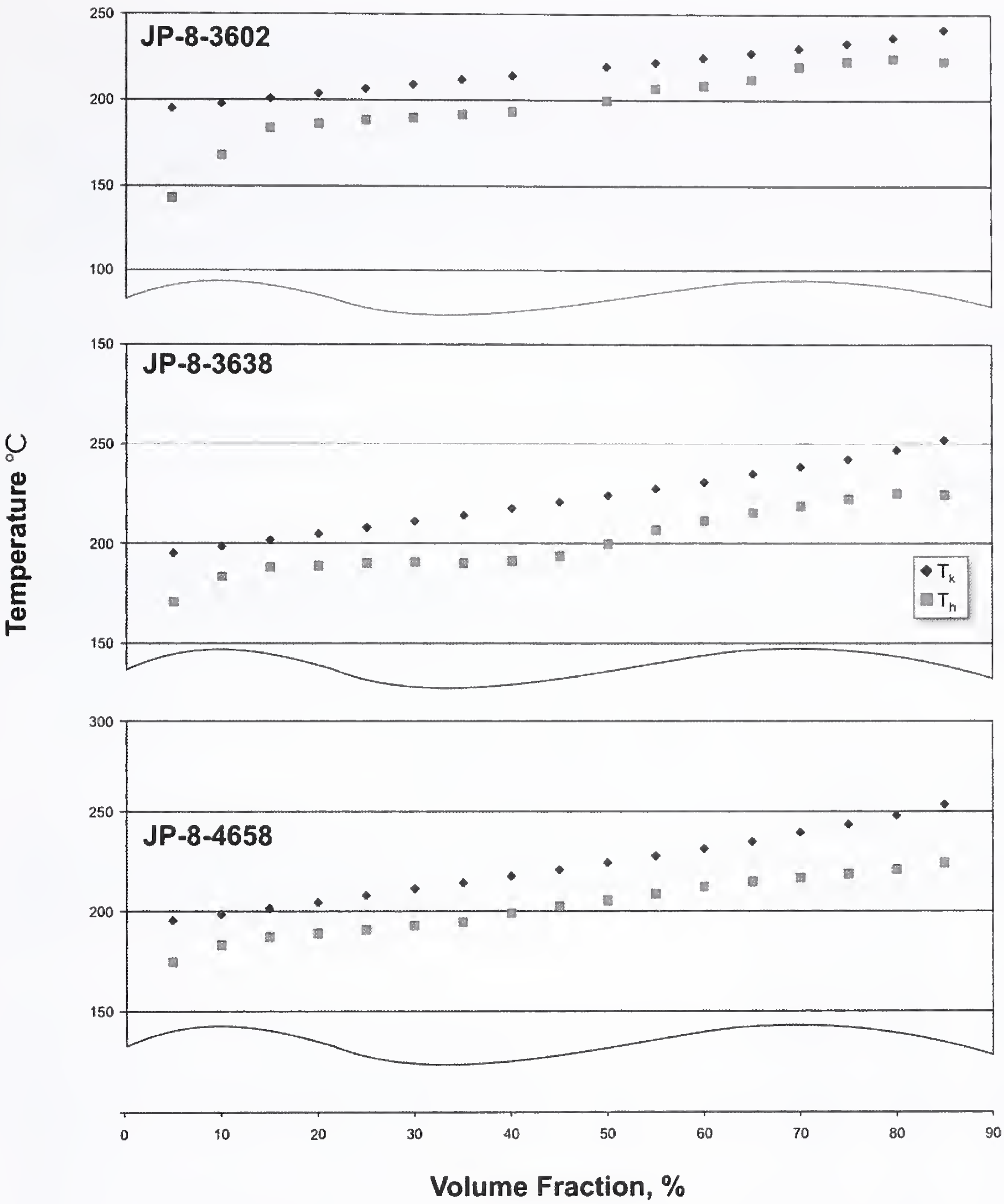

Figure 22: The relationship of T_k and T_h for the three Jet-A fluids measured in this work. The uncertainty is discussed in the text.

Table 14: A summary of the initial behavior of JP-8-3773, obtained directly from the flight line of Wright Patterson Air Force Base. In keeping with our advanced distillation curve protocol, the onset temperature is the temperature at which the first bubbles are observed. The sustained bubbling temperature is that at which the bubbling persists. The vapor rise temperature is that at which vapor is observed to rise into the distillation head, considered to be the initial boiling temperature of the fluid (highlighted in bold print). These temperatures have been corrected to 1 atm. with the Sidney Young equation. The uncertainties are discussed in the text.

Observed Temperature	**JP-8-3773, °C, 83.86 kPa**
onset	132.4
sustained	179.9
vapor rising	182.8

Table 15: Distillation curve data of JP-8-3773, obtained directly from the flight line of Wright Patterson Air Force Base. The temperatures have been adjusted to 1 atm with the modified Sydney Young equation; uncertainties are discussed in the text.

Distillate Volume Fraction, %	**JP-8-3773 83.86 kPa**	
	T_k, °C	T_h, °C
5	185.6	174.7
10	187.9	179.2
15	190.3	182.2
20	192.7	184.8
25	195.1	186.7
30	197.6	185.1
35	200.4	188.7
40	203.3	194.1
45	206.1	196.2
50	209.3	199.9
55	213.5	201.2
60	216.4	203.8
65	220.6	209.4
70	224.8	212.1
75	229.4	215.8
80	234.6	219.3
85	240.3	225.5

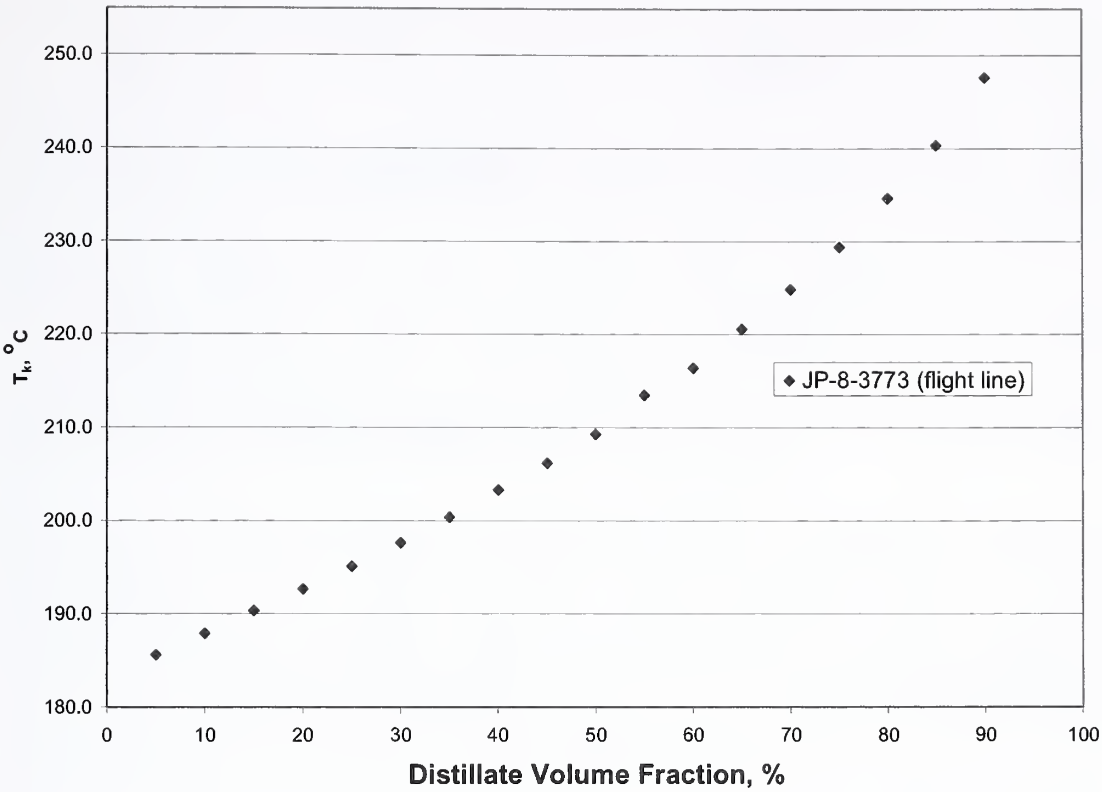

Figure 23: Distillation curve of JP-8-3773, obtained directly from the flight line of Wright Patterson Air Force Base. The temperatures have been adjusted to 1 atm with the modified Sydney Young equation; uncertainties are discussed in the text.

While the gross examination of the distillation curves is instructive and valuable for many design purposes, the composition channel of the advanced approach can provide even greater understanding and information content. One can sample and examine the individual fractions as they emerge from the condenser, as discussed in the introduction. Following the analytical procedure described, samples were collected and prepared for analysis. Chemical analyses of each fraction were done by gas chromatography with flame ionization detection and mass spectrometric detection. Representative chromatograms (measured by flame ionization detection) for each fraction of Jet-A-4658 are shown in Figure 24. The time axis is from 0 to 12 minutes for each chromatogram, and the abundance axis is presented in arbitrary units of area counts. It is clear that although there are many peaks on each chromatogram (30 – 40 major peaks, and 60 – 80 minor and trace peaks), these chromatograms are much simpler than those of the neat fluids, which can contain 300 - 400 peaks. At the very start of each chromatogram is the solvent front, which does not interfere with the sample. One can follow the progression of the chromatograms in Figure 24 as the distillate fraction becomes richer in the heavier components. This figure illustrates just one chemical analysis strategy that can be applied to the distillate fractions. It is possible to use any analytical technique that is applicable to solvent born liquid samples that might be desirable for a given application.

Figure 24: Chromatograms of distillate fractions of a typical Jet-A sample, in this case Jet-A-4658, presented in arbitrary units of intensity (from a flame ionization detector) plotted against time. One can see the solvent peaks very early in the chromatograms. The details of the chromatography are discussed in the text.

The distillate fractions of the three Jet-A samples and the S-8 sample were examined for hydrocarbon types by use of a mass spectrometric classification method summarized in ASTM Method D-2789[33]. In this method, one uses mass spectrometry (or gas chromatography – mass spectrometry) to characterize hydrocarbon samples into six types. The six types or families are paraffins, monocycloparaffins, dicycloparaffins, alkylbenzenes (or aromatics), indanes and tetralins (grouped as one classification), and naphthalenes. Although the method is specified only for application to low olefinic gasolines, and is subject to numerous interferences and uncertainties, it is of practical relevance to many complex fluid analyses, and is often applied to gas turbine fuels, rocket propellants and missile fuels. For the hydrocarbon type analysis of the distillate fraction samples, 1 µL injections were made into the GC-MS. Because of this consistent injection volume, no corrections were needed for sample volume.

The results of these hydrocarbon type analyses for the Jet-A and S-8 samples are presented in Tables 16a to 16e, and plotted in Figure 25. The first line in each of the tables reports the results of the analysis as applied to the entire sample (called the composite) rather than to distillate fractions. The data listed in this line are actually an average of two separate determinations; one done with a neat sample of the fuel (that is, with no added solvent) and the other with the sample in n-hexane. The volume of the neat sample was 0.2 µL, and only these mass spectra were corrected for sample volume. All of the distillate fractions presented in the table were measured in the same way as the composite (m/z range from 15 to 550 relative molecular mass units gathered in scanning mode, each spectrum corrected by subtracting trace air and water peaks).

In general, the hydrocarbon type fractions for the composite (the first row in each table) are consistent with the compositions obtained for the distillate fractions (the remaining rows of each table). Thus, taking the S-8 fluid as an example, the paraffin fraction for the composite sample was found to be 80.0 percent, while that of the distillate fractions ranged from 79.1 to 87.8. We have noted, however, that with the composite samples (which naturally produce a much more complex total ion chromatogram), one obtains many more non-integral m/z peaks on the mass spectrum. Thus, for a distillate fraction, one might obtain a peak at m/z = 43.0, while for the composite one might obtain m/z = 43.0, 43.15, etc., despite the resolution of the instrument being only 1 unit of mass. Our practice has been to round the fractional masses to the nearest integral mass, a practice that can sometimes cause bias. This is an unavoidable vagary of the instrument that can potentially be remedied with a higher resolution mass spectrometer. We maintain that the comparability among the distillate fractions is not affected by this characteristic, although the intercomparability between the distillate fractions and the composite should be approached with a bit more caution.

Table 16: Summary of the results of hydrocarbon family calculations based on the method of ASTM D-2789. The first three tables are for the individual lots of Jet-A, while the last is for the synthetic S-8.

Table 16a: Jet-A-3602:

Distillate Volume Fraction, %	Paraffins Vol %	Monocyclo-paraffins Vol %	Dicyclo-paraffins Vol %	Alkyl-aromatics Vol %	Indanes and Tetralins Vol %	Naphth-alenes Vol %
composite	*36.0*	*26.9*	*4.5*	*20.6*	*6.9*	*1.7*
0.025	25.5	30.3	6.1	34.7	2.9	0.4
10	27.5	27.0	7.4	33.2	4.3	0.7
20	27.5	26.7	10.4	28.4	5.9	1.0
30	28.2	26.6	10.8	27.0	6.3	1.1
35	30.0	26.4	9.6	26.4	6.5	1.2
40	29.1	26.6	11.6	24.3	7.0	1.4
45	30.1	26.9	11.0	23.4	7.2	1.5
50	32.9	26.6	8.8	22.8	7.4	1.5
60	28.9	26.8	13.3	19.9	9.0	2.1
70	31.0	28.3	12.4	17.1	9.1	2.2
80	31.5	29.0	12.8	14.0	10.0	2.8
Residue	34.3	32.5	13.9	6.8	7.9	4.5

Table 16b: Jet-A-3638:

Distillate Volume Fraction, %	Paraffins Vol %	Monocyclo-paraffins Vol %	Dicyclo-paraffins Vol %	Alkyl-aromatics Vol %	Indanes and Tetralins Vol %	Naphth-alenes Vol %
composite	*49.6*	*24.9*	*7.4*	*12.5*	*2.9*	*2.8*
0.025	36.9	30.0	6.2	24.6	1.3	1.0
10	42.6	26.1	4.2	25.0	0.9	1.3
20	45.4	25.0	4.1	23.3	0.8	1.4
30	42.2	26.6	6.7	21.0	1.7	1.9
35	42.9	26.4	7.1	19.1	1.8	2.6
40	41.0	26.7	8.4	19.5	2.2	2.2
45	40.9	27.0	9.0	18.5	2.4	2.3
50	42.0	27.0	8.7	17.6	2.3	2.5
60	42.5	27.3	9.0	15.8	2.5	2.9
70	44.8	27.4	8.1	13.7	2.5	3.5
80	44.6	27.6	9.5	11.1	2.9	4.3
Residue	43.2	27.7	12.0	3.9	3.1	10.1

Table 16c: Jet-A-4658:

Distillate Volume Fraction, %	Paraffins Vol %	Monocyclo-paraffins Vol %	Dicyclo-paraffins Vol %	Alkyl-aromatics Vol %	Indanes and Tetralins Vol %	Naphth-alenes Vol %
composite	*46.5*	*22.5*	*5.4*	*18.4*	*4.5*	*2.4*
0.025	40.4	27.3	3.4	27.3	1.2	0.5
10	39.8	25.1	4.5	27.2	2.6	0.8
20	41.2	24.6	4.4	25.6	3.1	1.1
30	40.9	25.2	5.8	22.1	4.3	1.6
35	43.2	24.5	4.3	21.9	4.2	1.8
40	43.3	25.3	4.8	20.0	4.6	2.0
45	41.7	25.9	6.4	18.7	5.0	2.3
50	42.9	25.8	5.6	18.1	5.1	2.4
60	43.1	26.4	6.7	15.0	5.9	2.9
70	43.8	27.1	7.4	11.8	6.3	3.6
80	48.7	29.9	7.0	6.3	4.6	3.3
Residue	49.7	31.9	7.0	3.4	3.4	4.5

Table 16d: S-8:

Distillate Volume Fraction, %	Paraffins Vol %	Monocyclo-paraffins Vol %	Dicyclo-paraffins Vol %	Alkyl-aromatics Vol %	Indanes and Tetralins Vol %	Naphth-alenes Vol %
composite	*80.0*	*17.3*	*0.9*	*0.1*	*0*	*1.9*
0.025	79.1	18.4	0.1	1.8	0.0	0.6
10	81.2	16.4	0.0	1.9	0.0	0.5
20	81.0	18.0	0.1	0.0	0.0	0.9
30	80.8	17.9	0.3	0.0	0.0	1.1
35	82.0	16.8	0.1	0.0	0.0	1.1
40	85.8	13.7	0.0	0.0	0.0	0.5
45	87.8	11.9	0.0	0.0	0.0	0.3
50	85.3	13.8	0.0	0.0	0.0	0.9
60	85.1	13.9	0.0	0.0	0.0	1.1
70	85.1	13.7	0.0	0.0	0.0	1.2
80	83.6	15.0	0.0	0.0	0.0	1.4
Residue	84.8	14.7	0.0	0.0	0.0	0.5

Table 16e: JP-8 3773:

Distillate Volume Fraction, %	Paraffins Vol %	Monocyclo-paraffins Vol %	Dicyclo-paraffins Vol %	Alkyl-aromatics Vol %	Indanes and Tetralins Vol %	Naphth-alenes Vol %
0.025	40.8	30.3	11.4	16.8	0.5	0.3
10	49.0	27.0	2.3	20.7	0.7	0.3
20	45.9	28.1	4.7	18.0	1.9	1.3
30	47.4	27.4	3.6	19.2	1.5	1.0
35	48.6	26.8	3.1	19.4	1.3	0.7
40	52.1	24.8	2.1	18.8	1.2	0.9
45	57.6	21.8	1.0	18.4	0.2	1.0
50	56.1	23.5	1.6	17.0	0.8	1.1
60	57.2	23.5	1.7	14.9	1.0	1.8
70	61.4	22.2	1.0	11.0	1.7	2.6
80	56.3	26.6	2.5	8.0	2.5	4.0
Residue	56.0	30.9	4.0	1.2	0.5	7.3

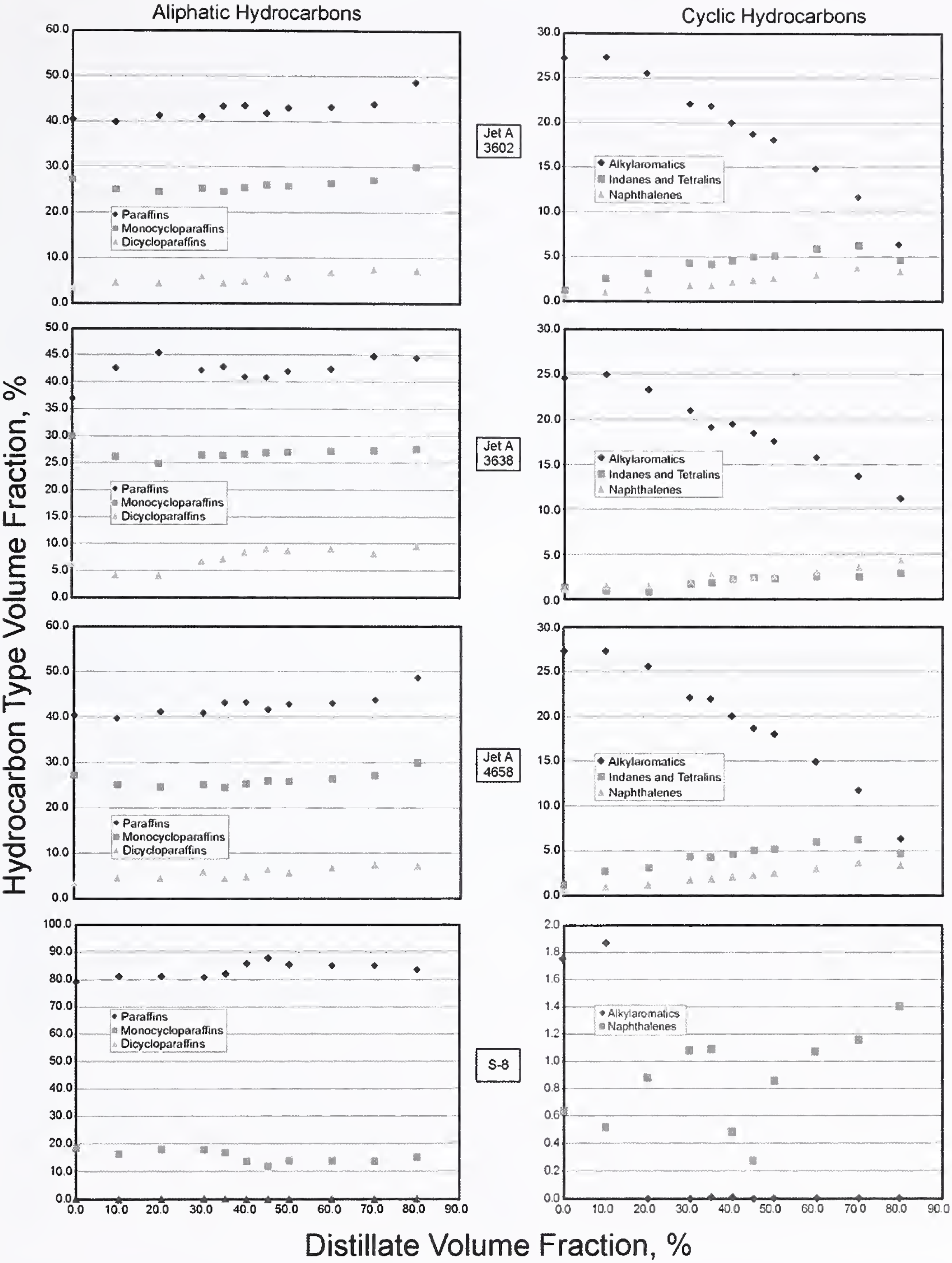

Figure 25: A plot of the hydrocarbon types resulting from the ASTM D-2789 analysis performed on Jet-A-3602, Jet-A-3638, Jet-A-4658 and S-8. The left side of the figure presents the aliphatic constituents, while the right side presents the cyclic constituents. The uncertainties are discussed in the text.

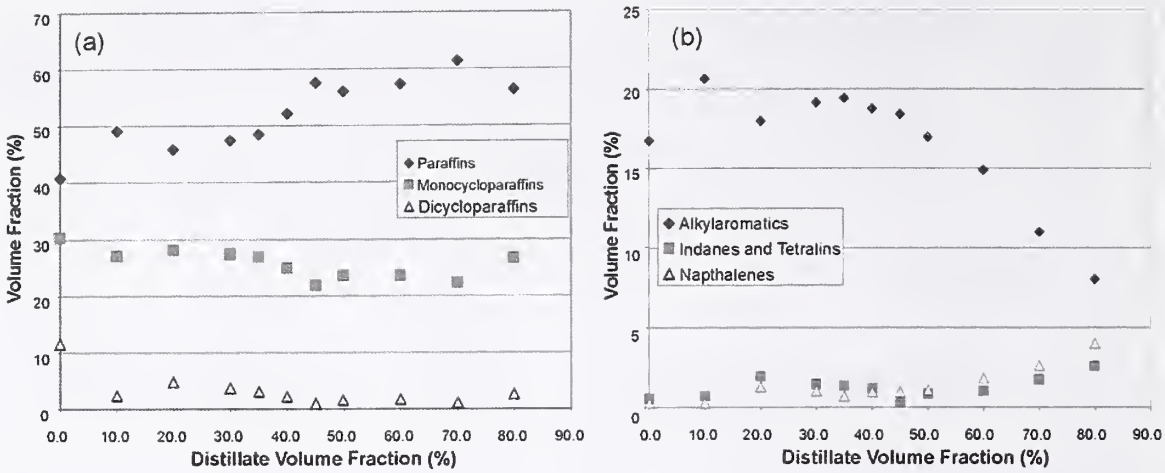

Figure 26: A plot of the hydrocarbon types resulting from the ASTM D-2789 analysis performed on JP-8-3773. The left side of the figure presents the aliphatic constituents, while the right side presents the cyclic constituents. The uncertainties are discussed in the text.

The distribution of hydrocarbon type as a function of distillate fraction is particularly instructive among the different Jet-A samples and with reference to Jet-A as compared to the synthetic S-8. We note from the data of Table 16a – 16d that Jet-A-3638 and Jet-A-4658 have very similar hydrocarbon family distributions. Moreover, the paraffin fractions of these fluids are significantly higher than those of Jet-A-3602. We also note that for Jet-A-3638 and Jet-A-4658, the alkylaromatic content is relatively close, while for the Jet-A-3602 it is much higher. This behavior is in striking contrast to the behavior apparent on the distillation curves, in which the curves of Jet-A-3602 and Jet-A-4658 appeared to be very similar, and the curve for Jet-A-3638 was at a lower temperature. This observation illustrates the importance of the composition channel of our distillation curve approach. Note also that this does not represent an inconsistency, since it is clear that differing distributions of hydrocarbon types can give rise to different volatilities. Despite having very similar volatility characteristics, Jet-A-3602 and Jet-A-4658 are very different chemically, a fact that would not be noted without the composition channel.

As a function of distillate volume fraction, one can see from Figure 25 that in general for the Jet-A fluids, the paraffin, monocycloparaffin and dicycloparaffin content remains essentially constant or increases very slightly. The alkylaromatic content decreases markedly, while the concentrations of the indanes and tetralins, and the naphthalenics compounds increase.

When one compares the Jet-A fluids with the synthetic S-8, the difference is very significant. Table 16d clearly shows that S-8 has a much higher paraffinic content than any of the Jet-A fluids. Moreover, the alkylaromatic content is very small. Indeed, the only aromatic constituents could be found in the very early emerging distillate fractions.

These two facts are consistent with the composition of the synthetic feed stock of this fluid, namely natural gas. One also notes the clear similarity of the Jet-A fluids with the JP-8, shown in Figure 26. These fluids differ only in the additive package, and this is not reflected in the volatility behavior.

Distillation Curve Measurements on Mixtures of Jet-A and S-8:

As part of the property measurement program for aviation fuels, we prepared mixtures of Jet-A-4658 with S-8, and made distillation curve measurements to examine how the properties would change.[18, 29] Mixtures were prepared volumetrically in mixing cylinders at ambient temperature and pressure. Mixtures of 25/75, 50/50, and 75/25 (vol/vol) of Jet-A with S-8 were prepared and measured. Typically, between four and six distillation curves were measured for each mixture with the same apparatus and approach as has been described in detail earlier. In Table 17, we present the initial boiling behaviors for these mixtures and in Table 18 we present the distillation curve data. The distillation curves are presented graphically in Figure 27.

Table 17: A summary of the initial behavior of the three mixtures (prepared on a volume basis) of Jet-A + S-8, along with the initial behaviors of the starting fluids. The temperatures have been adjusted to 1 atm with the modified Sydney Young equation; uncertainties are discussed in the text.

Observed Temperature, °C	**S-8 83.27 kPa**	**75/25 S-8 + Jet-A 83.67 kPa**	**50/50 S-8 + Jet-A 82.38 kPa**	**25/75 S-8 + Jet-A 83.51 kPa**	**Jet-A 4658 83.63 kPa**
Onset	163.0	160.9	154.9	161.8	139.9
Sustained	168.6	182.3	178.6	178.9	185.6
Vapor Rising	**181.9**	**184.8**	**186.6**	**189.1**	**190.5**

These data are presented graphically in Figure 27.

As with the as-delivered aviation fuels discussed earlier, the composition explicit data channel provided a chemical analysis of selected distillate cuts. The hydrocarbon type breakdown resulting from the ASTM D-2789 type analysis is presented in Table 19a-d and Figure 28.

Table 18: Representative distillation curve data for the three mixtures (prepared on a volume basis) of S-8 + Jet-A-4658 measured in this work. For reference, the data for the individual components, S-8 and Jet-A-4658, are also provided. These data are plotted in Figure 27. The temperatures have been adjusted to 1 atm with the modified Sydney Young equation; uncertainties are discussed in the text.

Distillate Volume Fraction, %	**S-8 83.27 kPa**		**75/25 S-8 + Jet-A 83.67 kPa**		**50/50 S-8 + Jet-A 82.38 kPa**		**25/75 S-8 + Jet-A 83.51 kPa**		**Jet-A 4658 83.63 kPa**	
	T_k, °C	T_h, °C	T_k, °C	T_h, °C	T_k, °C	T_h, °C	T_k, °C	T_h, °C	T_k, °C	T_h, °C
5	183.6	169.2	187.8	176.2	190.2	171.0	193.3	174.7	195.4	174.7
10	185.0	173.9	190.4	180.8	192.8	177.6	196.4	183.2	198.5	183.3
15	187.7	179.1	193.4	184.2	196.4	183.6	199.9	189.3	201.5	187.0
20	190.2	173.6	196.3	182.6	199.9	188.9	202.9	192.5	204.7	189.1
25	193.0	175.5	199.8	187.5	203.5	184.8	206.6	189.6	208.1	190.6
30	196.2	181.9	202.8	191.1	206.3	192.7	209.6	193.1	211.3	192.8
35	199.5	187.7	206.3	194.5	209.9	193.3	212.7	196.5	214.3	194.6
40	202.9	192.0	209.9	197.5	213.3	193.8	216.4	198.4	217.6	199.1
45	207.1	196.2	213.7	198.1	217.1	196.6	219.7	200.8	220.7	202.6
50	211.0	200.3	218.2	205.8	221.1	201.8	223.6	207.2	224.2	205.4
55	215.3	205.2	222.4	210.4	225.1	206.9	227.5	211.3	227.6	208.6
60	219.6	209.3	226.6	214.6	228.8	208.1	231.0	215.3	231.2	212.4
65	224.2	213.6	231.6	219.4	233.3	213.1	235.0	219.9	234.7	214.9
70	229.4	219.1	236.4	225.8	237.2	220.0	238.9	221.2	239.4	216.6
75	235.2	224.3	241.8	229.2	242.3	221.1	243.7	226.5	243.3	218.7
80	240.1	231.4	247.5	233.9	247.2	225.8	248.8	233.2	247.9	220.8
85	246.8	236.8	255.4	240.7	254.4	231.5	255.7	235.5	253.6	224.1

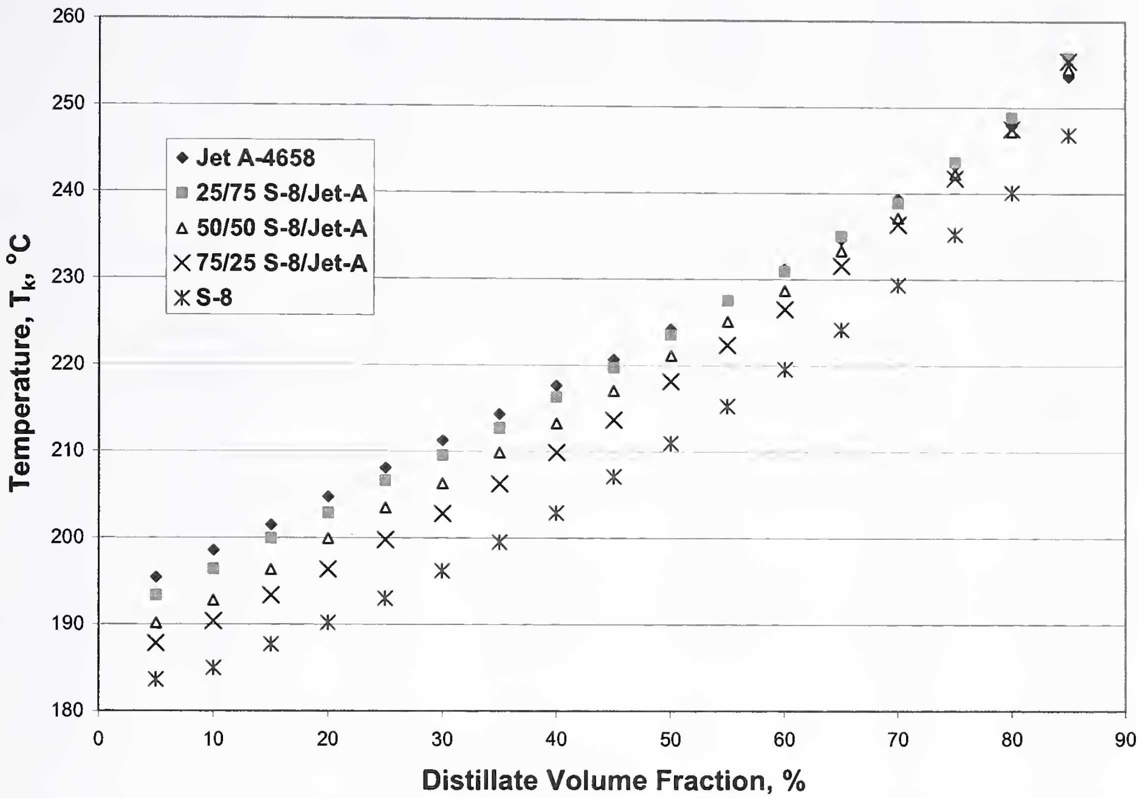

Figure 27: Representative distillation curves for each of the three mixtures of S-8 + Jet-A-4658 (prepared on a volume basis) measured in this work. For reference, the curves for the individual components, S-8 and Jet-A-4658, are also provided. The temperatures have been adjusted to 1 atm with the modified Sydney Young equation; uncertainties are discussed in the text.

Table 19: Summary of the results of hydrocarbon family calculations based on the method of ASTM D-2789.

Table 19a: 75/25 S-8/Jet-A:

Distillate Volume Fraction, %	Paraffins Vol %	Monocyclo-paraffins Vol %	Dicyclo-paraffins Vol %	Alkyl-aromatics Vol %	Indanes and Tetralins Vol %	Naphth-alenes Vol %
composite	*75.3*	*22.0*	*0.4*	*1.2*	*0.2*	*0.9*
0.025	74.1	22.2	0.2	3.2	0.0	0.3
10	77.9	19.1	0.1	2.6	0.0	0.3
20	76.7	19.9	0.1	2.9	0.0	0.4
30	76.6	20.0	0.1	2.9	0.0	0.5
35	77.6	19.2	0.1	2.7	0.0	0.4
40	75.9	20.1	0.3	3.0	0.2	0.6

45	81.5	16.3	0.0	1.9	0.0	0.2
50	78.1	18.9	0.2	2.3	0.1	0.5
60	78.9	18.4	0.1	1.7	0.1	0.7
70	72.3	21.6	1.4	2.3	0.8	1.6
80	84.1	15.2	0.0	0.1	0.0	0.6
Residue	83.1	16.5	0.0	0.0	0.0	0.4

Table 19b: 50/50 S-8/Jet-A:

Distillate Volume Fraction, %	Paraffins Vol %	Monocyclo-paraffins Vol %	Dicyclo-paraffins Vol %	Alkyl-aromatics Vol %	Indanes and Tetralins Vol %	Naphth-alenes Vol %
composite	*56.4*	*23.5*	*6.1*	*8.8*	*3.0*	*2.3*
0.025	66.7	22.9	0.4	9.6	0.0	0.3
10	67.9	23.3	0.5	7.8	0.2	0.4
20	68.9	22.3	0.5	7.7	0.2	0.4
30	70.6	20.9	0.3	7.4	0.3	0.5
35	70.8	20.9	0.4	7.1	0.3	0.4
40	71.3	20.5	0.4	6.8	0.4	0.6
45	73.2	19.3	0.3	6.4	0.3	0.5
50	71.9	20.0	0.4	6.2	0.8	0.8
60	70.4	21.7	0.6	5.2	1.1	1.0
70	73.1	20.9	0.4	3.4	1.0	1.2
80	76.9	19.4	0.1	1.5	0.9	1.2
Residue	72.3	25.9	0.3	0.2	0.1	1.2

Table 19c: 25/75 S-8/Jet-A:

Distillate Volume Fraction, %	Paraffins Vol %	Monocyclo-paraffins Vol %	Dicyclo-paraffins Vol %	Alkyl-aromatics Vol %	Indanes and Tetralins Vol %	Naphth-alenes Vol %
composite	*48.1*	*25.6*	*8.5*	*11.3*	*4.2*	*2.5*
0.025	56.2	26.5	1.3	15.3	0.4	0.3
10	56.7	25.1	1.5	15.5	0.7	0.5
20	60.9	22.3	0.7	15.2	0.5	0.5
30	56.7	24.6	1.8	14.5	1.6	0.8
35	58.1	23.9	1.5	14.1	1.6	0.8
40	57.0	24.9	1.9	13.3	1.9	1.0
45	59.9	23.6	1.2	12.4	1.8	1.1
50	60.7	23.4	1.3	11.5	1.9	1.2
60	65.5	21.5	0.6	8.9	2.1	1.4
70	62.4	24.9	1.3	6.9	2.6	1.9
80	59.9	27.1	2.7	4.9	3.0	2.4
Residue						

Table 19d: Jet-A 4658:

Distillate Volume Fraction, %	Paraffins Vol %	Monocyclo-paraffins Vol %	Dicyclo-paraffins Vol %	Alkyl-aromatics Vol %	Indanes and Tetralins Vol %	Naphth-alenes Vol %
composite	*46.5*	*22.5*	*5.4*	*18.4*	*4.5*	*2.4*
0.025	40.4	27.3	3.4	27.3	1.2	0.5
10	39.8	25.1	4.5	27.2	2.6	0.8
20	41.2	24.6	4.4	25.6	3.1	1.1
30	40.9	25.2	5.8	22.1	4.3	1.6
35	43.2	24.5	4.3	21.9	4.2	1.8
40	43.3	25.3	4.8	20.0	4.6	2.0
45	41.7	25.9	6.4	18.7	5.0	2.3
50	42.9	25.8	5.6	18.1	5.1	2.4
60	43.1	26.4	6.7	15.0	5.9	2.9
70	43.8	27.1	7.4	11.8	6.3	3.6
80	48.7	29.9	7.0	6.3	4.6	3.3
Residue	49.7	31.9	7.0	3.4	3.4	4.5

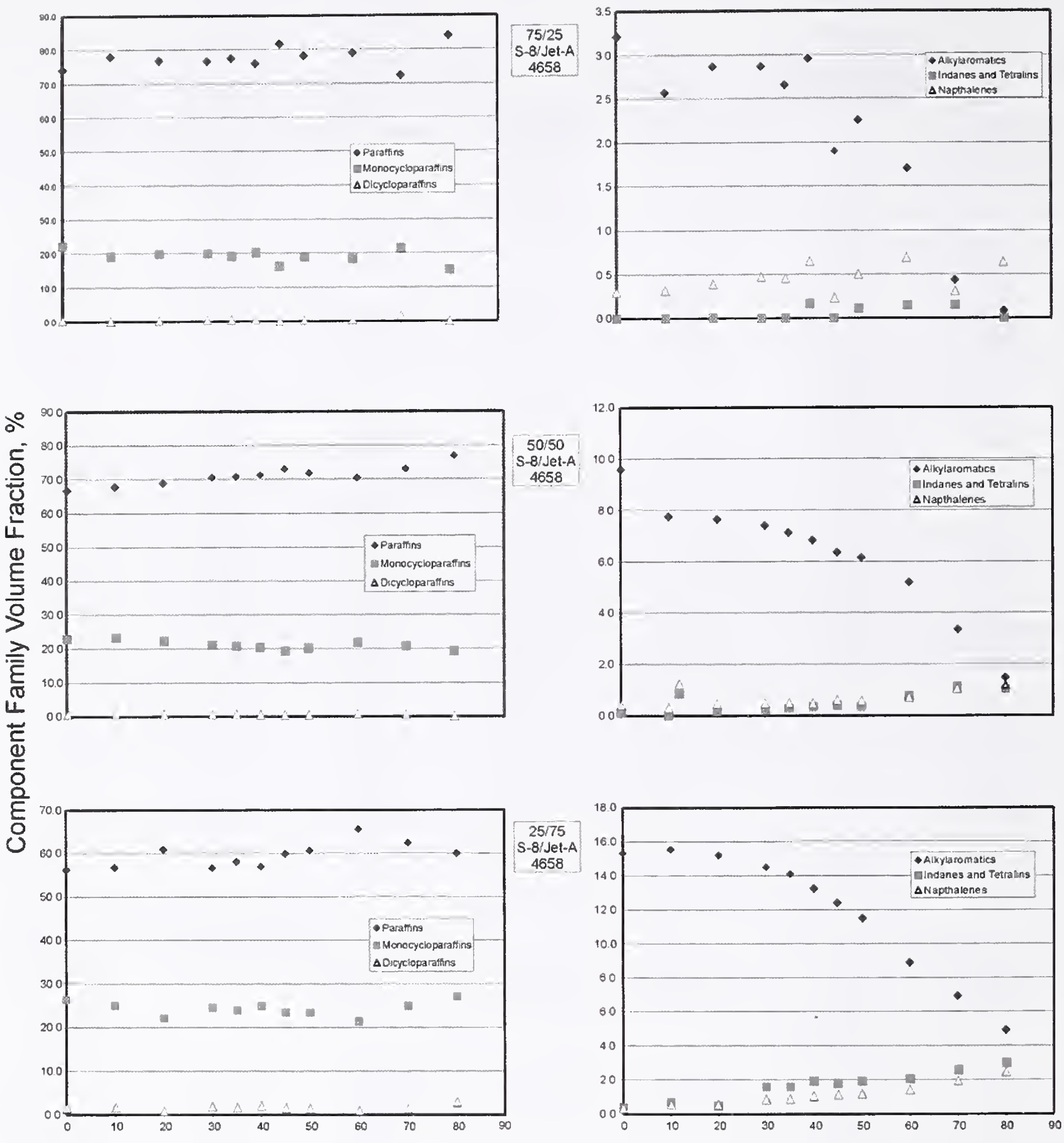

Figure 28: A plot of the hydrocarbon types resulting from the ASTM D-2789 analysis performed on three mixtures of Jet-A-4658 and S-8. The left side of the figure presents the aliphatic constituents, while the right side presents the cyclic constituents. The uncertainties are discussed in the text.

Density Measurements of Compressed Liquid Jet-A, JP-8 and S-8:

The apparatus described earlier[8] for the compressed liquid density measurements on methyl- and propylcyclohexane was used to measure the compressed liquid density for Jet-A, JP-8 and S-8.[34] these measurements were made over the temperature range of 270 K to 470 K and pressures to 50 MPa. We present these measurements in Tables 20 – 24, and Figures 29 - 33, which follow. Tables list compressed liquid densities of Jet-A-3602, Jet-A-3638 and Jet-A-4658, JP-8-3773 and S-8, respectively. The density measurements have an estimated uncertainty of 1.0 kg/m^3 which includes the uncertainty in temperature 0.03 K and pressure 0.01 MPa.

Table 20: Compressed liquid densities of Jet-A-3602

Temperature [K]	Pressure [MPa]	Density [kg/m^3]	Temperature [K]	Pressure [MPa]	Density [kg/m^3]
270.00	30.770	850.67	350.00	4.478	779.05
270.00	25.606	848.05	350.00	3.281	777.97
270.00	20.663	845.45	350.00	2.206	776.98
270.00	15.925	842.88	350.00	1.095	775.96
270.00	11.308	840.33	350.00	0.555	775.45
270.00	6.061	837.34	370.00	31.929	787.77
270.00	4.923	836.67	370.00	25.704	783.1
270.00	3.742	835.97	370.00	20.960	779.32
270.00	2.518	835.23	370.00	16.114	775.28
270.00	1.319	834.5	370.00	11.021	770.78
290.00	31.570	838.62	370.00	5.488	765.55
290.00	25.590	835.32	370.00	4.354	764.42
290.00	20.646	832.51	370.00	3.228	763.26
290.00	15.967	829.77	370.00	2.162	762.17
290.00	11.244	826.91	370.00	1.090	761.05
290.00	5.974	823.62	370.00	0.589	760.53
290.00	4.779	822.84	390.00	31.808	775.21
290.00	3.597	822.07	390.00	25.736	770.24
290.00	2.423	821.3	390.00	21.012	766.14
310.00	31.934	826.25	390.00	16.082	761.61
310.00	25.572	822.48	390.00	10.876	756.53
310.00	20.758	819.48	390.00	5.410	750.78
310.00	16.002	816.47	390.00	4.277	749.52
310.00	11.259	813.25	390.00	3.239	748.33
310.00	5.758	809.31	390.00	2.163	747.09
310.00	4.674	808.51	390.00	1.255	746.02
310.00	3.500	807.64	390.00	0.659	745.28
310.00	2.304	806.68	410.00	31.747	762.63
310.00	1.720	806.26	410.00	25.841	757.38
330.00	31.638	812.73	410.00	21.034	752.82
330.00	25.593	808.76	410.00	16.035	747.76

330.00	20.805	805.48	410.00	10.778	742.08
330.00	16.082	802.16	410.00	5.328	735.65
330.00	11.178	798.57	410.00	4.280	734.33
330.00	5.765	794.42	410.00	3.214	732.96
330.00	4.589	793.49	410.00	2.188	731.62
330.00	3.413	792.51	410.00	1.192	730.3
330.00	2.261	791.6	430.00	31.659	749.98
330.00	1.117	790.66	430.00	25.868	744.41
330.00	0.541	790.17	430.00	21.038	739.44
330.00	31.638	812.73	430.00	15.970	733.81
330.00	25.593	808.76	430.00	10.651	727.39
330.00	20.805	805.48	430.00	5.308	720.29
330.00	16.082	802.16	430.00	4.261	718.79
330.00	11.178	798.57	430.00	3.256	717.32
330.00	5.765	794.42	430.00	2.238	715.8
330.00	4.589	793.49	430.00	1.268	714.32
330.00	3.413	792.51	450.00	31.665	737.5
330.00	2.261	791.6	450.00	25.929	731.48
330.00	1.117	790.66	450.00	21.027	725.93
330.00	0.541	790.17	450.00	15.895	719.64
330.00	31.754	812.44	450.00	10.572	712.47
330.00	25.641	808.49	450.00	5.322	704.58
330.00	20.858	805.25	450.00	4.325	702.96
330.00	16.096	801.93	450.00	3.330	701.3
330.00	11.218	798.35	450.00	2.348	699.62
330.00	5.762	794.14	450.00	1.337	697.84
330.00	4.609	793.21	470.00	31.633	725.24
330.00	3.479	792.29	470.00	26.007	718.83
330.00	2.315	791.32	470.00	20.979	712.57
330.00	1.147	790.36	470.00	15.846	705.6
330.00	0.599	789.91	470.00	10.523	697.56
350.00	32.101	800.44	470.00	5.390	688.79
350.00	25.629	795.91	470.00	4.388	686.91
350.00	20.879	792.4	470.00	3.404	685.03
350.00	16.081	788.74	470.00	2.407	683.05
350.00	11.105	784.74	470.00	1.434	681.07
350.00	5.598	780.05			

Table 21: Compressed liquid densities of Jet-A-3638

Temperature [K]	Pressure [MPa]	Density [kg/m^3]	Temperature [K]	Pressure [MPa]	Density [kg/m^3]
270.00	30.045	827.22	370.00	5.088	740.92
270.00	25.104	824.61	370.00	4.066	739.86
270.00	20.148	821.94	370.00	3.048	738.73

270.00	15.155	819.16	370.00	2.027	737.62
270.00	10.128	816.28	370.00	1.006	736.51
270.00	5.058	813.27	390.00	30.017	750.57
270.00	4.043	812.66	390.00	25.082	746.29
270.00	3.019	812.03	390.00	20.133	741.78
270.00	1.994	811.40	390.00	15.156	736.95
270.00	0.971	810.76	390.00	10.141	731.75
290.00	30.076	814.46	390.00	5.075	726.09
290.00	25.140	811.64	390.00	4.062	724.89
290.00	20.184	808.73	390.00	3.047	723.67
290.00	15.201	805.71	390.00	2.027	722.43
290.00	10.175	802.55	390.00	1.006	721.17
290.00	5.109	799.24	410.00	30.020	738.07
290.00	4.093	798.55	410.00	25.080	733.42
290.00	3.072	797.86	410.00	20.128	728.48
290.00	2.050	797.16	410.00	15.147	723.16
290.00	1.028	796.45	410.00	10.131	717.38
310.00	30.079	801.81	410.00	5.066	711.01
310.00	25.134	798.75	410.00	4.050	709.64
310.00	20.174	795.57	410.00	3.029	708.24
310.00	15.187	792.26	410.00	2.008	706.81
310.00	10.159	788.77	410.00	0.985	705.36
310.00	5.090	785.07	430.00	30.008	725.40
310.00	4.075	784.30	430.00	25.067	720.35
310.00	3.053	783.51	430.00	20.112	714.93
310.00	2.031	782.73	430.00	15.129	709.05
310.00	1.009	781.93	430.00	10.111	702.59
330.00	30.043	788.77	430.00	5.049	695.38
330.00	25.110	785.43	430.00	4.028	693.82
330.00	20.156	781.94	430.00	3.009	692.23
330.00	15.172	778.28	430.00	1.984	690.59
330.00	10.148	774.42	430.00	0.960	688.90
330.00	5.084	770.34	450.00	29.957	712.75
330.00	4.069	769.48	450.00	25.019	707.25
330.00	3.050	768.61	450.00	20.073	701.31
330.00	2.031	767.74	450.00	15.096	694.80
330.00	1.010	766.85	450.00	10.079	687.56
350.00	30.055	775.92	450.00	5.020	679.37
350.00	25.118	772.28	450.00	4.003	677.59
350.00	20.163	768.48	450.00	2.985	675.74
350.00	15.181	764.48	450.00	1.964	673.84
350.00	10.159	760.23	450.00	0.939	671.87
350.00	5.092	755.70	470.00	29.936	700.26

350.00	4.073	754.74	470.00	25.002	694.28
350.00	3.059	753.78	470.00	20.051	687.75
350.00	2.037	752.80	470.00	15.078	680.53
350.00	1.017	751.81	470.00	10.062	672.39
370.00	30.053	763.11	470.00	4.997	662.99
370.00	25.114	759.16	470.00	3.981	660.92
370.00	20.159	755.03	470.00	2.957	658.76
370.00	15.176	750.65	470.00	1.941	656.54
370.00	10.157	745.98	470.00	0.922	654.23

Table 22: Compressed liquid densities of Jet-A-4658

Temperature [K]	Pressure [MPa]	Density [kg/m^3]	Temperature [K]	Pressure [MPa]	Density [kg/m^3]
270.00	30.015	837.52	370.00	4.010	751.72
270.00	25.010	834.93	370.00	3.011	750.70
270.00	20.002	832.28	370.00	2.006	749.66
270.00	15.007	829.56	370.00	1.013	748.61
270.00	10.007	826.76	370.00	0.499	748.06
270.00	4.999	823.86	390.00	30.008	761.81
270.00	4.010	823.27	390.00	25.012	757.62
270.00	2.999	822.67	390.00	20.018	753.21
270.00	2.005	822.07	390.00	15.007	748.52
270.00	1.007	821.46	390.00	10.009	743.54
270.00	0.508	821.16	390.00	5.007	738.18
290.00	30.001	824.78	390.00	4.008	737.05
290.00	25.002	822.00	390.00	3.008	735.91
290.00	19.999	819.11	390.00	2.001	734.74
290.00	15.002	816.15	390.00	1.009	733.55
290.00	10.004	813.08	390.00	0.503	732.93
290.00	5.005	809.92	410.00	30.004	749.32
290.00	4.005	809.26	410.00	25.012	744.75
290.00	3.009	808.60	410.00	20.013	739.94
290.00	2.009	807.94	410.00	15.000	734.79
290.00	1.010	807.27	410.00	10.009	729.27
290.00	0.507	806.93	410.00	5.007	723.26
310.00	30.013	811.77	410.00	4.008	721.99
310.00	25.011	808.70	410.00	3.008	720.69
310.00	20.013	805.54	410.00	2.002	719.37
310.00	15.010	802.27	410.00	1.013	718.05
310.00	10.009	798.88	410.00	0.516	717.36
310.00	5.006	795.34	430.00	29.999	736.86
310.00	3.999	794.61	430.00	25.007	731.93
310.00	3.006	793.87	430.00	20.009	726.68
310.00	2.009	793.13	430.00	15.005	721.00

310.00	1.009	792.38	430.00	10.023	714.88
310.00	0.508	792.00	430.00	5.012	708.11
330.00	29.999	799.02	430.00	4.017	706.66
330.00	25.010	795.71	430.00	3.004	705.17
330.00	20.007	792.28	430.00	2.010	703.68
330.00	15.012	788.72	430.00	1.012	702.13
330.00	10.013	784.99	430.00	0.508	701.34
330.00	5.006	781.09	450.00	29.996	724.54
330.00	4.015	780.29	450.00	25.003	719.19
330.00	3.008	779.48	450.00	20.006	713.44
330.00	2.005	778.65	450.00	15.002	707.18
330.00	1.014	777.81	450.00	10.002	700.31
330.00	0.513	777.39	450.00	5.018	692.70
350.00	29.995	786.59	450.00	4.002	691.02
350.00	25.009	783.03	450.00	3.010	689.34
350.00	20.013	779.32	450.00	2.013	687.61
350.00	15.006	775.43	450.00	1.006	685.81
350.00	10.005	771.34	450.00	0.508	684.89
350.00	5.012	767.03	470.00	29.993	712.33
350.00	4.010	766.12	470.00	25.002	706.52
350.00	3.005	765.20	470.00	20.012	700.22
350.00	2.007	764.28	470.00	15.020	693.32
350.00	1.005	763.34	470.00	10.016	685.63
350.00	0.504	762.87	470.00	5.005	676.93
370.00	30.005	774.22	470.00	4.002	675.03
370.00	25.011	770.35	470.00	3.001	673.07
370.00	20.009	766.29	470.00	2.008	671.06
370.00	15.010	762.03	470.00	1.014	668.98
370.00	10.015	757.53	470.00	0.514	667.89
370.00	5.007	752.72			

Table 23: Compressed-liquid densities of JP-8-3773

Temperature [K]	Pressure [MPa]	Density [kg/m^3]	Temperature [K]	Pressure [MPa]	Density [kg/m^3]
270.0	39.99	833.2	330.0	5.01	771.1
270.0	35.00	830.8	330.0	4.00	770.3
270.0	30.00	828.2	330.0	2.99	769.4
270.0	24.99	825.6	330.0	1.99	768.6
270.0	20.00	823.0	330.0	1.00	767.7
270.0	15.00	820.2	330.0	0.49	767.2
270.0	10.00	817.4	350.0	40.00	783.9
270.0	4.99	814.4	350.0	35.00	780.5
270.0	3.99	813.8	350.0	30.00	777.0
270.0	3.00	813.2	350.0	25.00	773.3

270.0	1.99	812.6	350.0	19.99	769.5
270.0	1.01	812.0	350.0	15.00	765.5
270.0	0.50	811.6	350.0	9.99	761.2
290.0	39.97	821.0	350.0	5.00	756.7
290.0	35.00	818.3	350.0	3.99	755.8
290.0	30.00	815.6	350.0	2.99	754.8
290.0	24.98	812.7	350.0	2.00	753.9
290.0	20.00	809.8	350.0	1.01	752.9
290.0	15.00	806.8	350.0	0.50	752.4
290.0	9.99	803.7	370.0	40.00	771.8
290.0	5.00	800.4	370.0	35.00	768.2
290.0	3.99	799.7	370.0	30.00	764.4
290.0	3.00	799.0	370.0	24.99	760.4
290.0	1.99	798.4	370.0	19.99	756.2
290.0	1.00	797.7	370.0	14.99	751.7
290.0	0.49	797.3	370.0	10.01	747.0
310.0	39.99	808.7	370.0	4.99	742.0
310.0	35.00	805.7	370.0	3.99	740.9
310.0	29.99	802.7	370.0	2.99	739.9
310.0	25.00	799.5	370.0	1.99	738.8
310.0	20.00	796.2	370.0	0.99	737.7
310.0	14.99	792.8	370.0	0.49	737.1
310.0	10.00	789.3	390.0	39.99	759.9
310.0	4.99	785.7	390.0	35.00	755.9
310.0	4.00	784.9	390.0	29.99	751.8
310.0	3.00	784.2	390.0	25.00	747.5
310.0	1.99	783.4	390.0	20.00	742.9
310.0	1.00	782.6	390.0	14.99	738.0
310.0	0.50	782.2	390.0	10.00	732.6
330.0	40.00	796.0	390.0	4.99	727.0
330.0	35.00	792.9	390.0	4.00	725.8
330.0	29.99	789.6	390.0	3.00	724.6
330.0	24.99	786.2	390.0	2.00	723.4
330.0	19.99	782.7	390.0	1.00	722.1
330.0	14.98	779.0	390.0	0.49	721.5
330.0	10.00	775.2	410.0	39.99	747.9
410.0	35.00	743.7	450.0	34.99	719.2
410.0	29.98	739.2	450.0	29.99	714.0
410.0	25.01	734.5	450.0	24.99	708.4
410.0	20.00	729.5	450.0	19.99	702.3
410.0	14.99	724.1	450.0	15.00	695.7
410.0	10.00	718.2	450.0	10.00	688.4
410.0	4.99	711.9	450.0	5.00	680.3
410.0	3.99	710.5	450.0	4.00	678.5
410.0	2.99	709.1	450.0	3.00	676.7
410.0	1.99	707.7	450.0	1.99	674.8

410.0	0.99	706.3	450.0	0.99	672.9
410.0	0.49	705.5	450.0	0.49	671.9
430.0	39.98	736.0	470.0	40.01	712.5
430.0	34.99	731.4	470.0	34.99	707.2
430.0	29.99	726.6	470.0	29.99	701.5
430.0	25.00	721.4	470.0	24.99	695.4
430.0	19.99	715.9	470.0	20.01	688.7
430.0	15.00	709.9	470.0	15.00	681.4
430.0	10.00	703.4	470.0	9.99	673.3
430.0	5.00	696.2	470.0	4.99	664.0
430.0	4.00	694.7	470.0	4.00	661.9
430.0	2.99	693.1	470.0	2.99	659.8
430.0	2.00	691.5	470.0	1.99	657.6
430.0	0.99	689.9	470.0	0.99	655.3
430.0	0.49	689.0	470.0	0.49	654.2
450.0	40.02	724.2			

Table 24: Compressed-liquid densities of S-8

Temperature [K]	Pressure [MPa]	Density [kg/m^3]	Temperature [K]	Pressure [MPa]	Density [kg/m^3]
270.0	30.09	786.2	330.0	1.01	725.1
270.0	25.15	783.6	330.0	0.51	724.7
270.0	20.20	780.9	350.0	30.01	735.5
270.0	15.21	778.1	350.0	25.01	731.7
270.0	10.19	775.1	350.0	20.01	727.7
270.0	5.12	772.1	350.0	15.00	723.5
270.0	4.10	771.4	350.0	10.01	719.1
270.0	3.07	770.8	350.0	5.00	714.3
270.0	2.05	770.1	350.0	4.01	713.4
270.0	1.02	769.5	350.0	3.01	712.3
270.0	0.51	769.1	350.0	2.00	711.3
290.0	30.04	773.6	350.0	1.01	710.3
290.0	25.10	770.7	350.0	0.50	709.8
290.0	20.14	767.7	370.0	30.02	723.2
290.0	15.15	764.6	370.0	25.02	719.0
290.0	10.13	761.3	370.0	20.01	714.7
290.0	5.06	757.8	370.0	15.02	710.1
290.0	4.05	757.1	370.0	10.00	705.1
290.0	3.02	756.4	370.0	5.01	699.9
290.0	2.00	755.6	370.0	4.01	698.8
290.0	0.97	754.9	370.0	3.01	697.6
290.0	0.46	754.5	370.0	2.00	696.4
310.0	29.97	760.5	370.0	1.01	695.3
310.0	25.03	757.3	370.0	0.50	694.7

310.0	20.07	754.0	390.0	30.02	711.0
310.0	15.09	750.6	390.0	25.00	706.5
310.0	10.07	747.0	390.0	20.01	701.7
310.0	5.00	743.1	390.0	15.01	696.6
310.0	3.98	742.3	390.0	10.00	691.1
310.0	2.96	741.5	390.0	5.00	685.2
310.0	1.94	740.7	390.0	4.00	683.9
310.0	0.92	739.8	390.0	3.00	682.6
310.0	0.40	739.4	390.0	2.01	681.3
310.0	2.99	741.4	390.0	1.00	680.0
310.0	2.01	740.5	390.0	0.50	679.3
310.0	1.01	739.7	410.0	30.01	698.7
310.0	0.51	739.3	410.0	25.01	693.8
330.0	30.00	747.9	410.0	20.01	688.6
330.0	25.01	744.4	410.0	15.00	683.0
330.0	20.01	740.8	410.0	10.01	676.9
330.0	15.01	737.0	410.0	5.00	670.1
330.0	10.01	733.0	410.0	4.00	668.7
330.0	5.01	728.7	410.0	3.00	667.2
330.0	4.01	727.9	410.0	2.01	665.7
330.0	3.01	727.0	410.0	1.00	664.1
330.0	2.01	726.1	410.0	0.50	663.3
430.0	29.99	686.4	450.0	4.00	636.9
430.0	25.02	681.1	450.0	3.00	634.9
430.0	20.00	675.3	450.0	2.01	632.9
430.0	15.00	669.1	450.0	1.01	630.8
430.0	10.01	662.2	450.0	0.50	629.7
430.0	5.00	654.6	470.0	30.01	662.2
430.0	4.01	653.0	470.0	25.01	655.9
430.0	3.01	651.3	470.0	20.01	649.0
430.0	2.00	649.5	470.0	15.01	641.3
430.0	1.01	647.7	470.0	10.01	632.6
430.0	0.49	646.8	470.0	5.01	622.7
450.0	30.02	674.3	470.0	4.02	620.5
450.0	25.01	668.4	470.0	3.01	618.1
450.0	20.02	662.1	470.0	2.00	615.7
450.0	15.00	655.2	470.0	1.00	613.2
450.0	10.00	647.5	470.0	0.50	611.9
450.0	5.01	638.8			

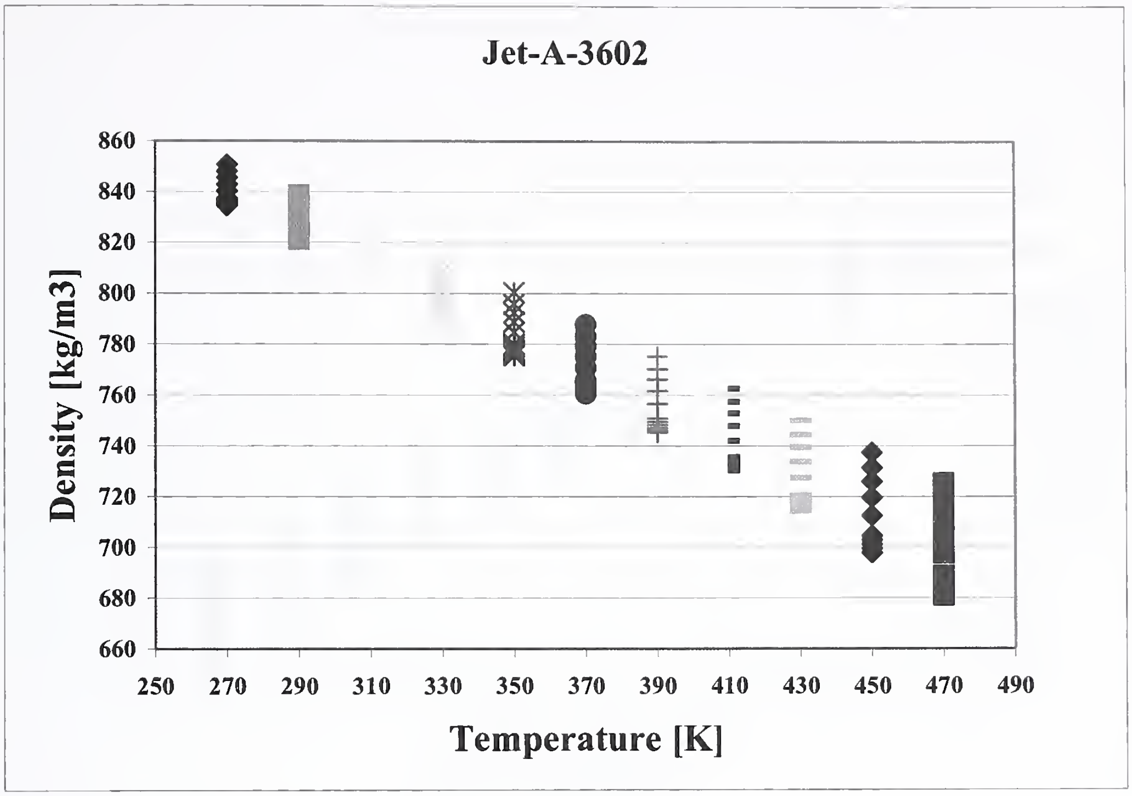

Figure 29: Compressed liquid densities of Jet A-3602.

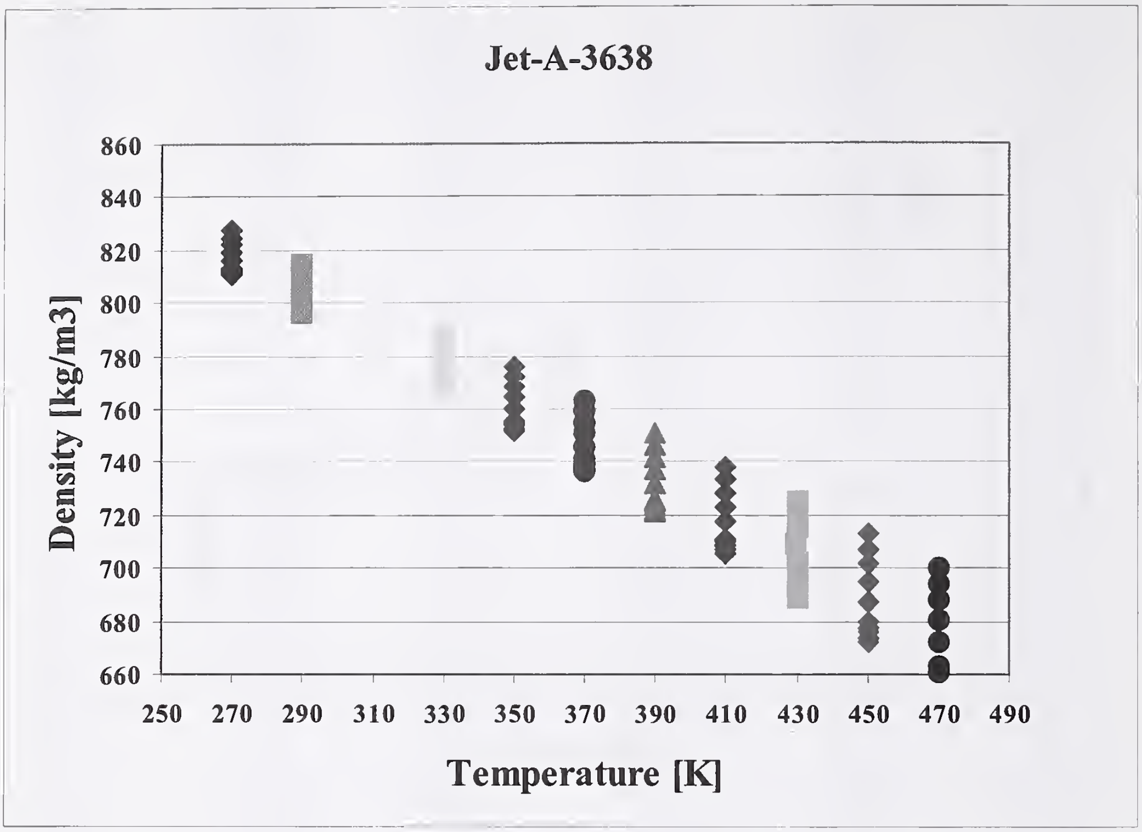

Figure 30: Compressed liquid densities of Jet A-3638.

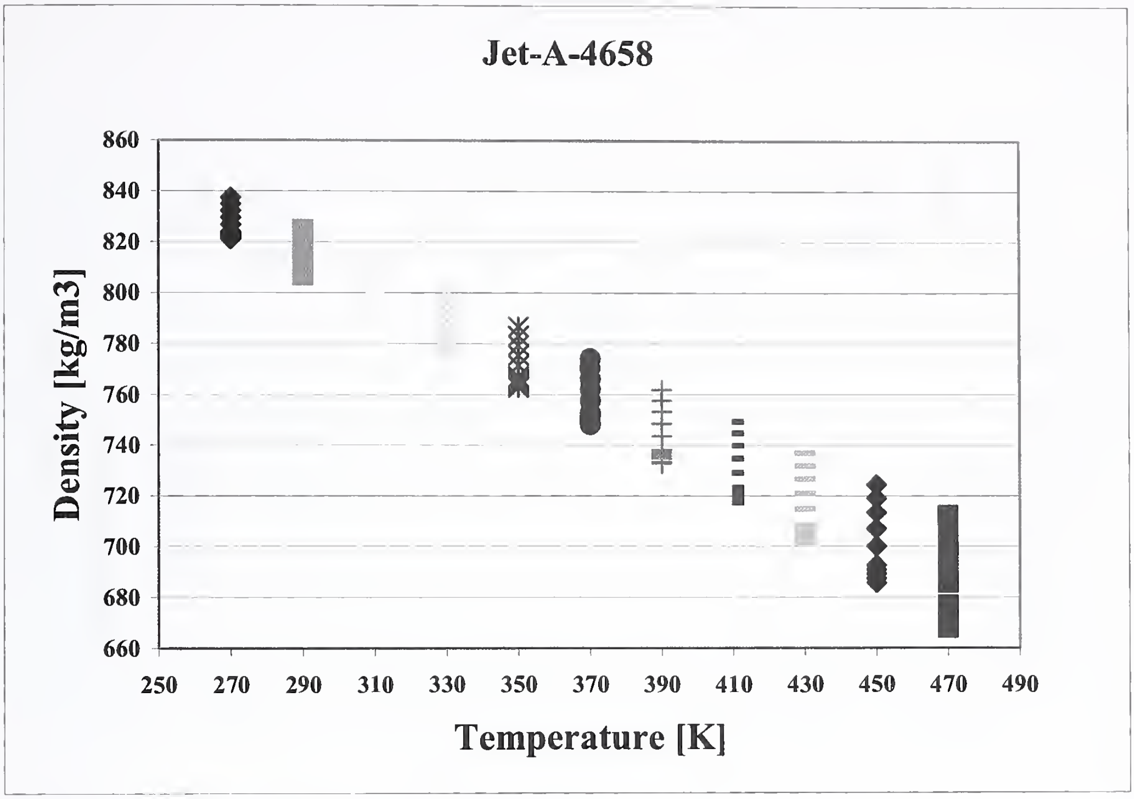

Figure 31: Compressed liquid densities of Jet A-3638.

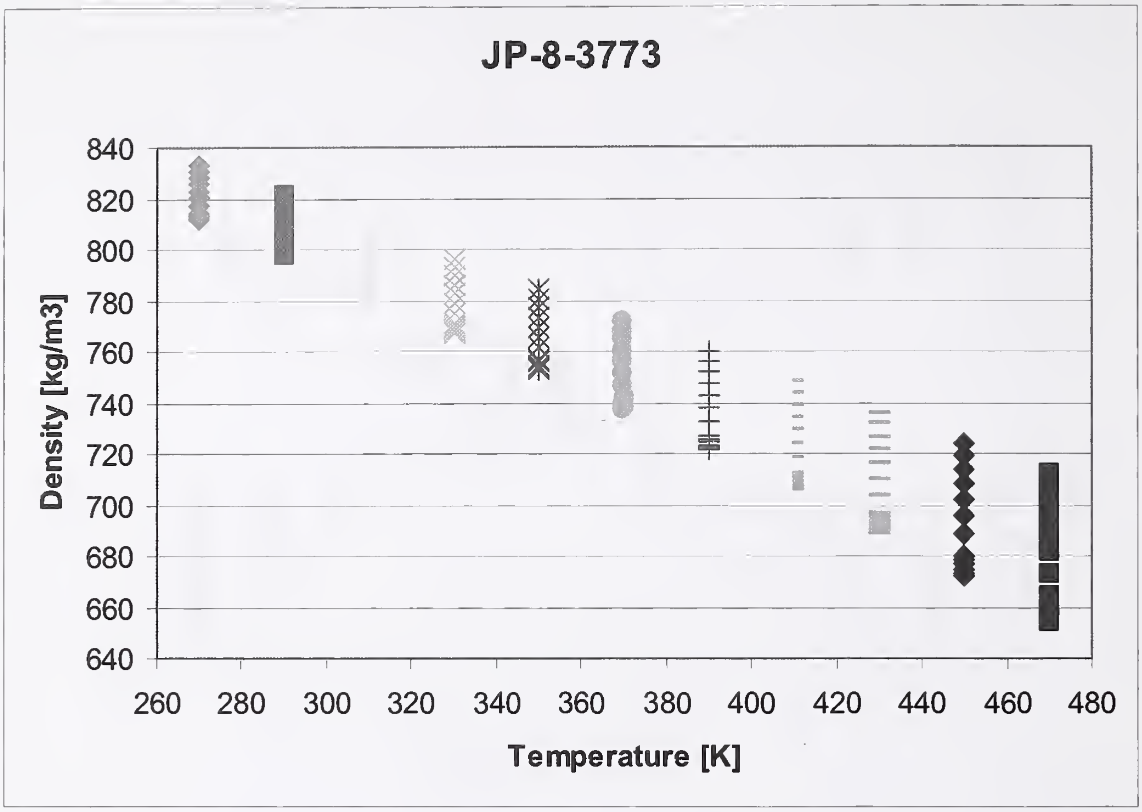

Figure 32: Compressed liquid densities of JP-8-3773.

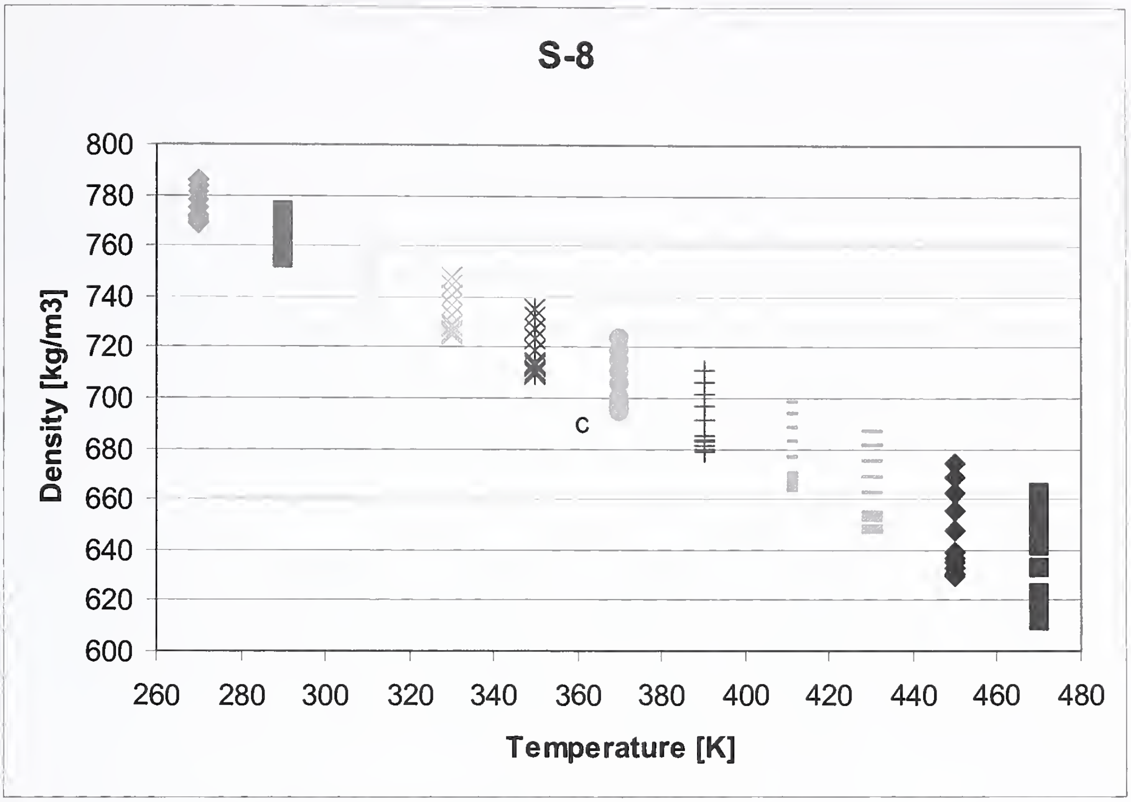

Figure 33: Compressed liquid densities of S-8.

Viscosity Measurements of Jet-A Fuels at Ambient Pressure:

The viscosities of two samples of Jet-A (3638 and 4658) was measured with a commercial viscodensimeter in the temperature range from 263.15 K to 373.15 K. The performance of the instrument hardware and firmware was examined by comparisons with certified viscosity standard liquids. The reference viscosities of two appropriate calibration liquids were reproduced by the instrument within 0.4 % and 0.8 %, respectively. Together, these two viscosity standards span the entire range of measured Jet-A fuel samples. The estimated uncertainty of the Jet-A fuel measurements reported here is deduced from this comparison. Above a viscosity of 0.94 mPa·s the reported uncertainty is 0.4 %; however, below this viscosity threshold the reported uncertainty is expanded to 1 % to match the more conservative manufacturer's estimate. We note that the reported uncertainty estimates are not derived from a strict statistical treatment. The measured absolute and kinematic viscosities of Jet-A-3638 and Jet-A-4658 are tabulated in Tables 25 and 26, respectively. Also included in Tables 25 and 26 are the measured densities and the estimated uncertainty value for each measured quantity. In addition to the tabulated data, the measured absolute and kinematic viscosities are illustrated in Figures 34 - 37.

Table 25: Viscosity Measurements for Jet-A-3638.

Temperature K	η mPa·s	u [η] mPa·s	ν $mm^2 \cdot s^{-1}$	u [ν] $mm^2 \cdot s^{-1}$	ρ $kg \cdot m^{-3}$	u [ρ] $kg \cdot m^{-3}$
373.150	0.47418	0.00474	0.64796	0.00648	731.78	0.51
368.150	0.49836	0.00498	0.67746	0.00678	735.64	0.50
363.150	0.52412	0.00524	0.70877	0.00709	739.46	0.50
358.150	0.55200	0.00552	0.74261	0.00743	743.32	0.50
353.150	0.58223	0.00582	0.77927	0.00779	747.14	0.50
348.150	0.61503	0.00615	0.81899	0.00819	750.94	0.50
343.150	0.65078	0.00651	0.86223	0.00862	754.74	0.50
338.150	0.68986	0.00690	0.90944	0.00910	758.54	0.50
333.150	0.73269	0.00733	0.96111	0.00961	762.34	0.50
328.150	0.77984	0.00780	1.0179	0.0102	766.10	0.50
323.150	0.83198	0.00832	1.0807	0.0046	769.90	0.50
318.150	0.88983	0.00890	1.1502	0.0049	773.64	0.50
313.150	0.95426	0.00392	1.2275	0.0052	777.38	0.50
308.150	1.0264	0.0042	1.3140	0.0056	781.14	0.50
303.150	1.1076	0.0046	1.4112	0.0060	784.90	0.50
298.150	1.1995	0.0050	1.5210	0.0065	788.62	0.50
293.150	1.3041	0.0054	1.6458	0.0071	792.36	0.50
288.150	1.4240	0.0059	1.7887	0.0077	796.10	0.50
283.150	1.5624	0.0065	1.9535	0.0084	799.82	0.50
278.150	1.7235	0.0072	2.1449	0.0093	803.56	0.50
273.150	1.9134	0.0081	2.3703	0.0104	807.26	0.50
268.150	2.1393	0.0090	2.6380	0.0116	810.96	0.51
263.150	2.4106	0.0102	2.9590	0.0130	814.68	0.51

Table 26: Viscosity Measurements for Jet-A-4658

Temperature K	η mPa·s	u [η] mPa·s	ν $mm^2 \cdot s^{-1}$	u [ν] $mm^2 \cdot s^{-1}$	ρ $kg \cdot m^{-3}$	u [ρ] $kg \cdot m^{-3}$
373.150	0.53287	0.00533	0.71680	0.00717	743.38	0.51
368.150	0.56121	0.00561	0.75113	0.00751	747.16	0.50
363.150	0.59165	0.00592	0.78785	0.00788	750.96	0.50
358.150	0.62466	0.00625	0.82765	0.00828	754.74	0.50
353.150	0.66055	0.00661	0.87086	0.00871	758.50	0.50
348.150	0.69968	0.00700	0.91789	0.00919	762.26	0.50
343.150	0.74245	0.00743	0.96926	0.00970	765.98	0.51
338.150	0.78941	0.00790	1.0256	0.0103	769.76	0.50
333.150	0.84115	0.00842	1.0876	0.0109	773.46	0.50
328.150	0.89844	0.00900	1.1561	0.0116	777.16	0.50
323.150	0.96220	0.00397	1.2322	0.0053	780.88	0.51
318.150	1.0335	0.0043	1.3172	0.0056	784.56	0.50
313.150	1.1136	0.0046	1.4126	0.0061	788.26	0.50
308.150	1.2041	0.0050	1.5203	0.0065	791.98	0.50
303.150	1.3070	0.0054	1.6426	0.0071	795.68	0.50
298.150	1.4249	0.0059	1.7825	0.0077	799.38	0.50
293.150	1.5608	0.0065	1.9436	0.0084	803.06	0.50
288.150	1.7188	0.0072	2.1306	0.0092	806.72	0.51
283.150	1.9043	0.0079	2.3498	0.0101	810.40	0.50
278.150	2.1239	0.0088	2.6089	0.0112	814.10	0.50
273.150	2.3878	0.0100	2.9199	0.0127	817.78	0.50
268.150	2.7078	0.0113	3.2966	0.0143	821.40	0.50
263.150	3.1011	0.0130	3.7586	0.0163	825.08	0.50

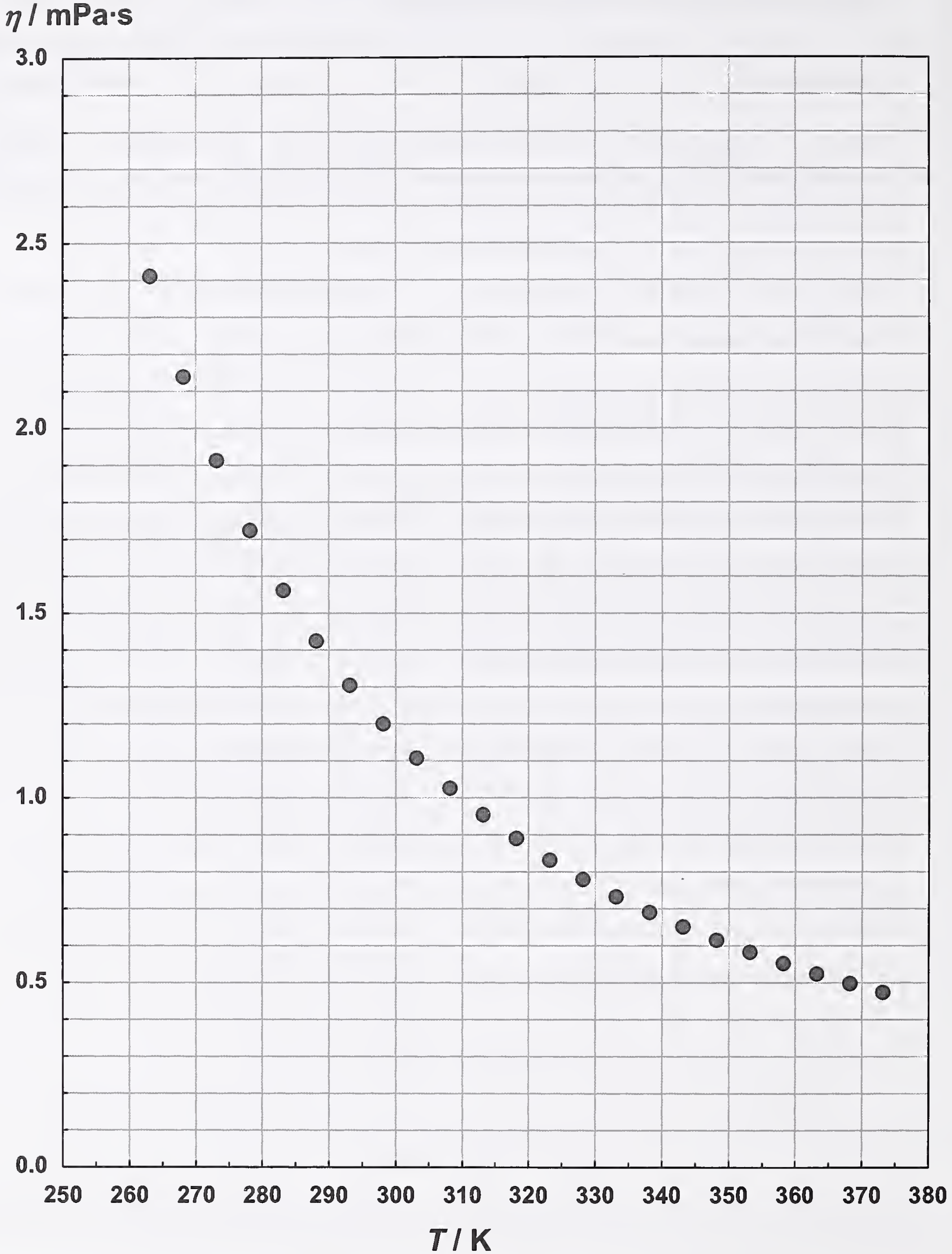

Figure 34: Measurements of the absolute viscosity of Jet-A-3638. The uncertainty is discussed in the text.

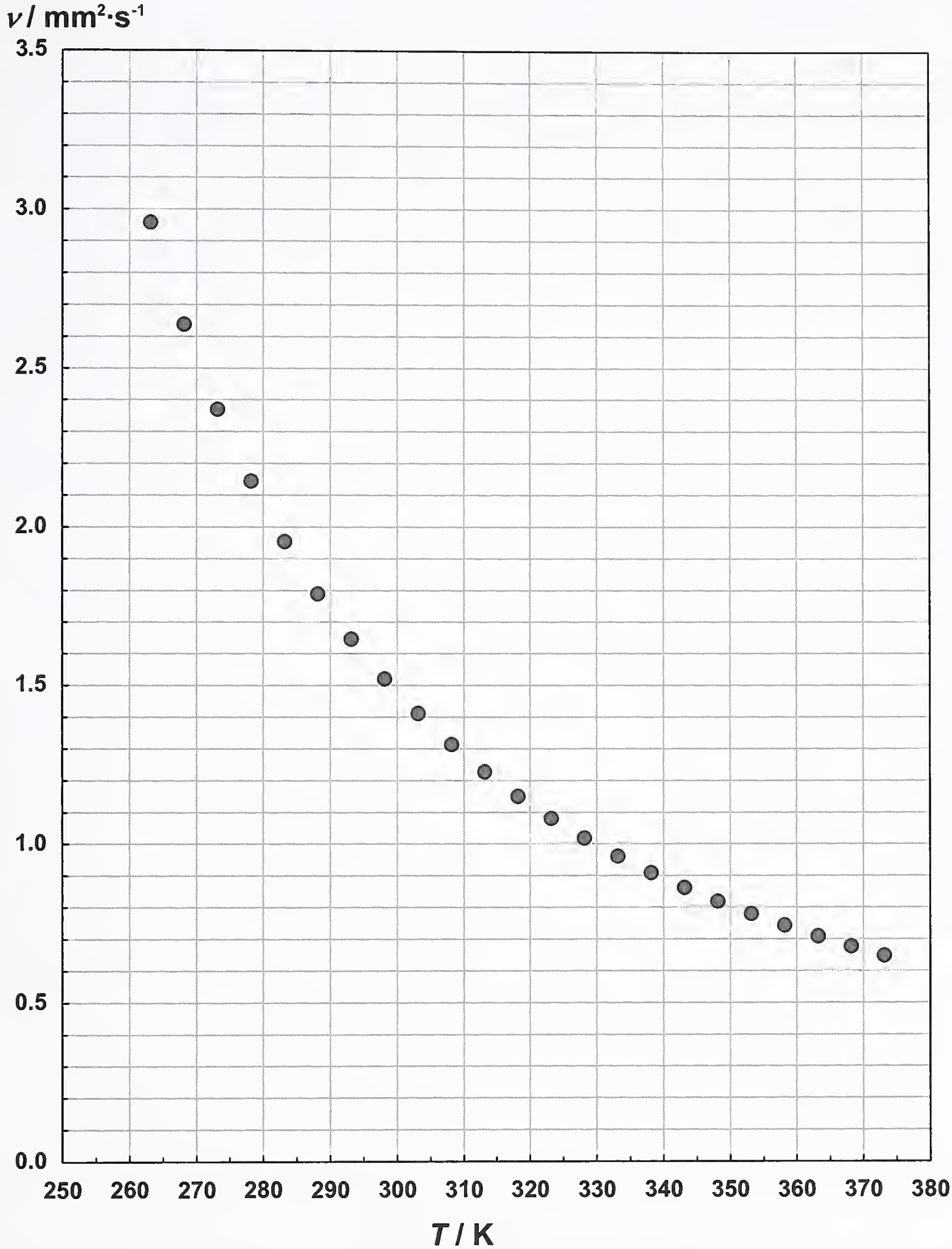

Figure 35: Measurements of the kinematic viscosity of Jet-A-3638. The uncertainty is discussed in the text.

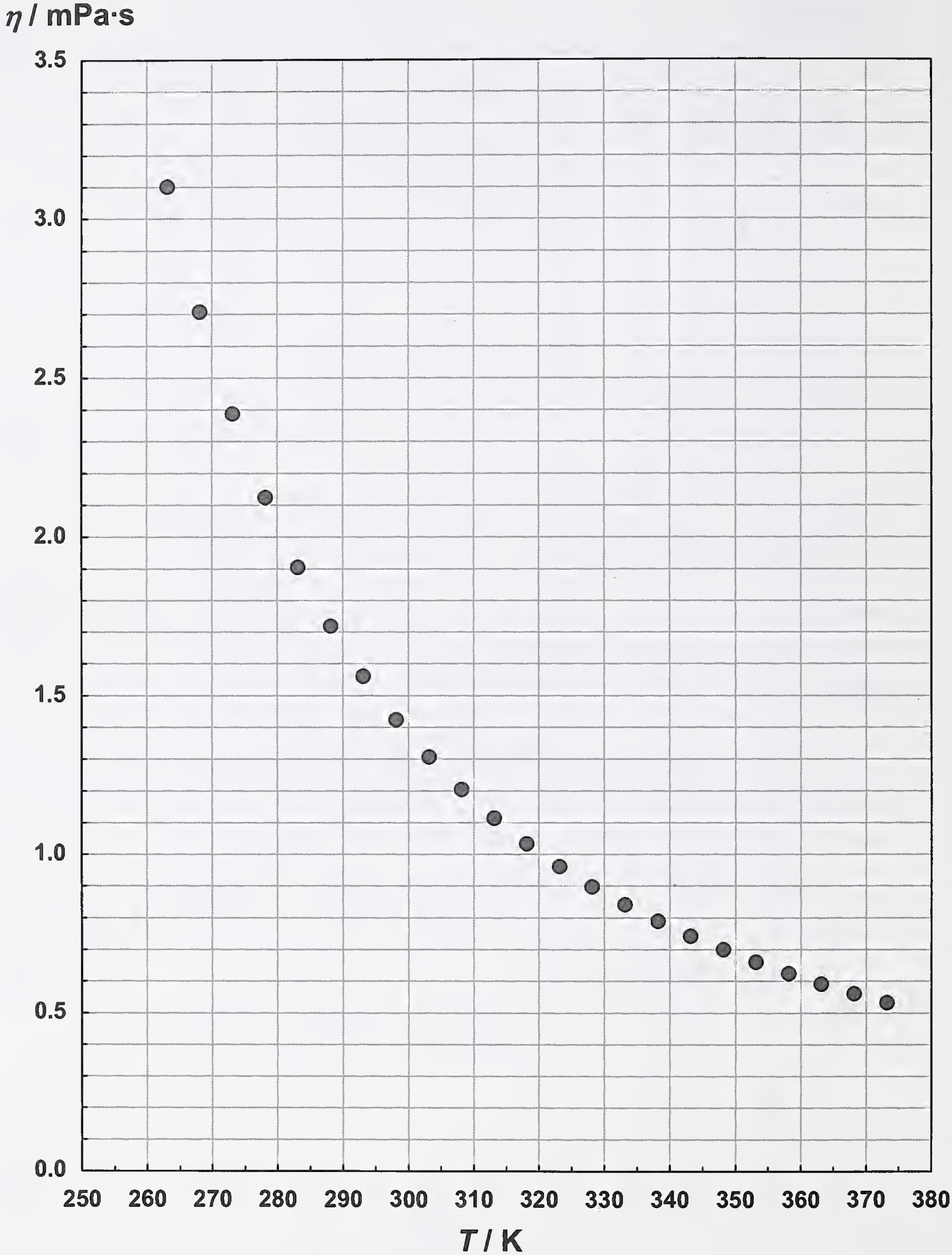

Figure 36: Measurements of the absolute viscosity of Jet-A-4648. The uncertainty is discussed in the text.

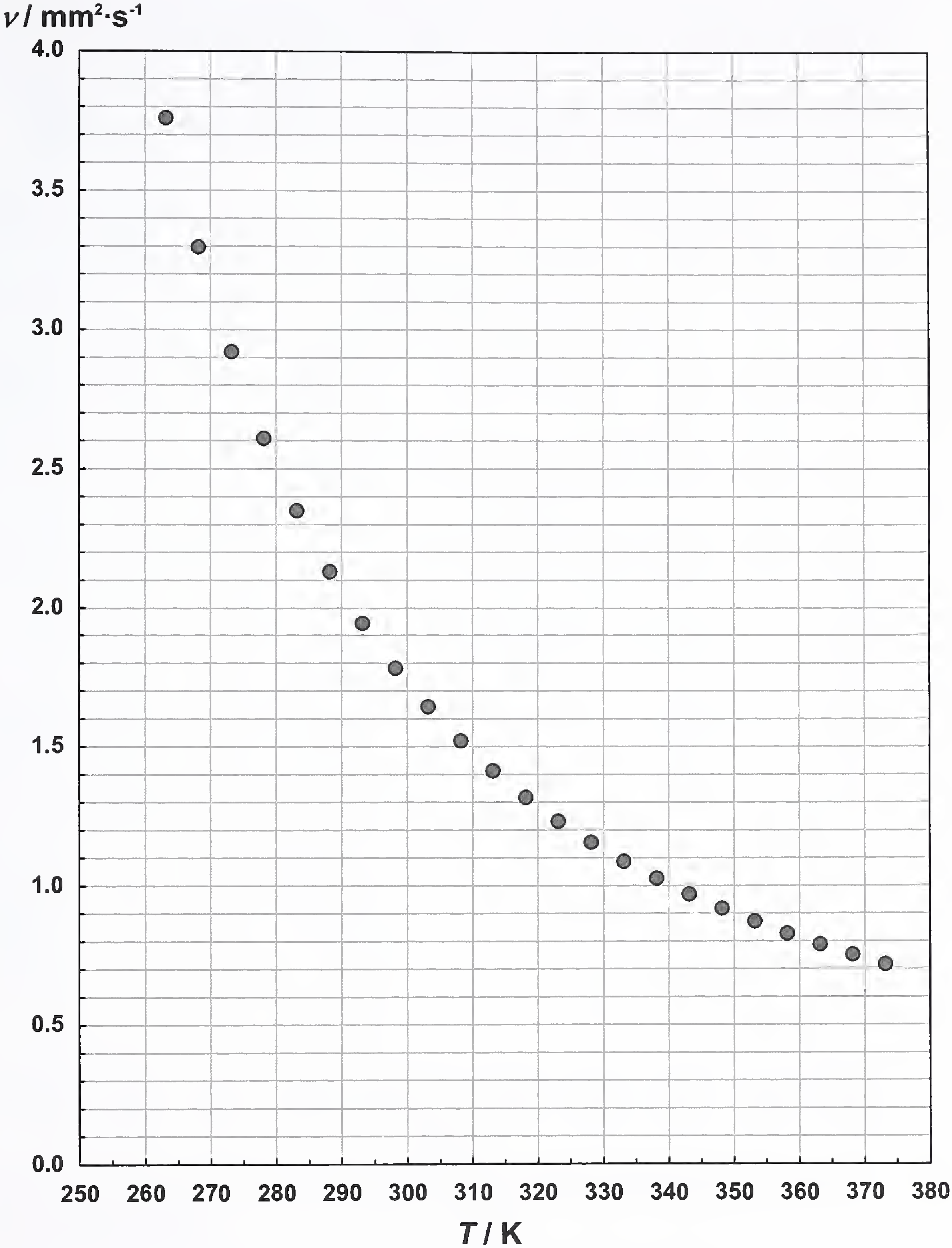

Figure 37: Measurements of the kinematic viscosity of Jet-A-4648. The uncertainty is discussed in the text.

The kinematic viscosity of JP-8-3773 was measured at ambient pressure in the temperature range 293.15 K to 373.15 K. These measurements are presented in Table 27. The instrument used was a commercial automated open gravitational flow viscometer with a suspended-level Ubbelohde glass capillary of 200 mm length with upper reservoir bulbs for a kinematic viscosity range from 0.3 $mm^2 \cdot s^{-1}$ to 30 $mm^2 \cdot s^{-1}$. This instrument was described earlier for the measurements done on methyl- and propylcyclohexane. These data are presented graphically in Figure 38.

Table 27: The kinematic viscosity of JP-8-3773 at an ambient pressure of 83 kPa.

JP-8 3773	
Temperature *T*	**Kinematic viscosity** *ν*
K	$\mathbf{mm^2 \cdot s^{-1}}$
293.15	1.692
303.15	1.442
313.15	1.250
323.15	1.099
333.15	0.9775
343.15	0.8768
353.15	0.7889
363.15	0.7172
373.15	0.6559

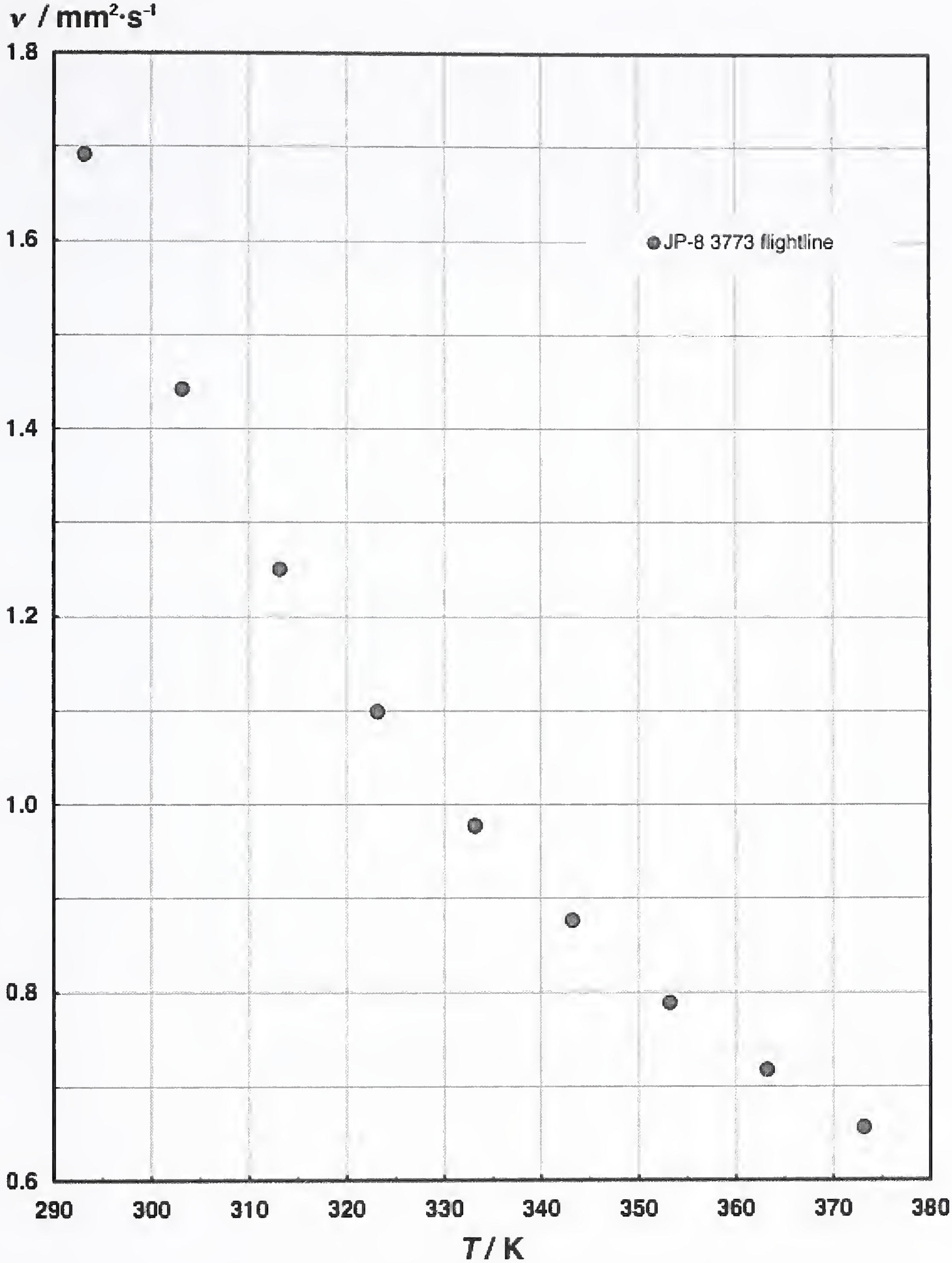

Figure 38: Measurements of the kinematic viscosity of JP-8-3773. The uncertainty is discussed in the text.

Thermal Conductivity Measurements of the Compressed Liquid Aviation Fuels:

Transient hot-wire measurements of the thermal conductivity were made on each of the three liquid samples of Jet-A-3602, Jet-A-3638, Jet-A-4658, JP-8-3773 and S-8. For each sample, measurements were made along 11 isotherms at temperatures from 300 to 500 K with pressures up to 70 MPa. The transient hot-wire instrument has been described in detail above in the treatment of the measurements on methyl- and propylcyclohexane. The tabulated thermal conductivity measurements are extensive and are therefore provided in Appendix I. The measurements are depicted graphically in Figures 39 - 43.

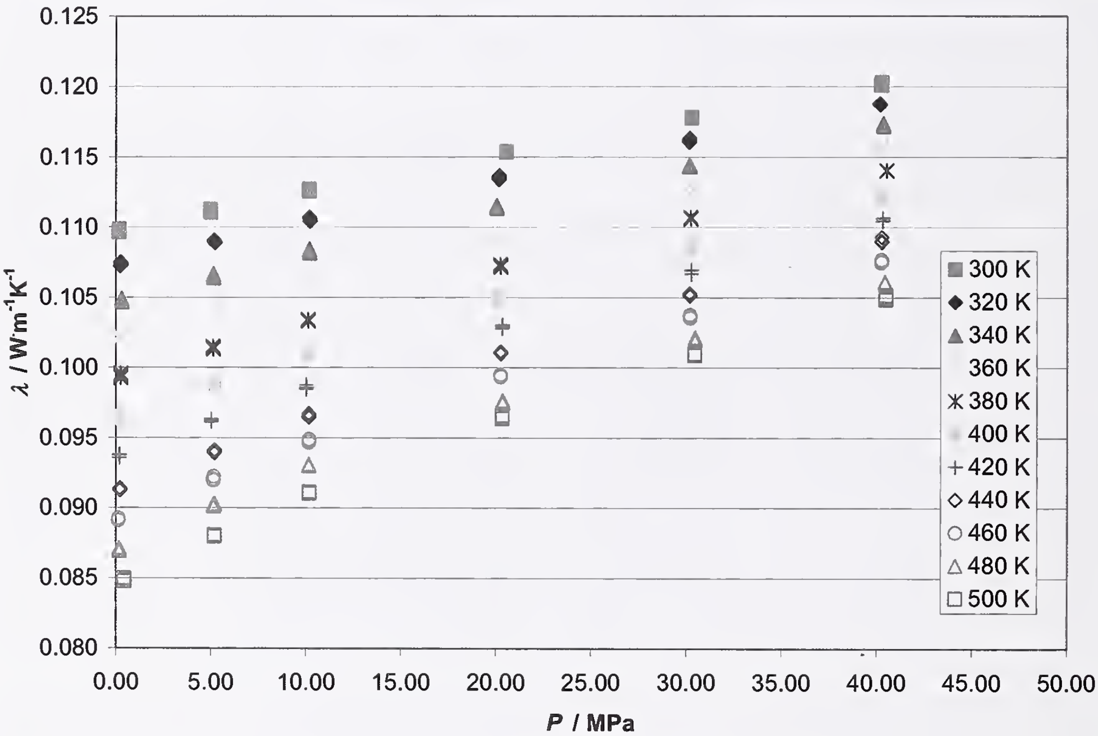

Figure 39: Thermal conductivity of Jet-A-3602 in the liquid phase.

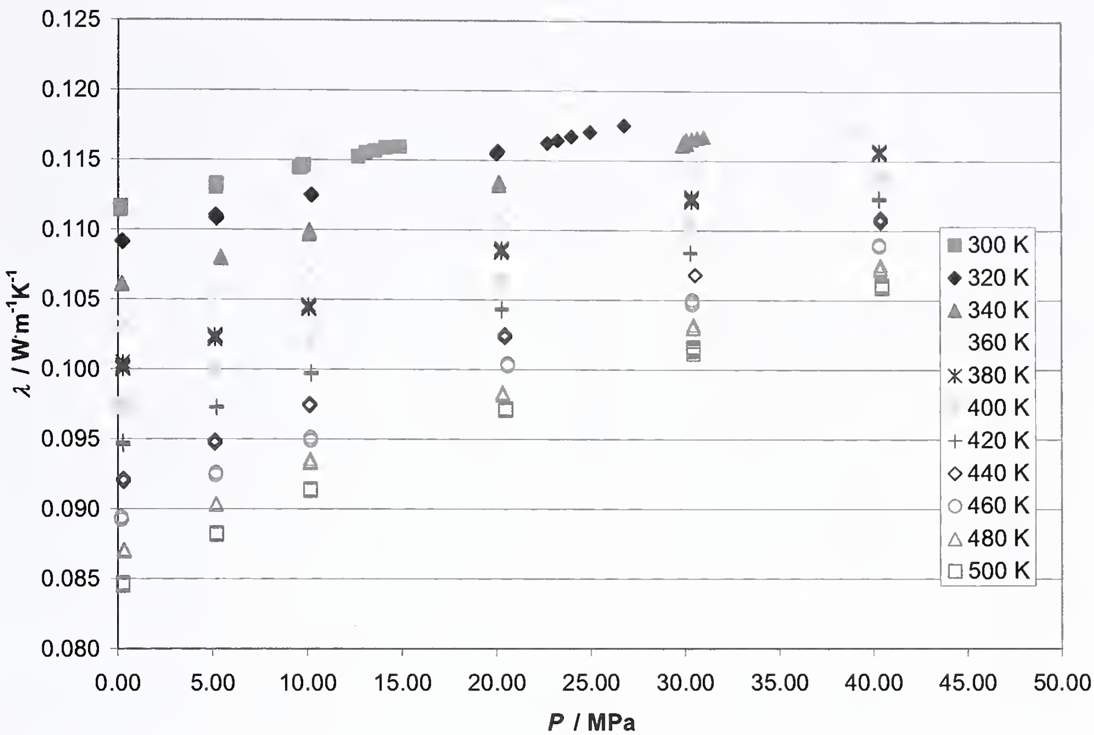

Figure 40: Thermal conductivity of Jet-A-3638 in the liquid phase.

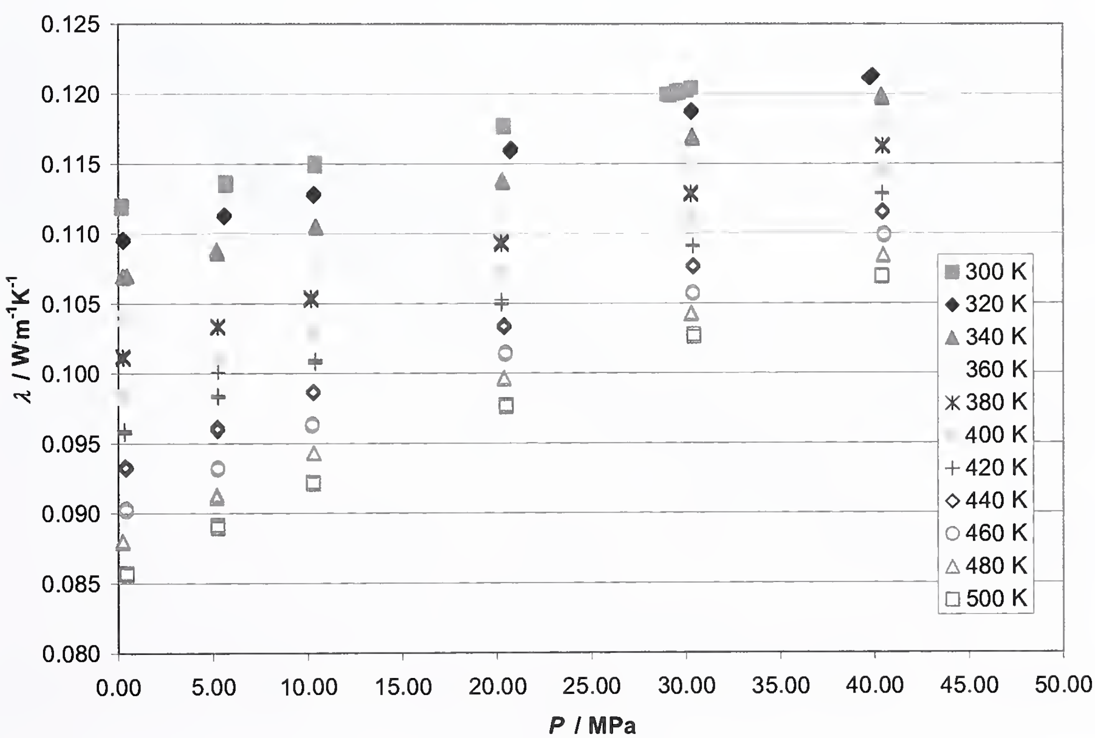

Figure 41: Thermal conductivity of Jet-A-4658 in the liquid phase.

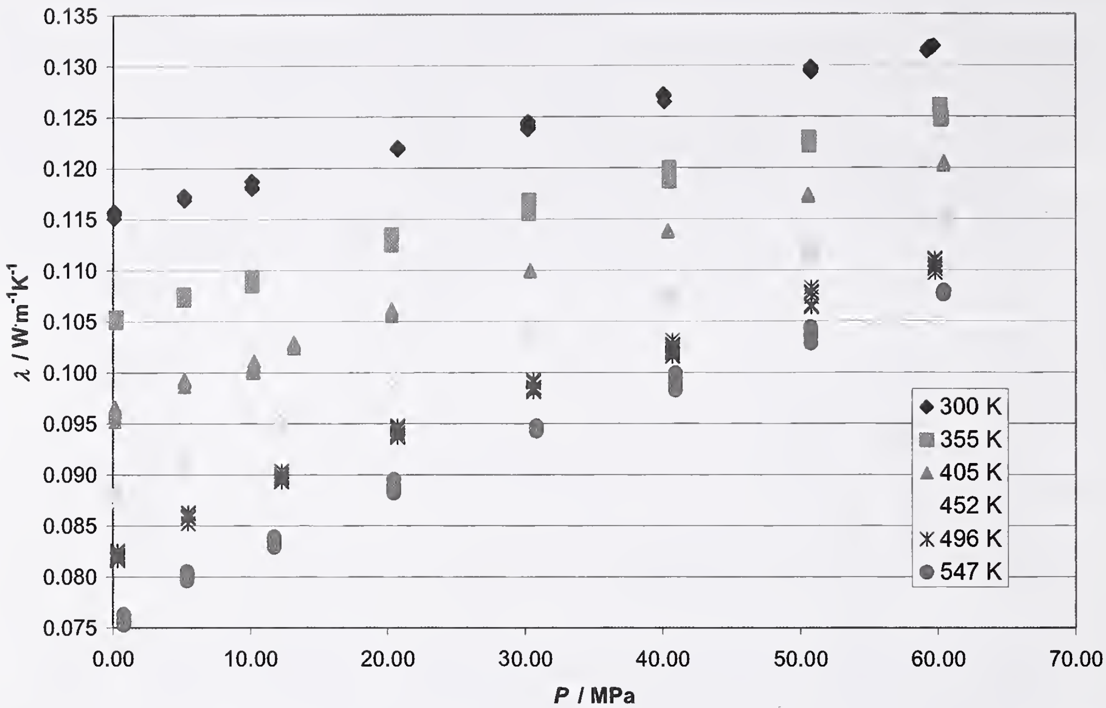

Figure 42: Thermal conductivity of JP-8-3773 from 0.1 MPa to 70 MPa.

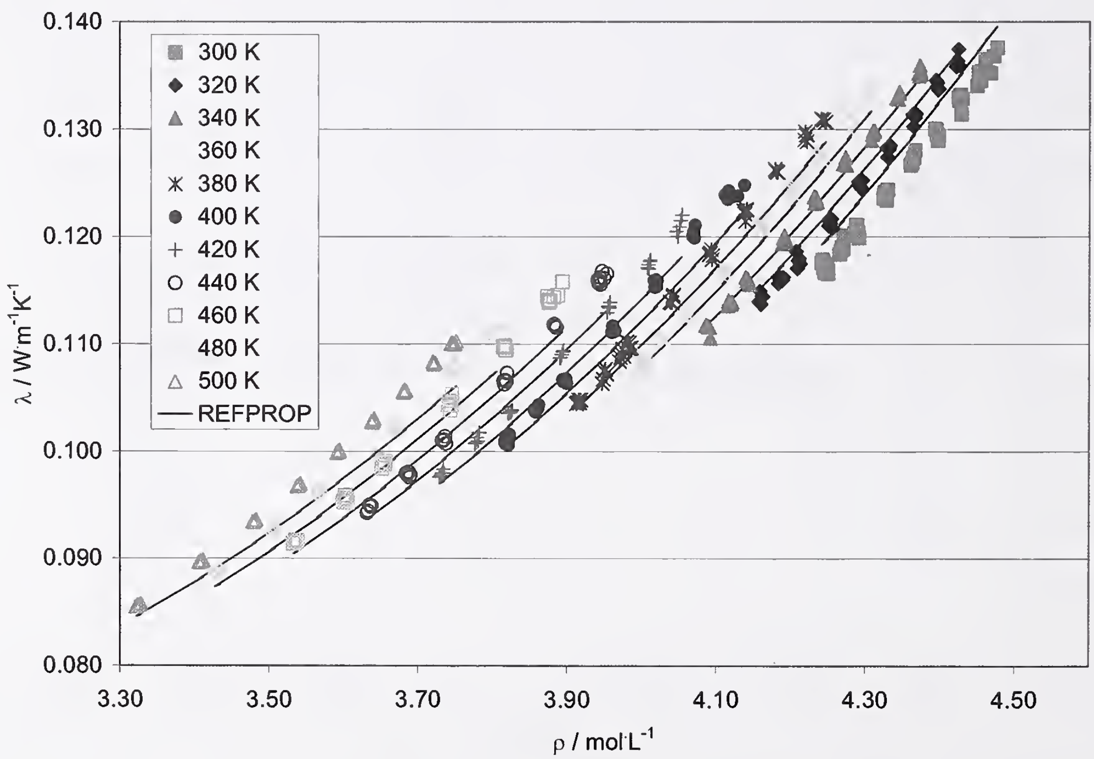

Figure 43: Thermal conductivity of S-8 at pressures from 0.1 MPa to 70 MPa.

Heat Capacities of Jet Fuels S-8 and JP-8:

The heat capacities of jet fuels JP-8-3373 and S-8 were measured with a commercial differential scanning calorimeter. Samples were contained in high-pressure sample containers during the measurements. These high-pressure containers are constructed of stainless steel, and are plated with gold on internal surfaces. These containers are sealed with a gold disk sandwiched between the upper lid and the lower portion of the vessel. The cells are rated for pressures of approximately 15 MPa. The internal volumes of these cells are approximately 30 μl. The high-pressure cells were used because the heat capacity measurements extended to above the normal boiling point of the jet fuels. In practice, measurements can be made at different filled fractions of the internal volume of the cells and these values can be extrapolated to complete filling to eliminate contributions from the vaporization of the liquid in the cells. The vaporization enthalpy was sufficiently negligible throughout the temperature range, that the larger fractions-filled measurements could be taken as being free of vapor-space. The capsules were filled and sealed within a glove bag that had been swept with dry nitrogen gas for at least an hour prior to cell filling. The sealed vessels were weighed on a microbalance with resolution of 1 μg.

Crushed pieces of SRM 720, synthetic sapphire, were used to calibrate the heat flux of the calorimeter with the same high-pressure cell that was used for the fluid heat capacity measurements. The mass of fluid sealed in the high-pressure cell was always much smaller than the mass of the cell. The empty cell parts had a mass of approximately 0.66 g and the sample masses ranged from 5 mg to 19 mg.

If vaporization enthalpies are significant, then the observed specific heat capacity of the two phase system will decrease with a decrease of vapor space in the sample vessel; or equivalently, the observed two phase heat capacity would decrease with increasing filled fraction of the sample cell. This behavior was not observed to temperatures of up to 473 K. In fact slight increases in the observed two phase heat capacity were observed with increasing filled fraction of the vessel.

Using a vapor volume of 5 μl, the ideal gas law, a representative enthalpy of vaporization of 50 $kJ \cdot mol^{-1}$, and a hypothetical increase in pressure of 0.1 MPa over 50 K, the contribution of the vaporization enthalpy to the observed two-phase heat capacity would be 0.0074 $J \cdot K^{-1} \cdot g^{-1}$, which is less than the run-to-run irreproducibility. Observed heat capacities were obtained by equilibrating the calorimeter at 223 K for 10 min or longer, scanning at 5 $K \cdot min^{-1}$ to 473 K and equilibrating at 473 K for 10 min. The equilibration periods were used to establish a baseline that was subtracted from the heat-flux against time thermal curve. Heat flux curves for the empty high-pressure cells in the reference and sample sides of the calorimeter were determined and averaged. The average heat flux curve for the empty vessel was subtracted from baseline-adjusted heat flux curves for the vessel filled with either sapphire or one of the jet fuels.

A correction factor for the heat flux was determined as a ratio of the true heat capacity of SRM 720 to that obtained from the average of several heat flux curves. This ratio was then multiplied by the observed heat capacity for the jet fuels to correct for heat-flux error (as in ASTM International Standard Method E968). The calorimeter obtains approximately 3000 readings for each thermal scan, not including the equilibration periods. With four or five replicates per filling and an average over three fillings, close to half a million data points might be processed to obtain a heat capacity curve. These are shown for JP-8-3773 and S-8 in figures 44 and 45. In order to reduce this number individual data points were collated near nominal temperatures. A single curve was then fitted to all these collated readings to obtain the heat capacity of each of the jet fuels. The statistics calculated for the fitted curve thus include the variances due to: 1) irreproducibility in vessel filling and sealing; 2) calorimetric noise; 3) run-to-run variability for the same vessel filling; 4) vessel placement irreproducibilities. The last two are the largest contributors to imprecision.

The least-squares generated equation for the heat capacity at ambient pressure of JP-8 is:

$$Cp/Cp^\circ = (2.193 \pm 0.0055) + (3.996 \pm 0.0011) \times 10^{-3}(T/T^\circ - 363.15)$$

The least-squares generated equation for the heat capacity of S-8 at ambient pressure is:

$$Cp/Cp^\circ = (2.527 \pm 0.0118) + (2.804 \pm 0.0024) \times 10^{-3}(T/T^\circ - 363.15)$$

where T° is 1 K, Cp° is 1 ($J \cdot K^{-1} \cdot g^{-1}$), and the difference between the saturation heat capacity and the constant pressure heat capacity was assumed to be negligible. The uncertainties attached to the parameters are 1 standard deviation. The random factors that contribute to those uncertainties of the parameters were stated in a previous paragraph.

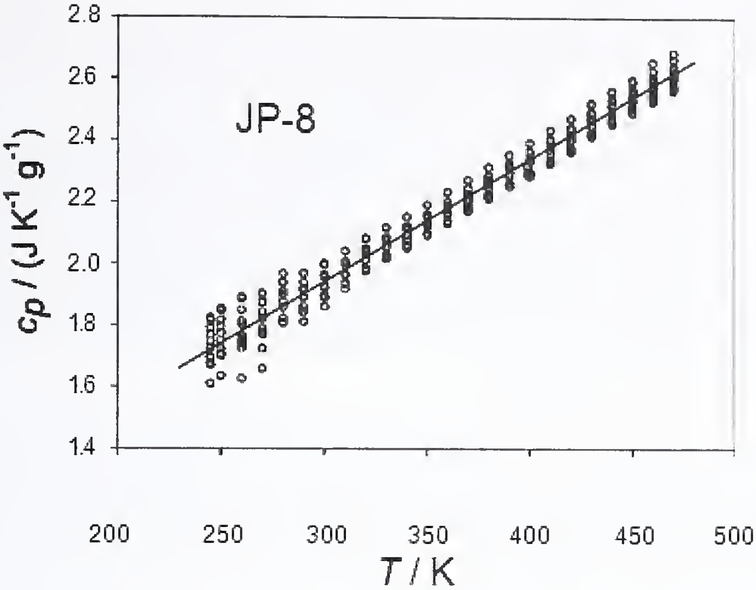

Figure 44: Heat capacity at constant pressure of JP-8-3773 as a function of temperature.

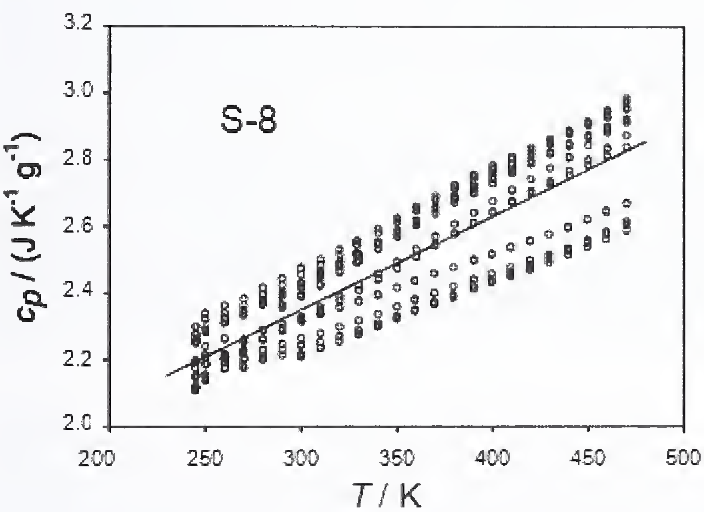

Figure 45: Heat capacity at constant pressure of JP-8-3773 as a function of temperature.

Development of the Thermodynamic and Transport Model:
The procedure for developing a surrogate mixture can be summarized as follows. First, a chemical analysis is performed to identify the composition of the fuel sample. From this analysis, a list of candidate fluids is constructed, including compounds representative of the various chemical families (branched or linear paraffins, alkenes, aromatics, mono or polycyclic paraffins, etc.) found in the sample. For each of these possible pure-fluid constituents, an equation of state, a viscosity surface and a thermal conductivity surface are developed, and a mixture model is used that incorporates the pure-fluid equations for both thermodynamic and transport properties. The fluids in the surrogate mixture and their compositions are then chosen by determining the composition that minimizes the difference between the predicted and experimental data for the distillation curve, density, sound speed, viscosity and thermal conductivity.

From the gas chromatography and mass spectrometry analysis of the Jet-A samples, we compiled a list of potential candidate fluids for a surrogate model. These fluids are listed in Table 28, along with their normal boiling point and their boiling points at an atmospheric pressure of 83 kPa (the typical local pressure of our laboratory, located at 1655 m above sea level). The list contains fluids used in our earlier work on RP-1, RP-2, and S-8, but in addition includes aromatic compounds such as toluene, o-xylene and tetralin that were not used in model for either S-8 or RP-1 and RP-2.[35, 36] For each mono-branched alkane identified in the chemical analysis, a representative species was selected as a candidate constituent fluid for the surrogates. In other words, for our purposes, all *x*-methylnonanes are represented as a single methylnonane. Similarly, we used a particular *x,y*-dimethylnonane to represent the dimethylnonane family. A major factor governing the specific choice of compound to represent a moiety was the availability of property data: priority was given to compounds for which the most abundant and reliable experimental measurements were available. For each possible constituent fluid, we searched the open literature as well as databases such as the NIST TDE program, DIPPR, and Landolt-Börnstein for experimental physical property data. For some of the fluids, the data were sparse and were supplemented with predicted values from the TDE and DIPPR Diadem programs[37].

Because our modeling approach requires thermophysical property models for all pure constituent fluids, it was necessary to have available equations of state and surfaces for the viscosity and thermal conductivity for each of the potential constituent pure fluids. Details of this procedure are available in other work, so we provide only a brief summary here[35, 36, 38, 39]. With the available experimental data supplemented with predictions obtained from the TDE program, we developed Helmholtz-form equations of state similar to the form developed by Span and Wagner that can represent not only the vapor pressure and density, but also other properties such as the speed of sound and heat capacity[40]. For viscosity and thermal conductivity, we primarily used an extended corresponding-states model, with n-dodecane as a reference fluid. When sufficient data were available, the representation of the viscosity or thermal conductivity was improved by fitting the data to correction functions for the shape factors. In the absence of experimental data, we used the predictive method of Van Velzen for viscosity, and the method of Baroncini for thermal conductivity (as implemented in the DIPPR Diadem program). Additionally, we incorporated earlier work on the thermal conductivity of methyl and propylcyclohexane to represent the alkyl cyclohexane family in terms of a scaled form of the thermal conductivity correlation developed for propylcyclohexane.

For calculations of the thermodynamic properties of mixtures, we used the mixture model incorporated into the REFPROP[41] computer program. This model includes an algorithm for estimating binary interaction parameters when data are unavailable for a particular fluid pair. The model for calculating the transport properties of a mixture is an extended corresponding-states method. In addition, we used an algorithm developed in earlier work to compute the distillation curve; this procedure incorporates data from an improved advanced distillation curve metrology.[35, 36, 38, 39]

The properties measurements discussed earlier formed the basis of the experimental data set used to obtain the surrogate models. We then used a multi-property, nonlinear regression procedure to minimize the differences between the experimental data and the predictions of the model. This is used to determine the components and their relative abundances to define the surrogate fluid mixtures for each aviation fuel sample. The objective function was the sum of the squared percentage differences between the experimental data and the predicted value. The independent variables were the compositions of the fluid mixture. Our initial guess included all of the components in Table 28. Successive calculations gave very small concentrations of some components. These were removed from the mixture and the minimization process was repeated until further reductions in the number of components resulted in unacceptably large deviations with the experimental data.

The final compositions of the surrogate mixtures are summarized in Table 29. Each surrogate model contains eight components. The surrogate for the composite Jet-A-4658 contains more of the heavier cycloalkanes than the Jet-A-3638 sample, and also contains hexadecane. The Jet-A-3638 sample contains some propylcyclohexane, and more of the lighter components. This is not unexpected because the distillation curves indicate that the Jet-A-4658 sample contains more of the higher boiling components.

In Figures 46 to 52, we present comparisons of our surrogate models with experimental data. Figure 46 shows the density as a function of temperature at atmospheric pressure (83 kPa). The models agree with the data to within their experimental uncertainty (0.1 %). The density of the two different samples differs from each other by approximately 1.5 %. Figures 47 and 48 show the deviations in density between the experimental measurements as a function of pressure, over the temperature range 270 K to 470 K for the Jet-A-3638 and the Jet-A-4658 samples. The experimental uncertainty of these data is 0.1 %. The models both show increasing deviations as the pressure increases, but remain within 0.5 %.

Table 28. Potential constituent fluids for the surrogate fuel mixtures

Compound	CAS no.	Class	No. of carbon atoms	Boiling point at 83 kPa (K)	Normal boiling point (K)
heptane	142-82-5	linear paraffin	7	364.90	371.53
toluene	108-88-3	aromatic	7	376.87	383.75
octane	111-65-9	linear paraffin	8	391.75	398.77
ortho-xylene	95-47-6	aromatic	8	410.16	417.54
nonane	111-84-2	linear paraffin	9	416.54	423.81
propylcyclohexane	1678-92-8	monocyclic paraffin	9	422.13	429.86
5-methylnonane	15869-85-9	branched paraffin	10	430.7	438.3
decane	124-18-5	linear paraffin	10	439.6	447.3
trans-decalin	493-02-7	dicyclic paraffin	10	452.0	460.4
tetralin	119-64-2	aromatic	10	472.31	480.75
2-methyldecane	6975-98-0	branched paraffin	11	454.4	462.3
2,4-dimethylnonane	17302-24-8	branched paraffin	11	437.6	445.4
undecane	1120-21-4	linear paraffin	11	461.1	469.0
pentylcyclohexane	4292-92-6	monocyclic paraffin	11	468.3	476.7
1-methyldecalin	2958-75-0	dicyclic paraffin	11	469.6	478.2
3-methylundecane	1002-43-3	branched paraffin	12	478.1	486.3
dodecane	112-40-3	linear paraffin	12	481.2	489.4
hexylcyclohexane	4292-75-5	monocyclic paraffin	12	489.7	498.4
5-methyldodecane	17453-93-9	branched paraffin	13	494.7	503.2
tridecane	629-50-5	linear paraffin	13	500.2	508.7
heptylcyclohexane	5617-41-4	monocyclic paraffin	13	509.2	517.9
2-methyltridecane	1560-96-9	branched paraffin	14	512.7	521.1
tetradecane	629-59-4	linear paraffin	14	518.1	526.7
pentadecane	629-62-9	linear paraffin	15	535.0	543.8
hexadecane	544-76-3	linear paraffin	16	551.0	560.1

Table 29. Composition of the Surrogate Mixtures

Fluid Name	Jet-A-4658 surrogate composition, mole fraction	Jet-A-3638 surrogate composition, mole fraction
propylcylcohexane	0.000	0.009
hexylcyclohexane	0.000	0.275
heptylcyclohexane	0.255	0.000
methyldecalin	0.081	0.014
5-methylnonane	0.148	0.068
2-methyldecane	0.164	0.347
n-tetradecane	0.068	0.027
n-hecadecane	0.030	0.000
ortho-xylene	0.055	0.120
tetralin	0.199	0.140

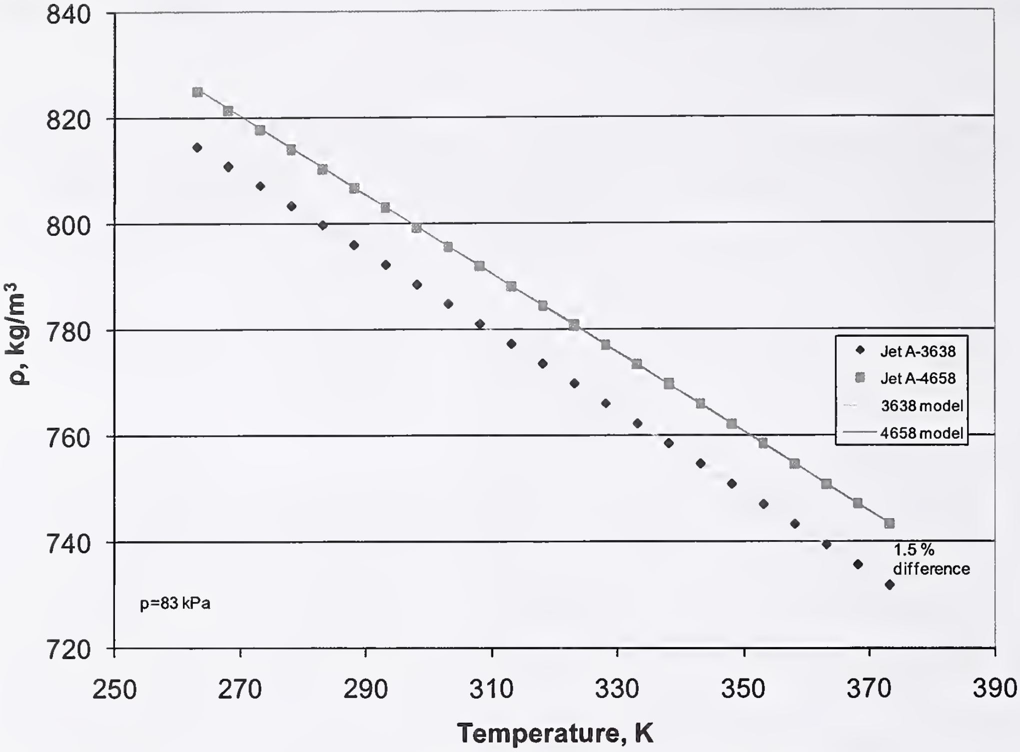

Figure 46: Plot of density as a function of temperature for the Jet-A samples at 83 kPa.

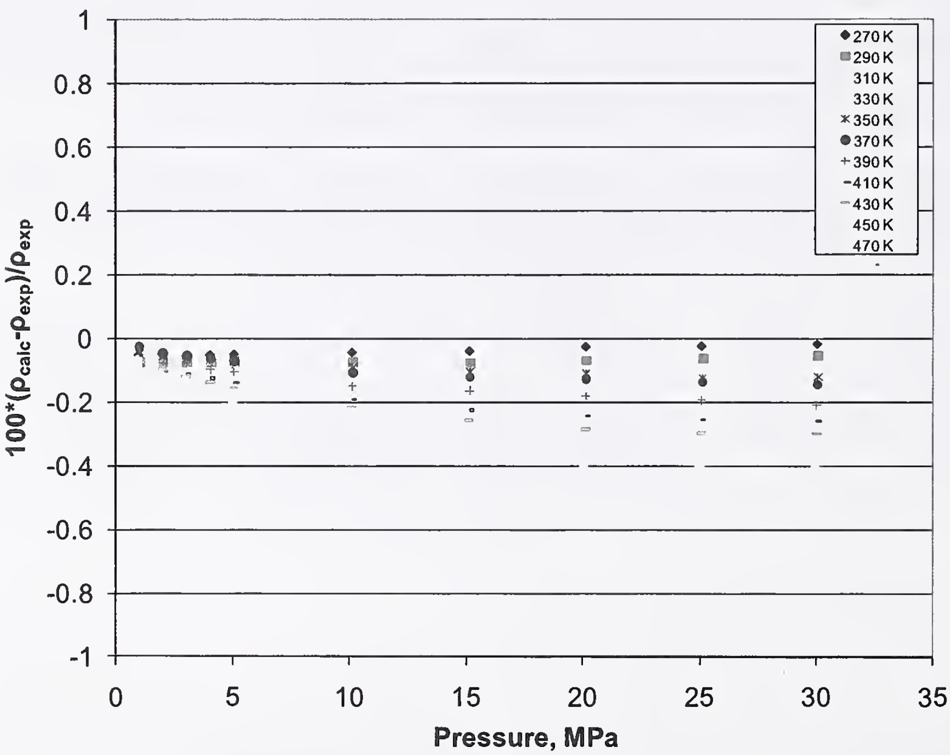

Figure 47: Deviation plot for density as a function of pressure for sample Jet-A-3638.

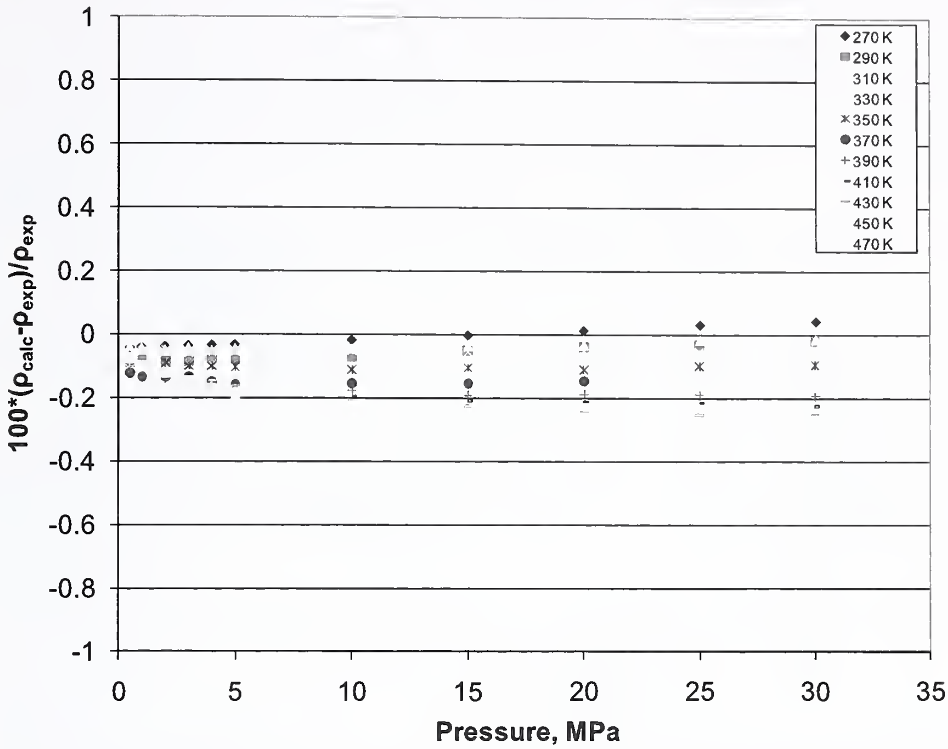

Figure 48: Deviation plot for density as a function of pressure for sample Jet-A-4658

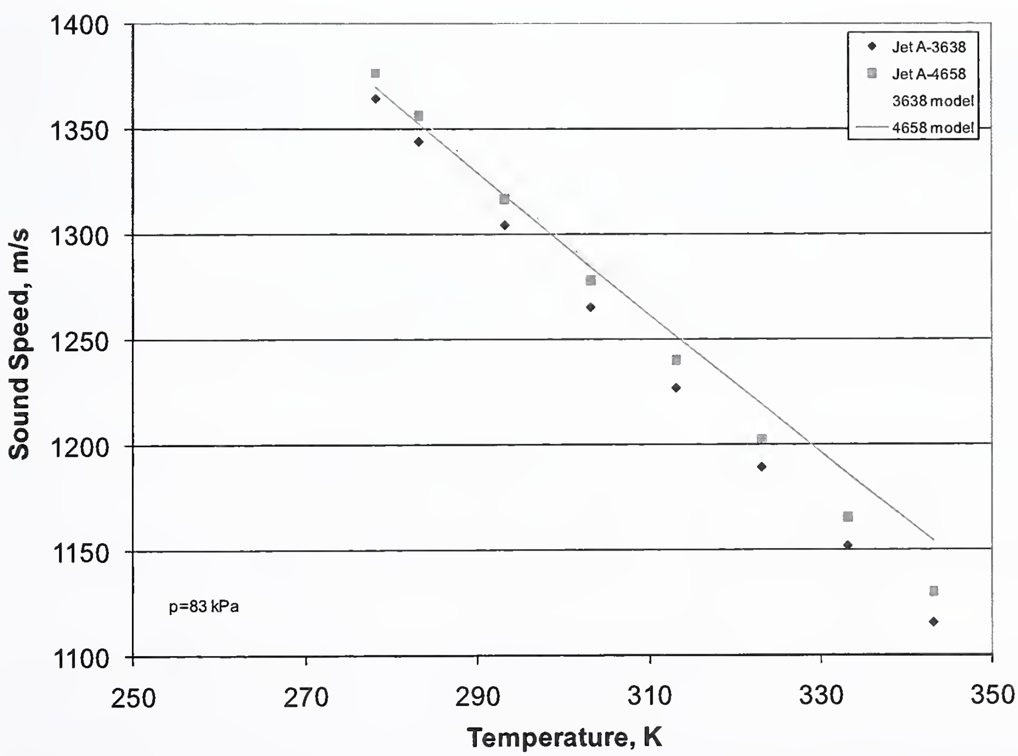

Figure 49: Calculated and experimental speed of sound for the Jet-A samples at 83 kPa

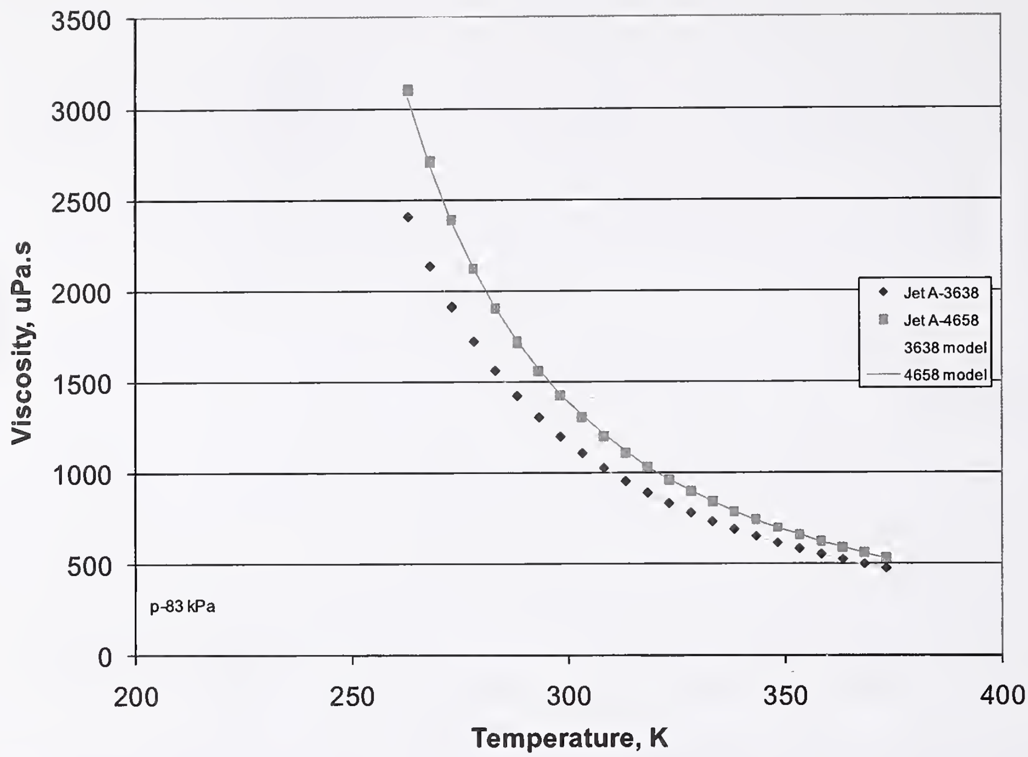

Figure 50: Plot of calculated and experimental viscosity for the Jet-A samples at 83 kPa.

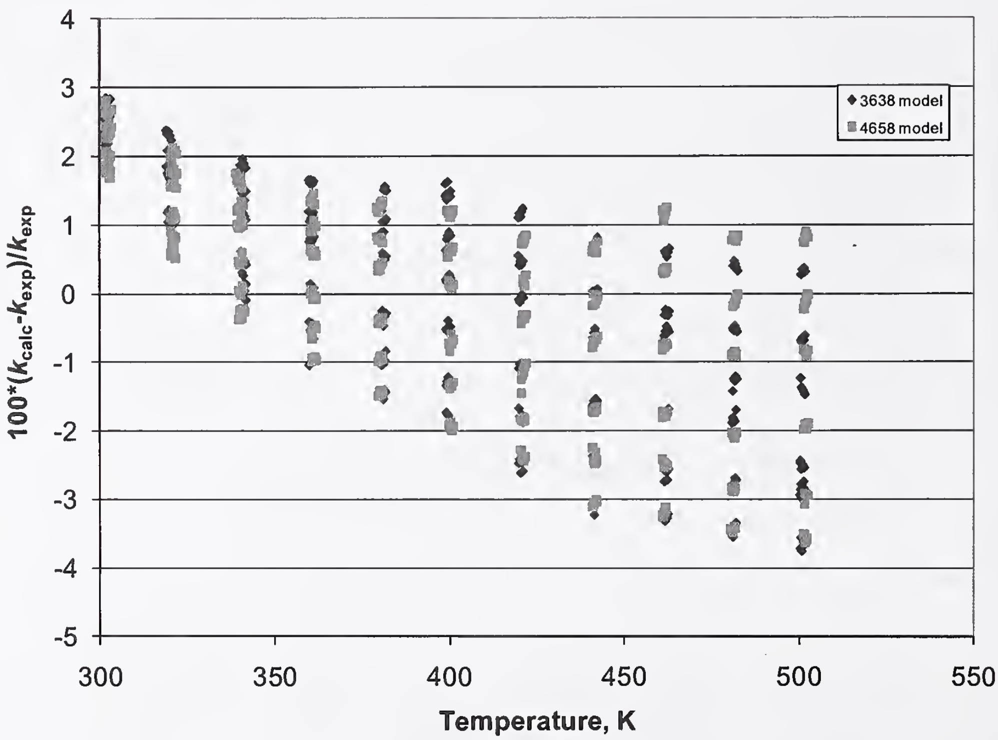

Figure 51: Deviation plot of calculated and experimental thermal conductivity for the Jet-A samples at pressures to 40 MPa

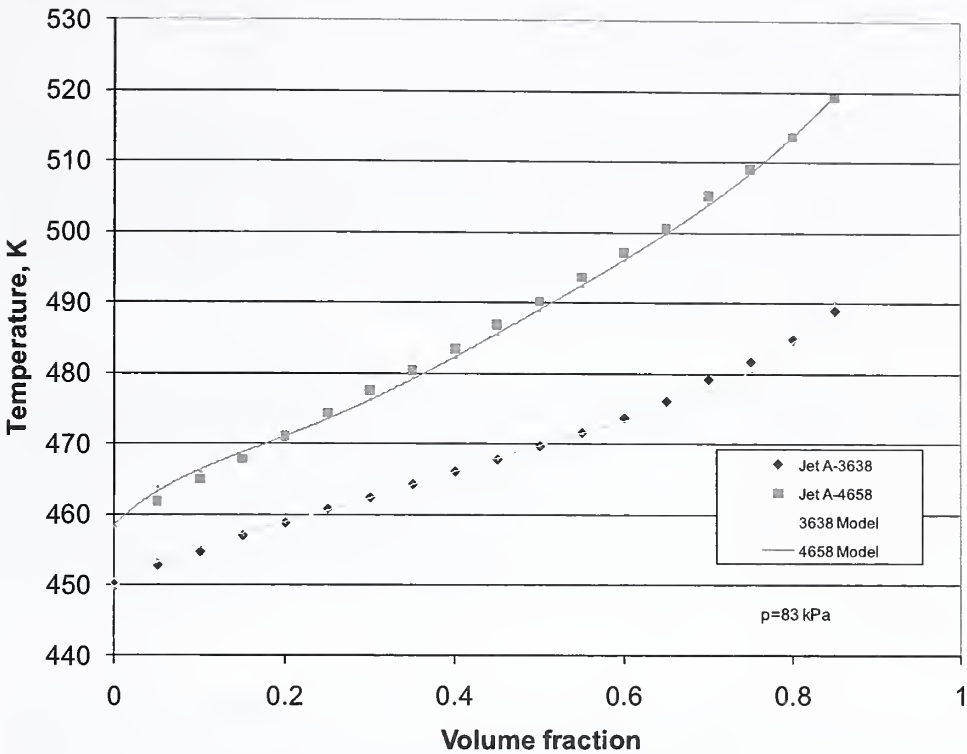

Figure 52: Distillation curves for the Jet-A samples, measured and calculated from the model.

The experimental values of the speed of sound and those calculated from the surrogate models are presented in Figure 49. All measurements were taken at ambient atmospheric pressure, and have an estimated uncertainty of 0.1 %. Neither of the models is able to represent the data to within their experimental uncertainty and systematically over predict the speed of sound; however, all models have deviations within 3.5 %.

Figure 50 is a plot of the calculated and experimental viscosity at atmospheric pressure as a function of temperature. This property is very sensitive to changes in composition, as indicated by an approximately 20 % difference in viscosity of the two samples at 270 K. The model was tuned so that the viscosity is represented by the model to within 3 %.

Figure 51 demonstrates the performance of the surrogate models for the thermal conductivity. The measurements covered temperatures from approximately 300 K to a maximum of 500 K, at pressures up to 40 MPa and were obtained from a transient hot-wire apparatus with an estimated uncertainty of 1 %. The present surrogate models represent the data to within 4 % over the range of conditions studied

Our final comparison with experimental data is presented in Figure 52, which shows the calculated and experimental advanced distillation curves. The distillation curves of the Jet-A-3638 and Jet-A-4658 sample differ significantly; at the end of the distillation they differ by 30 °C. The surrogate models are able to capture the behavior of each sample.

The volatility, as indicated by the advanced distillation curve, and the viscosity are very sensitive to changes in composition of the fuels.

Our surrogate models represent the thermophysical properties of the two samples studied. Work is in progress to develop a methodology to represent the Jet-A fuels as a single model that will characterize the fuels in terms of compositionally sensitive properties such as points on the distillation curve and viscosities. In addition, comparisons with existing surrogate models are in progress, and also further development of the equation of state models to improve the representation of the properties.

The composition of the surrogate mixture model for S-8, containing seven components, is summarized in Table 30. The computed distillation curve and the experimental data are shown in Figure 53. The difference between the calculated and experimental distillation temperatures is always within 1 %. The lightest (n-nonane) and heaviest fluids (n-hexadecane) are present only in small amounts and determine the initial boiling behavior and the tail of the distillation curve. The overall shape of the distillation curve is due primarily to only four major components: 2,6-dimethyloctane, 3-methyldecane, n-tridecane and n-tetradecane.

In Figures 54 to 57, we present comparisons of the S-8 surrogate model with experimental data. Figure 54 shows deviations of experimental and calculated surrogate density for S-8. The measurements cover the temperature range 233 K to 470 K at pressures to 30 MPa, and have an average absolute deviation (AAD) of 1.5 %

Figure 55 shows the deviations of experimental and calculated sound speeds for S-8. All of the sound speed measurements were made at local atmospheric pressure. The deviations are within 2.5 %, which exceeds the experimental uncertainty but is acceptable given the uncertainties in the constituent fluids and the mixture model.

Figure 56 shows the deviations of experimental and calculated viscosity at atmospheric pressure for S-8. The deviations are within about 5 % over the temperature range investigated.

Figure 57 shows the deviations of experimental and calculated thermal conductivity over pressures from atmospheric to 70 MPa at temperatures to 500 K. The predictions from the surrogate model are within 6 %, with the largest deviations at the lower temperatures.

Table 30. Composition of surrogate mixture for S-8

Fluid	S-8 surrogate composition, mole fraction
n-nonane	0.03
2,6-dimethyloctane	0.28
3-methyldecane	0.34
n-tridecane	0.13
n-tetradecane	0.20
n-pentadecane	0.015
n-hexadecane	0.005

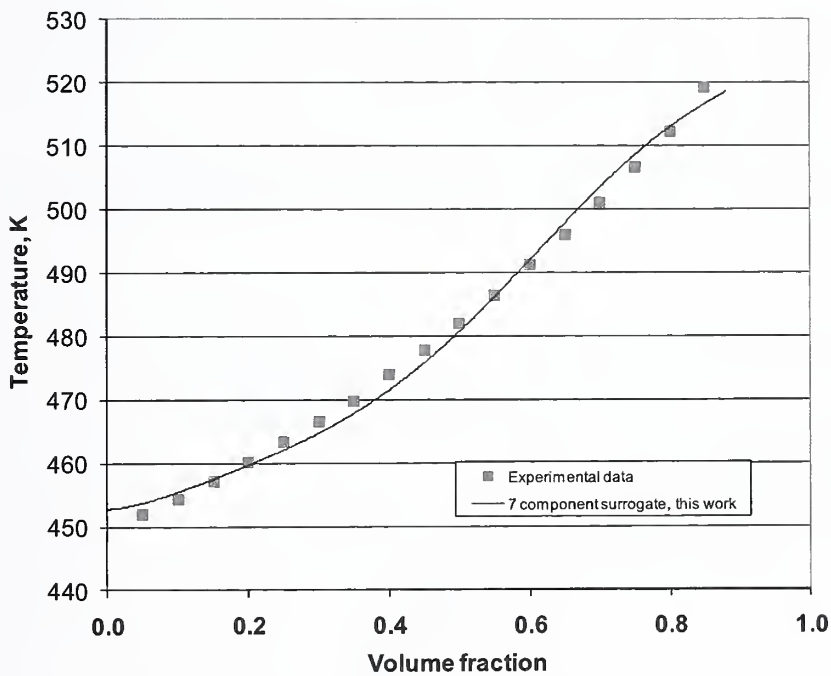

Figure 53. Distillation curve for S-8, showing the experimental and modeled curves.

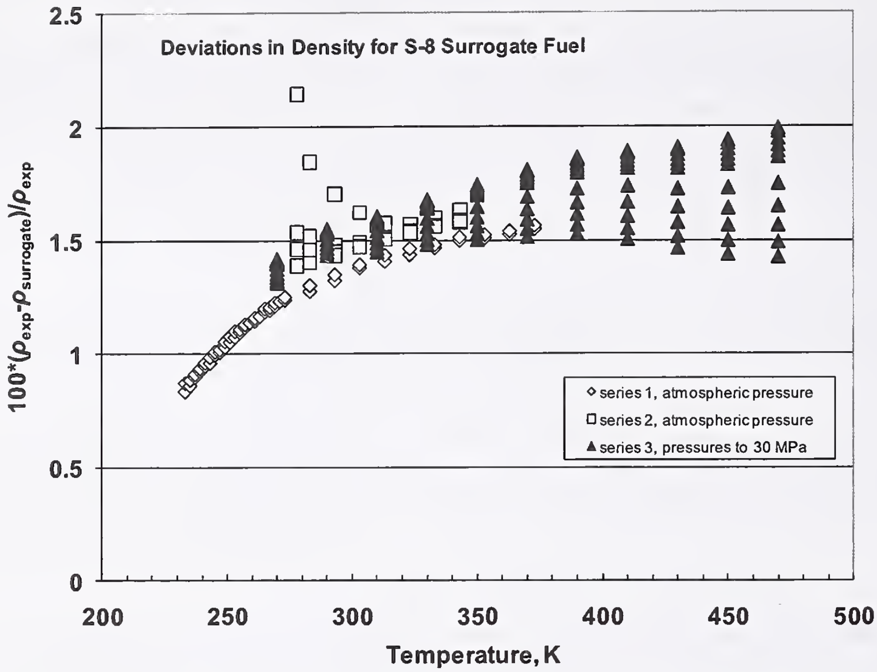

Figure 54: Deviations of experimental and calculated surrogate density for S-8.

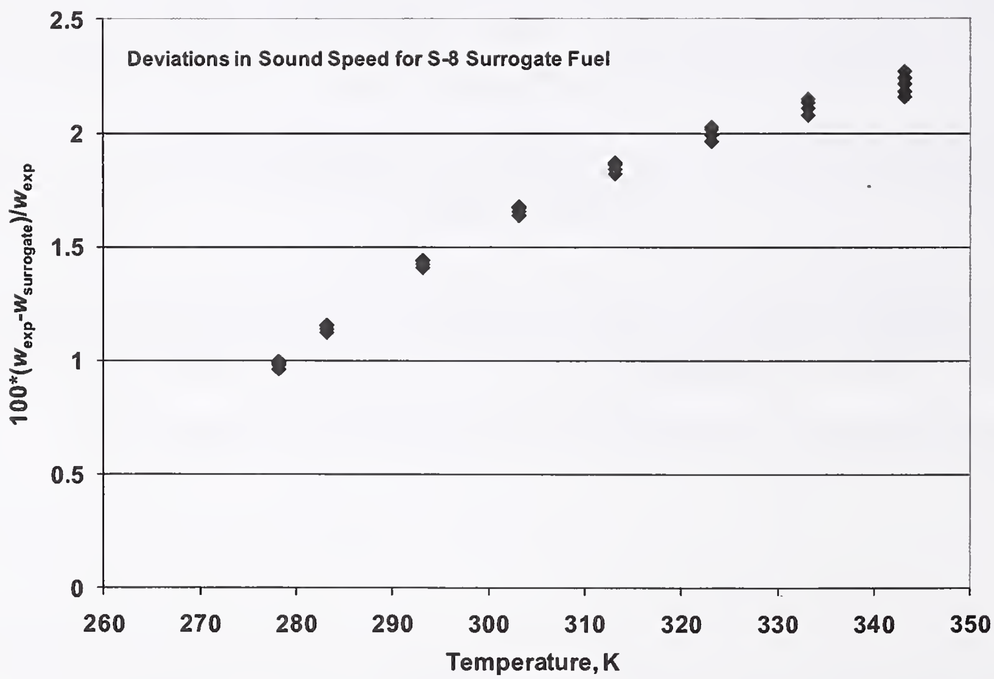

Figure 55: Deviations of experimental and calculated surrogate sound speed for S-8.

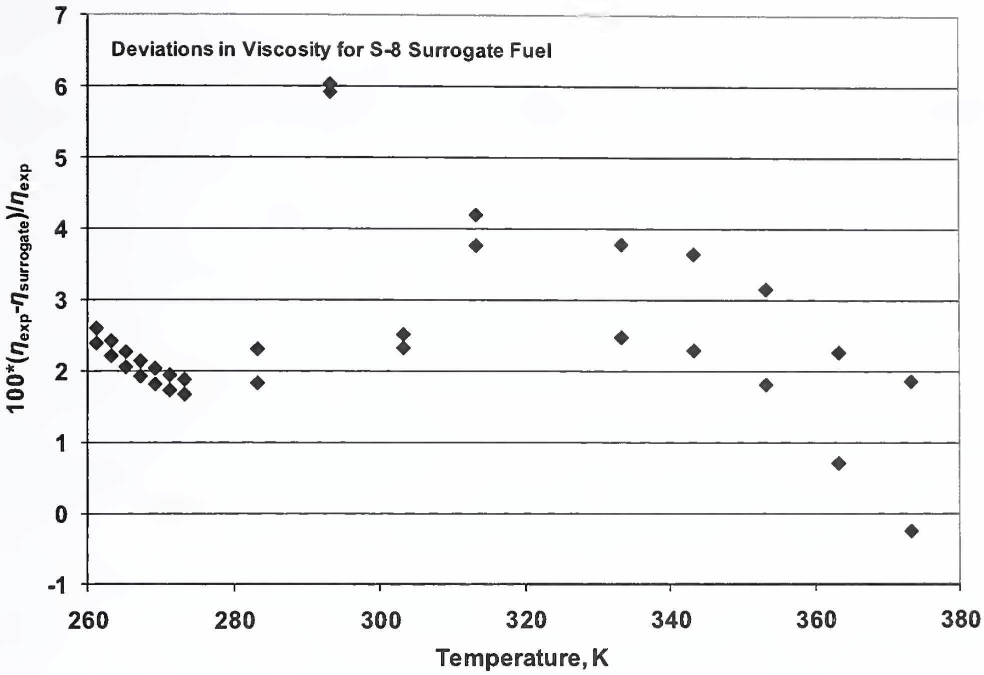

Figure 56: Deviations of experimental and calculated viscosity for S-8.

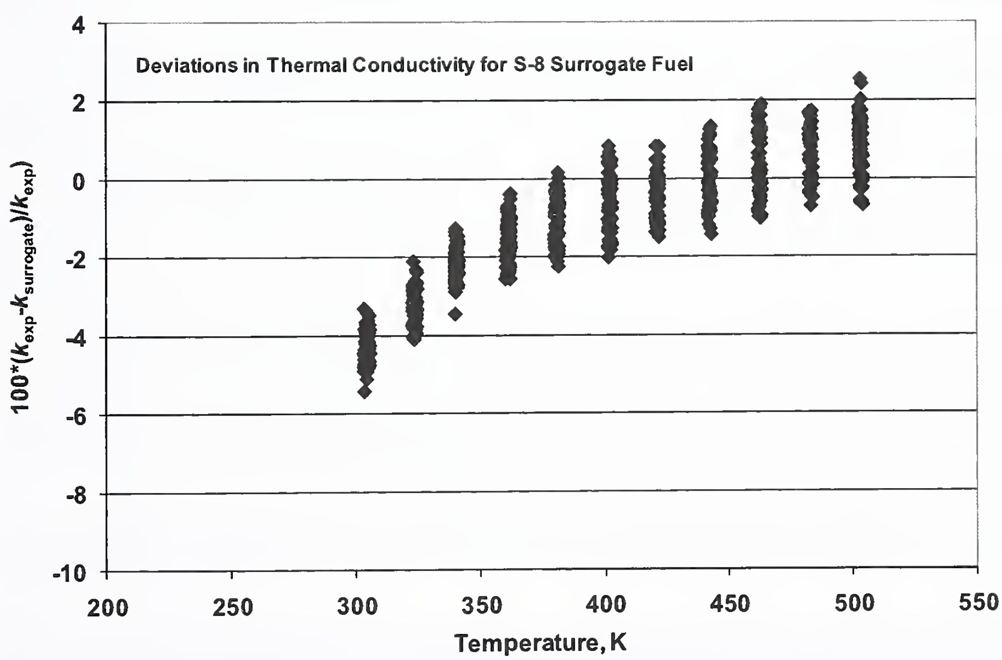

Figure 57: Deviations of experimental and calculated thermal conductivity for S-8.

References:

1. Bruno, T. J., Svoronos, P.D.N., *CRC Handbook of Basic Tables for Chemical Analysis, 2nd. ed.* Taylor and Francis CRC Press: Boca Raton, 2004.

2. Bruno, T. J., Svoronos, P.D.N., *CRC Handbook of Fundamental Spectroscopic Correlation Charts*. Taylor and Francis CRC Press: Boca Raton, 2005.

3. Andersen, P. C., Bruno, T.J., Thermal decomposition kinetics of RP-1 rocket propellant. *Ind. Eng. Chem. Res.* 2005, 44, (6), 1670-1676.

4. Andersen, W. A., Bruno, T.J., Rapid screening of fluids for chemical stability in organic Rankine cycle applications. *Ind. Eng. Chem. Res.* 2005, 44, 5560-5566.

5. Widegren, J. A., Bruno, T.J., Thermal decomposition kinetics of the aviation fuel Jet-A. *Ind. Eng. Chem. Res.* 2008, 47, (13), 4342-4348.

6. Widegren, J. A., Bruno, T.J., Thermal decomposition kinetics of propylcyclohexane. *Ind. Eng. Chem. Res.* 2009, 48, (2), 654-659.

7. Bruno, T. J., Conditioning of flowing multiphase samples for chemical analysis. *Sep. Sci. Technol.* 2005, 40, (8), 1720-1732.

8. Outcalt, S. L., McLinden, M.O., Automated densimeter for the rapid characterization of industrial fluids. *Ind. Eng. Chem. Res.* 2007, 46, 8264 - 8269.

9. Laesecke, A., Outcalt, S.L. and Brumback, K., Density and Speed of Sound Measurements of Methyl- and Propylcyclohexane. *Energy and Fuels* 2008, 22, 2629 - 2636.

10. Perkins, R. A.; Huber, M. L., Measurement and correlation of the thermal conductivity of pentafluoroethane (R125) from 190 K to 512 K at pressures to 70 MPa. *Journal of Chemical and Engineering Data* 2006, 51, (3), 898-904.

11. Perkins, R. A.; Laesecke, A.; Nieto de Castro, C. A., Polarized Transient Hot Wire Thermal Conductivity Measurements. *Fluid Phase Equilibria* 1992, 80, 275-286.

12. Bruno, T. J., Improvements in the measurement of distillation curves - part 1: a composition-explicit approach. *Ind. Eng. Chem. Res.* 2006, 45, 4371-4380.

13. Bruno, T. J., Method and apparatus for precision in-line sampling of distillate. *Sep. Sci. Technol.* 2006, 41, (2), 309-314.

14. Smith, B. L., Bruno, T.J., Advanced distillation curve measurement with a model predictive temperature controller. *Int. J. Thermophys.* 2006, 27, 1419-1434.

15. Bruno, T. J.; Smith, B. L., Enthalpy of combustion of fuels as a function of distillate cut: application of an advanced distillation curve method. *Energy & Fuels* 2006, 20, 2109-2116.

16. Bruno, T. J., Thermodynamic, transport and chemical properties of "reference" JP-8. *Book of Abstracts, Army Research Office and Air Force Office of Scientific Research, 2006 Contractor's meeting in Chemical Propulsion* 2006, 15-18.

17. Bruno, T. J., The properties of S-8. In Final Report for MIPR F4FBEY6237G001, Air Force Research Laboratory: 2006.

18. Bruno, T. J., Laesecke, A., Outcalt, S.L., Seelig, H-D, Smith, B.L., *Properties of a 50/50 Mixture of Jet-A + S-8, NIST-IR-6647.* 2007.

19. Bruno, T. J., Wolk, A., Naydich, A., Stabilization of biodiesel fuel at elevated Temperature with Hydrogen Donors: evaluation with the advanced distillation curve method. *Energy & Fuels* 2008, in press.

20. Bruno, T. J., Wolk, A., Naydich, A., Composition-explicit distillation curves for mixtures of gasoline with four-carbon alcohols (butanols). *Energy & Fuels* 2008, in press.

21. Ott, L. S., Smith, B.L., Bruno, T.J., Advanced distillation curve measurements for corrosive fluids: application to two crude oils. *Fuel* 2008, 87, 3055-3064.

22. Ott, L. S., Smith, B.L., Bruno, T.J., Advanced distillation curve measurement: application to a bio-derived crude oil prepared from swine manure. *Fuel* 2008, 87, 3379-3387.

23. Ott, L. S., Smith, B.L., Bruno, T.J., Composition-explicit distillation curves of mixtures of diesel fuel with biomass-derived glycol ester oxygenates: a fuel design tool for decreased particulate emissions. *Energy and Fuels* 2008, 22, 2518-2526.

24. Ott, L. S., Hadler, A., Bruno, T.J., Variability of the rocket propellants RP-1, RP-2, and TS-5: application of a composition- and enthalpy-explicit distillation curve method. *Ind. Eng. Chem. Res.* 2008, 47 (23), 9225-9233.

25. Ott, L. S., Bruno, T.J., Variability of biodiesel fuel and comparison to petroleum-derived diesel fuel: application of a composition and enthalpy explicit distillation curve method. *Energy & Fuels* 2008, 22, 2861-2868.

26. Smith, B. L., Bruno, T.J., Improvements in the measurement of distillation curves: part 3 - application to gasoline and gasoline + methanol mixtures. *Ind. Eng. Chem. Res.* 2007, 46, 297-309.

27. Smith, B. L., Bruno, T.J., Improvements in the measurement of distillation curves: part 4- application to the aviation turbine fuel Jet-A. *Ind. Eng. Chem. Res.* 2007, 46, 310-320.

28. Smith, B. L., Bruno, T.J., Composition-explicit distillation curves of aviation fuel JP-8 and a coal based jet fuel. *Energy & Fuels* 2007, 21, 2853-2862.

29. Smith, B. L., Bruno, T.J., Application of a Composition-Explicit Distillation Curve Metrology to Mixtures of Jet-A + Synthetic Fischer-Tropsch S-8. *J. Propul. Power* 2008, 24, (3), 619 - 623.

30. Smith, B. L., Ott, L.S., Bruno, T.J., Composition-explicit distillation curves of diesel fuel with glycol ether and glycol ester oxygenates: a design tool for decreased particulate emissions. *Environ. Sci. Tech.* 2008, 42, (20), 7682-7689.

31. Smith, B. L., Ott, L.S., Bruno, T.J., Composition-explicit distillation curves of commercial biodiesel fuels: comparison of petroleum derived fuel with B20 and B100. *Ind. Eng. Chem. Res.* 2008, 47, (16), 5832-5840.

32. Ott, L. S., Smith, B.L., Bruno, T.J., Experimental test of the Sydney Young equation for the presentation of distillation curves. *J. Chem. Thermodynam.* 2008, 40, 1352-1357.

33. Standard Test Method for Boiling Range Distribution of Petroleum Fractions by Gas Chromatography, ASTM Standard D2887-02, ASTM Annual Book of Standards, 2004. In 2004.

34. Outcalt, S. L., Laesecke, A., Freund, M.B., Density and speed of sound measurements of Jet A and S 8 aviation turbine fuels. *Energy & Fuels* 2009, 23, (3), 1626-1633.

35. Huber, M. L., Smith, B.L., Ott, L.S., Bruno, T.J., Surrogate Mixture Model for the Thermophysical Properties of Synthetic Aviation Fuel S-8: Explicit Application of the Advanced Distillation Curve. *Energy & Fuels* 2008, 22, 1104 - 1114.

36. Huber, M. L., Lemmon, E.W., Diky, V., Smith, B.L., Bruno, T.J., Chemically authentic surrogate mixture model for the thermophysical properties of a coal-derived-liquid fuel. *Energy and Fuels* 2008, 22, 3249-3257.

37. Rowley, R. L., Wilding, W.V., Oscarson, J.L., Zundel, N.A., Marshall, T.L., Daubert, T.E., Danner, R.P., , DIPPR Data Compilation of Pure Compound Properties, Design Institute for Physical Properties AIChE, New York, NY, 2004. In.

38. Huber, M. L., Lemmon, E., Ott, L.S., Bruno, T.J., Preliminary surrogate mixture models for rocket propellants RP-1 and RP-2. *Energy & Fuels* 2009, 23, 3083-3088.

39. Huber, M. L., Lemmon, E., Bruno, T.J., Effect of RP-1 compositional variability on thermophysical properties. *Energy & Fuels* 2009, 23, 5550-5555.

40. Span, R.; Wagner, W., Equations of state for technical applications. I. Simultaneously optimized functional forms for nonpolar and polar fluids. *International Journal of Thermophysics* 2003, 24, (1), 1-39.

41. Lemmon, E. W., McLinden, M.O., Huber, M.L., REFPROP, Reference fluid thermodynamic and transport properties, NIST Standard Reference Database 23. National Institute of Standards and Technology, Gaithersburg, MD, 2005: 2005.

Appendix I: Thermal Conductivity Measurements for Aviation Fuels

Table A1. Thermal conductivity of Jet-A-3602 in the liquid phase.

Point ID	T_0 (K)	T_e (K)	P_e (MPa)	λ_e (W·m^{-1}K^{-1})	q (W·m^{-1})
1001	298.295	296.274	1.984	0.1108	0.4694
1003	298.672	296.292	1.968	0.1106	0.5496
1005	299.099	296.325	1.961	0.1106	0.6375
1007	299.543	296.349	1.948	0.1105	0.7320
1009	300.022	296.374	1.939	0.1105	0.8329
1011	301.639	299.624	0.174	0.1099	0.4651
1013	301.987	299.627	0.174	0.1098	0.5446
1015	302.367	299.627	0.175	0.1097	0.6317
1017	302.774	299.622	0.170	0.1098	0.7254
1019	303.214	299.627	0.163	0.1096	0.8254
1021	301.619	299.634	4.975	0.1113	0.4651
1023	301.964	299.636	4.980	0.1112	0.5446
1025	302.346	299.639	4.984	0.1112	0.6316
1027	302.750	299.642	4.983	0.1110	0.7252
1029	303.180	299.640	4.971	0.1111	0.8253
1031	301.609	299.651	10.178	0.1127	0.4654
1033	301.951	299.654	10.176	0.1126	0.5450
1035	302.316	299.651	10.187	0.1125	0.6320
1037	302.713	299.650	10.197	0.1126	0.7254
1039	303.138	299.649	10.198	0.1126	0.8253
1041	301.570	299.672	20.550	0.1153	0.4651
1043	301.900	299.670	20.553	0.1153	0.5446
1045	302.265	299.672	20.554	0.1154	0.6317
1047	302.653	299.670	20.555	0.1154	0.7253
1049	303.070	299.672	20.549	0.1153	0.8253
1051	301.529	299.686	30.277	0.1178	0.4651
1053	301.859	299.689	30.274	0.1178	0.5447
1055	302.206	299.683	30.275	0.1178	0.6317
1057	302.590	299.682	30.278	0.1178	0.7253
1059	303.003	299.685	30.282	0.1178	0.8252
1061	301.527	299.694	40.263	0.1201	0.4653
1063	301.842	299.688	40.266	0.1202	0.5448
1065	302.199	299.693	40.251	0.1203	0.6320
1067	302.576	299.694	40.236	0.1201	0.7258
1069	302.972	299.689	40.224	0.1202	0.8259
2001	321.196	319.226	0.225	0.1072	0.4427
2003	321.505	319.239	0.249	0.1075	0.5181
2005	321.891	319.253	0.261	0.1075	0.6009
2007	322.305	319.266	0.273	0.1074	0.6899
2009	322.750	319.280	0.290	0.1073	0.7849
2011	321.338	319.407	5.164	0.1090	0.4424
2013	321.693	319.425	5.179	0.1091	0.5179
2015	322.008	319.426	5.194	0.1090	0.6006
2017	322.419	319.441	5.207	0.1089	0.6895
2019	322.853	319.454	5.218	0.1089	0.7845
2021	321.614	319.717	10.194	0.1107	0.4420
2023	321.952	319.724	10.206	0.1106	0.5174
2025	322.320	319.731	10.216	0.1105	0.6002
2027	322.722	319.745	10.222	0.1105	0.6891
2029	323.143	319.750	10.228	0.1104	0.7840
2031	321.722	319.865	20.180	0.1137	0.4419

2033	322.056	319.876	20.156	0.1136	0.5177
2035	322.403	319.872	20.157	0.1135	0.6005
2037	322.796	319.885	20.158	0.1134	0.6895
2039	323.204	319.887	20.169	0.1134	0.7844
2041	321.702	319.958	30.172	0.1163	0.4417
2043	322.025	319.967	30.161	0.1161	0.5174
2045	322.366	319.966	30.155	0.1162	0.6002
2047	322.745	319.978	30.158	0.1160	0.6891
2049	323.148	319.980	30.154	0.1162	0.7841
2051	321.861	320.074	40.148	0.1187	0.4418
2053	322.169	320.078	40.154	0.1188	0.5173
2055	322.514	320.084	40.161	0.1188	0.6000
2057	322.883	320.088	40.170	0.1188	0.6889
2059	323.263	320.086	40.178	0.1187	0.7837
3001	341.527	339.564	0.293	0.1049	0.4213
3003	341.762	339.569	0.303	0.1049	0.4932
3005	342.136	339.581	0.312	0.1049	0.5720
3007	342.535	339.593	0.320	0.1047	0.6567
3009	342.953	339.599	0.327	0.1048	0.7472
3011	341.537	339.694	5.129	0.1067	0.4211
3013	341.871	339.700	5.135	0.1066	0.4931
3015	342.231	339.708	5.142	0.1065	0.5719
3017	342.624	339.717	5.150	0.1064	0.6566
3019	343.036	339.724	5.154	0.1064	0.7471
3021	341.610	339.798	10.188	0.1084	0.4210
3023	341.932	339.803	10.183	0.1083	0.4930
3025	342.286	339.805	10.173	0.1084	0.5720
3027	342.669	339.815	10.171	0.1081	0.6569
3029	343.081	339.822	10.170	0.1082	0.7474
3031	341.664	339.918	20.026	0.1115	0.4212
3033	341.980	339.921	20.019	0.1115	0.4934
3035	342.323	339.928	20.050	0.1115	0.5718
3037	342.688	339.930	20.056	0.1114	0.6565
3039	343.084	339.935	20.066	0.1113	0.7469
3041	341.704	339.991	30.148	0.1143	0.4212
3043	342.013	339.996	30.153	0.1143	0.4932
3045	342.347	340.000	30.179	0.1145	0.5717
3047	342.703	339.998	30.188	0.1144	0.6564
3049	343.088	340.005	30.194	0.1143	0.7468
3051	341.750	340.067	40.334	0.1174	0.4209
3053	342.047	340.068	40.339	0.1174	0.4928
3055	342.372	340.071	40.336	0.1173	0.5717
3057	342.724	340.073	40.341	0.1173	0.6564
3059	343.098	340.080	40.349	0.1172	0.7468
4001	360.637	358.790	0.166	0.1022	0.4031
4003	360.911	358.795	0.175	0.1023	0.4719
4005	361.273	358.804	0.171	0.1021	0.5474
4007	361.655	358.810	0.167	0.1021	0.6287
4009	362.064	358.817	0.169	0.1021	0.7154
4011	360.656	358.894	5.232	0.1042	0.4031
4013	360.979	358.902	5.238	0.1041	0.4719
4015	361.327	358.908	5.242	0.1041	0.5474
4017	361.704	358.912	5.247	0.1040	0.6285
4019	362.105	358.921	5.251	0.1040	0.7151
4021	360.745	358.982	10.164	0.1061	0.4030
4023	361.062	358.988	10.169	0.1060	0.4719

4025	361.405	358.992	10.175	0.1060	0.5474
4027	361.774	359.000	10.182	0.1059	0.6285
4029	362.163	359.000	10.190	0.1058	0.7150
4031	360.798	359.072	20.275	0.1095	0.4029
4033	361.097	359.074	20.279	0.1095	0.4718
4035	361.433	359.079	20.278	0.1094	0.5472
4037	361.789	359.079	20.267	0.1093	0.6285
4039	362.173	359.087	20.268	0.1093	0.7152
4041	360.765	359.136	30.385	0.1128	0.4028
4043	361.111	359.137	30.390	0.1127	0.4718
4045	361.438	359.143	30.392	0.1126	0.5472
4047	361.785	359.145	30.380	0.1127	0.6285
4049	362.149	359.143	30.372	0.1126	0.7152
4051	360.846	359.196	40.225	0.1158	0.4030
4053	361.133	359.200	40.223	0.1157	0.4720
4055	361.443	359.199	40.234	0.1157	0.5473
4057	361.786	359.205	40.246	0.1156	0.6283
4059	362.149	359.211	40.250	0.1156	0.7148
5001	380.967	379.179	0.263	0.0995	0.3856
5003	381.285	379.183	0.259	0.0996	0.4516
5005	381.632	379.192	0.257	0.0994	0.5239
5007	382.008	379.199	0.258	0.0993	0.6015
5009	382.401	379.203	0.258	0.0994	0.6845
5011	380.987	379.257	5.121	0.1015	0.3855
5013	381.303	379.264	5.115	0.1015	0.4516
5015	381.644	379.268	5.114	0.1015	0.5238
5017	382.011	379.272	5.116	0.1014	0.6014
5019	382.397	379.278	5.117	0.1013	0.6842
5021	381.059	379.335	10.120	0.1035	0.3857
5023	381.369	379.345	10.123	0.1034	0.4516
5025	381.697	379.346	10.132	0.1034	0.5237
5027	382.053	379.348	10.136	0.1033	0.6012
5029	382.431	379.351	10.143	0.1033	0.6840
5031	381.064	379.398	20.233	0.1074	0.3857
5033	381.357	379.402	20.245	0.1073	0.4514
5035	381.683	379.406	20.250	0.1072	0.5236
5037	382.022	379.406	20.255	0.1072	0.6011
5039	382.385	379.405	20.260	0.1072	0.6840
5041	381.066	379.457	30.226	0.1107	0.3855
5043	381.351	379.458	30.231	0.1106	0.4514
5045	381.660	379.459	30.236	0.1106	0.5235
5047	381.996	379.464	30.236	0.1106	0.6011
5049	382.353	379.466	30.239	0.1106	0.6840
5051	381.067	379.512	40.517	0.1140	0.3855
5053	381.341	379.514	40.520	0.1140	0.4513
5055	381.646	379.516	40.523	0.1141	0.5235
5057	381.963	379.513	40.527	0.1140	0.6011
5059	382.314	379.516	40.511	0.1140	0.6841
6001	401.768	399.994	0.177	0.0966	0.3696
6003	402.070	399.990	0.180	0.0965	0.4328
6005	402.405	399.993	0.182	0.0965	0.5019
6007	402.761	399.991	0.183	0.0963	0.5763
6009	403.144	399.993	0.175	0.0964	0.6558
6011	401.679	400.005	5.188	0.0988	0.3695
6013	401.979	400.006	5.189	0.0988	0.4327
6015	402.306	400.008	5.189	0.0988	0.5018

6017	402.656	400.007	5.190	0.0987	0.5762
6019	403.022	400.004	5.193	0.0987	0.6556
6021	401.697	400.022	10.130	0.1010	0.3696
6023	401.986	400.019	10.134	0.1011	0.4327
6025	402.304	400.017	10.137	0.1010	0.5019
6027	402.655	400.022	10.139	0.1009	0.5763
6029	403.013	400.016	10.141	0.1008	0.6556
6031	401.635	400.041	20.129	0.1050	0.3698
6033	401.916	400.040	20.139	0.1051	0.4330
6035	402.219	400.038	20.144	0.1049	0.5021
6037	402.550	400.036	20.145	0.1048	0.5765
6039	402.906	400.039	20.149	0.1050	0.6558
6041	401.612	400.056	30.252	0.1087	0.3697
6043	401.880	400.053	30.252	0.1087	0.4329
6045	402.178	400.052	30.255	0.1087	0.5020
6047	402.500	400.052	30.257	0.1086	0.5764
6049	402.845	400.056	30.258	0.1085	0.6558
6051	401.546	400.067	40.273	0.1122	0.3699
6053	401.823	400.072	40.275	0.1120	0.4331
6055	402.108	400.067	40.273	0.1122	0.5023
6057	402.416	400.068	40.276	0.1122	0.5767
6059	402.751	400.066	40.287	0.1121	0.6560
7001	421.914	420.177	0.184	0.0938	0.3547
7003	422.223	420.186	0.188	0.0938	0.4153
7005	422.558	420.190	0.190	0.0938	0.4817
7007	422.914	420.191	0.188	0.0938	0.5532
7009	423.301	420.201	0.188	0.0936	0.6294
7011	421.903	420.239	5.025	0.0963	0.3546
7013	422.192	420.238	5.029	0.0964	0.4152
7015	422.525	420.246	5.031	0.0962	0.4815
7017	422.866	420.244	5.030	0.0962	0.5529
7019	423.244	420.251	5.032	0.0961	0.6291
7021	421.997	420.334	10.039	0.0988	0.3547
7023	422.291	420.340	10.040	0.0986	0.4153
7025	422.609	420.341	10.039	0.0985	0.4817
7027	422.946	420.345	10.039	0.0986	0.5531
7029	423.299	420.340	10.036	0.0985	0.6293
7031	422.289	420.384	20.334	0.1029	0.3542
7033	422.558	420.382	20.336	0.1028	0.4147
7035	422.860	420.382	20.337	0.1029	0.4810
7037	423.187	420.387	20.337	0.1030	0.5523
7039	423.531	420.386	20.331	0.1028	0.6285
7041	422.000	420.422	20.356	0.1031	0.3538
7043	422.277	420.423	20.354	0.1030	0.4144
7045	422.580	420.424	20.348	0.1029	0.4807
7047	422.904	420.427	20.345	0.1029	0.5520
7049	423.252	420.429	20.340	0.1029	0.6282
7051	421.974	420.463	30.268	0.1070	0.3540
7053	422.237	420.462	30.265	0.1070	0.4145
7055	422.531	420.464	30.265	0.1067	0.4808
7057	422.842	420.464	30.262	0.1069	0.5521
7059	423.171	420.461	30.259	0.1067	0.6282
7061	421.925	420.484	40.327	0.1106	0.3540
7063	422.180	420.482	40.327	0.1107	0.4144
7065	422.512	420.483	40.330	0.1105	0.4808
7067	422.812	420.482	40.316	0.1106	0.5522

7069	423.137	420.483	40.306	0.1104	0.6284
8001	441.838	440.120	0.223	0.0913	0.3407
8003	442.140	440.122	0.223	0.0913	0.3989
8005	442.412	440.122	0.224	0.0913	0.4626
8007	442.758	440.124	0.223	0.0914	0.5312
8009	443.121	440.124	0.218	0.0914	0.6044
8011	441.768	440.142	5.197	0.0941	0.3405
8013	442.051	440.142	5.198	0.0941	0.3987
8015	442.358	440.138	5.198	0.0940	0.4625
8017	442.702	440.144	5.192	0.0941	0.5311
8019	443.056	440.140	5.189	0.0939	0.6044
8021	441.769	440.152	10.163	0.0967	0.3406
8023	442.045	440.151	10.164	0.0965	0.3987
8025	442.347	440.148	10.165	0.0966	0.4625
8027	442.680	440.155	10.165	0.0966	0.5311
8029	443.028	440.152	10.164	0.0965	0.6043
8031	441.711	440.183	20.255	0.1012	0.3406
8033	441.977	440.185	20.254	0.1011	0.3988
8035	442.265	440.181	20.254	0.1011	0.4626
8037	442.585	440.187	20.256	0.1010	0.5311
8039	442.915	440.179	20.259	0.1010	0.6042
8041	441.635	440.197	30.162	0.1052	0.3408
8043	441.897	440.201	30.172	0.1051	0.3990
8045	442.176	440.198	30.178	0.1053	0.4627
8047	442.476	440.198	30.182	0.1052	0.5312
8049	442.792	440.190	30.183	0.1051	0.6044
8051	441.591	440.197	40.247	0.1090	0.3408
8053	441.892	440.196	40.249	0.1093	0.3991
8055	442.168	440.196	40.257	0.1089	0.4628
8057	442.462	440.199	40.261	0.1090	0.5314
8059	442.769	440.191	40.264	0.1090	0.6045
9001	461.280	459.599	0.148	0.0893	0.3283
9003	461.578	459.603	0.145	0.0893	0.3845
9005	461.902	459.607	0.138	0.0891	0.4462
9007	462.247	459.612	0.135	0.0891	0.5124
9009	462.610	459.612	0.138	0.0891	0.5829
9011	461.254	459.647	5.152	0.0923	0.3283
9013	461.544	459.654	5.144	0.0920	0.3845
9015	461.851	459.648	5.140	0.0921	0.4461
9017	462.186	459.655	5.134	0.0921	0.5124
9019	462.543	459.658	5.134	0.0920	0.5830
9021	461.240	459.693	10.181	0.0949	0.3284
9023	461.512	459.693	10.174	0.0948	0.3847
9025	461.815	459.698	10.172	0.0947	0.4462
9027	462.137	459.697	10.175	0.0948	0.5123
9029	462.479	459.701	10.182	0.0948	0.5827
9031	461.164	459.730	20.252	0.0995	0.3283
9033	461.416	459.725	20.253	0.0995	0.3845
9035	461.706	459.726	20.256	0.0994	0.4459
9037	462.012	459.726	20.260	0.0994	0.5120
9039	462.384	459.722	20.262	0.0994	0.5826
9041	461.193	459.750	30.196	0.1038	0.3286
9043	461.448	459.753	30.195	0.1037	0.3848
9045	461.724	459.752	30.199	0.1037	0.4462
9047	462.020	459.758	30.206	0.1036	0.5123
9049	462.322	459.747	30.209	0.1035	0.5828

9051	461.127	459.771	40.275	0.1076	0.3284
9053	461.412	459.770	40.269	0.1076	0.3846
9055	461.678	459.771	40.258	0.1077	0.4462
9057	461.973	459.775	40.248	0.1076	0.5125
9059	462.280	459.778	40.244	0.1075	0.5831
10001	482.140	480.490	0.183	0.0871	0.3163
10003	482.424	480.488	0.183	0.0871	0.3704
10005	482.742	480.496	0.183	0.0872	0.4297
10007	483.033	480.497	0.184	0.0869	0.4933
10009	483.391	480.498	0.184	0.0871	0.5611
10011	482.078	480.517	5.144	0.0903	0.3162
10013	482.341	480.510	5.145	0.0903	0.3702
10015	482.642	480.510	5.146	0.0902	0.4294
10017	482.966	480.513	5.146	0.0902	0.4931
10019	483.312	480.511	5.147	0.0901	0.5610
10021	482.227	480.677	5.215	0.0903	0.3160
10023	482.511	480.684	5.214	0.0903	0.3700
10025	482.806	480.680	5.210	0.0903	0.4292
10027	483.138	480.686	5.210	0.0902	0.4929
10029	483.481	480.686	5.209	0.0902	0.5608
10031	482.183	480.688	10.157	0.0931	0.3160
10033	482.446	480.684	10.158	0.0931	0.3700
10035	482.738	480.686	10.159	0.0931	0.4292
10037	483.049	480.687	10.160	0.0930	0.4927
10039	483.380	480.683	10.161	0.0930	0.5606
10041	481.966	480.703	20.361	0.0975	0.3161
10043	482.213	480.697	20.361	0.0977	0.3701
10045	482.494	480.698	20.361	0.0977	0.4293
10047	482.982	480.693	20.360	0.0975	0.4931
10049	483.304	480.699	20.359	0.0975	0.5611
10051	482.044	480.705	30.461	0.1022	0.3162
10053	482.282	480.698	30.461	0.1021	0.3702
10055	482.650	480.698	30.461	0.1020	0.4295
10057	482.933	480.694	30.460	0.1020	0.4932
10059	483.244	480.699	30.460	0.1019	0.5611
10061	482.044	480.700	40.419	0.1060	0.3162
10063	482.282	480.703	40.419	0.1061	0.3703
10065	482.544	480.705	40.419	0.1061	0.4295
10067	482.815	480.699	40.421	0.1060	0.4932
10069	483.115	480.703	40.421	0.1061	0.5611
11001	502.136	500.513	0.435	0.0850	0.3053
11003	502.423	500.518	0.436	0.0849	0.3575
11005	502.729	500.523	0.444	0.0849	0.4145
11007	503.059	500.522	0.446	0.0848	0.4759
11009	503.416	500.524	0.448	0.0848	0.5414
11011	502.132	500.548	5.197	0.0880	0.3052
11013	502.409	500.554	5.190	0.0880	0.3574
11015	502.708	500.555	5.188	0.0881	0.4147
11017	503.028	500.554	5.186	0.0881	0.4761
11019	503.370	500.558	5.191	0.0880	0.5416
11021	502.074	500.580	10.192	0.0911	0.3051
11023	502.329	500.576	10.193	0.0911	0.3572
11025	502.630	500.589	10.195	0.0911	0.4144
11027	502.935	500.583	10.196	0.0910	0.4758
11029	503.273	500.589	10.194	0.0910	0.5414
11031	501.983	500.625	20.349	0.0965	0.3051

11033	502.232	500.622	20.338	0.0966	0.3574
11035	502.537	500.625	20.333	0.0965	0.4146
11037	502.832	500.626	20.331	0.0964	0.4761
11039	503.146	500.627	20.334	0.0964	0.5417
11041	501.790	500.637	30.448	0.1010	0.3051
11043	502.027	500.636	30.449	0.1010	0.3572
11045	502.296	500.641	30.451	0.1010	0.4144
11047	502.580	500.646	30.451	0.1009	0.4758
11049	503.060	500.637	30.452	0.1009	0.5415
11051	501.948	500.658	40.475	0.1052	0.3053
11053	502.176	500.659	40.477	0.1051	0.3574
11055	502.436	500.663	40.478	0.1050	0.4146
11057	502.703	500.658	40.479	0.1049	0.4761
11059	502.992	500.661	40.480	0.1049	0.5417

Table A2. Thermal conductivity for Jet-A-3638 in the liquid phase.

Point ID	T_0 (K)	T_e (K)	P_e (MPa)	λ_e (W·m^{-1}K^{-1})	q (W·m^{-1})
1001	299.529	301.523	0.139	0.1117	0.4632
1003	299.531	301.866	0.140	0.1116	0.5423
1005	299.527	302.236	0.140	0.1116	0.6291
1007	299.530	302.637	0.140	0.1115	0.7223
1009	299.530	303.069	0.127	0.1114	0.8221
1011	299.541	301.455	5.175	0.1133	0.4631
1013	299.541	301.793	5.170	0.1132	0.5423
1015	299.542	302.160	5.164	0.1132	0.6290
1017	299.537	302.552	5.162	0.1131	0.7222
1019	299.538	302.976	5.158	0.1130	0.8216
1021	299.545	301.430	9.801	0.1147	0.4631
1023	299.549	301.767	9.739	0.1146	0.5423
1025	299.545	302.175	9.678	0.1145	0.6291
1027	299.545	302.567	9.619	0.1145	0.7223
1029	299.541	302.982	9.563	0.1144	0.8218
1031	299.557	301.435	14.851	0.1160	0.4633
1033	299.554	301.773	14.119	0.1159	0.5424
1035	299.550	302.138	13.551	0.1157	0.6291
1037	299.548	302.529	13.074	0.1155	0.7223
1039	299.548	302.949	12.663	0.1152	0.8217
2001	317.067	319.004	0.189	0.1092	0.4431
2003	317.087	319.364	0.211	0.1092	0.5187
2005	317.102	319.748	0.227	0.1091	0.6016
2007	317.120	320.165	0.242	0.1091	0.6907
2009	317.132	320.601	0.256	0.1091	0.7858
2011	317.272	319.133	5.134	0.1111	0.4427
2013	317.289	319.483	5.148	0.1108	0.5183
2015	317.303	319.862	5.163	0.1110	0.6012
2017	317.316	320.265	5.178	0.1109	0.6902
2019	317.328	320.695	5.184	0.1108	0.7854
2021	317.532	319.448	10.150	0.1125	0.4428
2023	317.541	319.782	10.176	0.1125	0.5182
2025	317.555	320.153	10.194	0.1125	0.6010
2027	317.563	320.549	10.207	0.1124	0.6900

2029	317.578	320.976	10.218	0.1124	0.7851
2031	317.685	319.483	20.061	0.1157	0.4425
2033	317.698	319.819	20.045	0.1156	0.5180
2035	317.707	320.181	20.024	0.1156	0.6008
2037	317.719	320.568	20.007	0.1155	0.6898
2039	317.730	320.979	19.988	0.1155	0.7848
2041	317.831	319.597	26.754	0.1175	0.4425
2043	317.836	320.009	24.973	0.1170	0.5180
2045	317.835	320.372	23.951	0.1167	0.6008
2047	317.844	320.761	23.234	0.1164	0.6898
2049	317.853	321.174	22.684	0.1163	0.7848
3001	338.468	340.321	0.207	0.1062	0.4206
3003	338.473	340.647	0.212	0.1062	0.4925
3005	338.478	341.008	0.209	0.1060	0.5713
3007	338.488	341.403	0.204	0.1060	0.6561
3009	338.492	341.818	0.203	0.1060	0.7466
3011	338.636	340.492	5.414	0.1081	0.4206
3013	338.640	340.813	5.403	0.1081	0.4927
3015	338.644	341.163	5.407	0.1080	0.5714
3017	338.652	341.546	5.416	0.1081	0.6560
3019	338.661	341.951	5.425	0.1079	0.7463
3021	338.700	340.494	10.105	0.1099	0.4204
3023	338.709	340.821	10.092	0.1100	0.4925
3025	338.710	341.164	10.079	0.1097	0.5714
3027	338.717	341.539	10.083	0.1097	0.6560
3029	338.716	341.932	10.091	0.1097	0.7463
3031	338.769	340.523	20.136	0.1132	0.4204
3033	338.773	340.831	20.134	0.1135	0.4922
3035	338.773	341.165	20.120	0.1135	0.5712
3037	338.773	341.527	20.110	0.1132	0.6560
3039	338.782	341.918	20.106	0.1132	0.7464
3041	338.824	340.487	30.069	0.1165	0.4204
3043	338.825	340.787	30.046	0.1165	0.4922
3045	338.829	341.114	30.015	0.1164	0.5709
3047	338.832	341.468	29.965	0.1163	0.6558
3049	338.837	341.848	29.932	0.1164	0.7463
3051	338.851	340.561	30.996	0.1167	0.4204
3053	338.853	340.861	30.654	0.1166	0.4922
3055	338.857	341.192	30.363	0.1165	0.5709
3057	338.857	341.547	30.107	0.1162	0.6555
3059	338.861	341.924	29.862	0.1161	0.7462
4001	358.082	359.910	0.281	0.1033	0.4023
4003	358.089	360.234	0.287	0.1033	0.4710
4005	358.091	360.587	0.293	0.1032	0.5463
4007	358.097	360.960	0.300	0.1032	0.6272
4009	358.101	361.361	0.305	0.1031	0.7135
4011	358.150	359.922	5.079	0.1053	0.4021
4013	358.153	360.235	5.084	0.1054	0.4709
4015	358.156	360.575	5.090	0.1053	0.5461
4017	358.164	360.948	5.094	0.1052	0.6270
4019	358.164	361.338	5.097	0.1051	0.7133
4021	358.222	359.987	10.072	0.1073	0.4021
4023	358.225	360.296	10.075	0.1072	0.4708
4025	358.229	360.633	10.059	0.1072	0.5464
4027	358.228	360.991	10.055	0.1071	0.6274
4029	358.235	361.379	10.056	0.1070	0.7138

4031	358.276	359.984	20.197	0.1111	0.4021
4033	358.279	360.281	20.200	0.1109	0.4708
4035	358.279	360.602	20.203	0.1109	0.5461
4037	358.282	360.955	20.187	0.1109	0.6273
4039	358.284	361.328	20.184	0.1108	0.7137
4041	358.321	359.970	30.400	0.1144	0.4021
4043	358.322	360.259	30.403	0.1145	0.4708
4045	358.322	360.569	30.396	0.1145	0.5463
4047	358.325	360.911	30.398	0.1143	0.6271
4049	358.322	361.269	30.387	0.1145	0.7138
4051	358.350	359.945	39.278	0.1175	0.4021
4053	358.350	360.225	39.136	0.1174	0.4709
4055	358.347	360.531	39.002	0.1173	0.5462
4057	358.354	360.868	38.876	0.1172	0.6271
4059	358.352	361.221	38.753	0.1171	0.7135
5001	378.914	380.728	0.241	0.1005	0.3849
5003	378.916	381.040	0.238	0.1003	0.4507
5005	378.914	381.370	0.241	0.1001	0.5227
5007	378.916	381.732	0.247	0.1000	0.6000
5009	378.918	382.123	0.251	0.1000	0.6826
5011	378.953	380.690	5.093	0.1025	0.3847
5013	378.955	380.990	5.098	0.1023	0.4504
5015	378.952	381.315	5.100	0.1024	0.5223
5017	378.954	381.672	5.103	0.1022	0.5997
5019	378.951	382.047	5.104	0.1021	0.6824
5021	378.969	380.661	10.042	0.1046	0.3848
5023	378.966	380.954	10.049	0.1044	0.4504
5025	378.970	381.279	10.052	0.1044	0.5224
5027	378.970	381.628	10.054	0.1044	0.5997
5029	378.969	381.995	10.055	0.1043	0.6824
5031	378.996	380.608	20.271	0.1086	0.3846
5033	378.995	380.892	20.266	0.1085	0.4503
5035	378.993	381.204	20.257	0.1087	0.5225
5037	378.993	381.538	20.249	0.1085	0.6000
5039	378.996	381.953	20.241	0.1084	0.6829
5041	379.013	380.596	30.354	0.1124	0.3847
5043	379.011	380.867	30.353	0.1123	0.4504
5045	379.010	381.172	30.355	0.1123	0.5224
5047	379.005	381.495	30.345	0.1122	0.6000
5049	379.012	381.851	30.337	0.1120	0.6828
5051	379.023	380.533	40.332	0.1157	0.3847
5053	379.028	380.805	40.332	0.1156	0.4504
5055	379.022	381.097	40.332	0.1157	0.5224
5057	379.025	381.414	40.324	0.1155	0.5999
5059	379.021	381.751	40.308	0.1155	0.6828
6001	397.146	398.949	0.309	0.0974	0.3704
6003	397.154	399.261	0.317	0.0975	0.4336
6005	397.164	399.606	0.325	0.0975	0.5029
6007	397.171	399.973	0.332	0.0974	0.5774
6009	397.182	400.367	0.338	0.0973	0.6569
6011	397.207	398.971	0.132	0.0975	0.3700
6013	397.223	399.296	0.129	0.0975	0.4333
6015	397.227	399.638	0.131	0.0972	0.5026
6017	397.231	399.996	0.136	0.0973	0.5770
6019	397.238	400.388	0.145	0.0973	0.6564
6021	397.311	398.985	5.093	0.1001	0.3699

6023	397.324	399.294	5.092	0.0999	0.4332
6025	397.327	399.625	5.093	0.0998	0.5025
6027	397.335	399.977	5.098	0.0997	0.5768
6029	397.336	400.353	5.106	0.0997	0.6562
6031	397.394	399.055	10.156	0.1023	0.3699
6033	397.398	399.351	10.160	0.1023	0.4331
6035	397.406	399.675	10.160	0.1022	0.5024
6037	397.410	400.023	10.162	0.1021	0.5768
6039	397.415	400.391	10.170	0.1021	0.6562
6041	397.466	399.068	20.278	0.1064	0.3698
6043	397.473	399.354	20.272	0.1064	0.4331
6045	397.470	399.659	20.271	0.1062	0.5024
6047	397.477	399.996	20.274	0.1063	0.5768
6049	397.481	400.355	20.279	0.1062	0.6563
6051	397.558	399.115	30.305	0.1104	0.3698
6053	397.561	399.390	30.307	0.1103	0.4329
6055	397.557	399.682	30.309	0.1102	0.5021
6057	397.564	400.006	30.310	0.1103	0.5766
6059	397.569	400.352	30.312	0.1102	0.6561
6061	397.633	399.142	40.400	0.1138	0.3698
6063	397.631	399.405	40.402	0.1138	0.4329
6065	397.637	399.699	40.401	0.1138	0.5021
6067	397.642	400.009	40.400	0.1140	0.5766
6069	397.636	400.335	40.400	0.1139	0.6561
7001	418.050	419.815	0.253	0.0948	0.3548
7003	418.054	420.122	0.261	0.0947	0.4153
7005	418.061	420.455	0.265	0.0947	0.4817
7007	418.072	420.720	0.270	0.0946	0.5529
7009	418.077	421.104	0.278	0.0945	0.6290
7011	418.139	419.756	5.182	0.0973	0.3547
7013	418.147	420.046	5.186	0.0974	0.4152
7015	418.150	420.372	5.190	0.0973	0.4816
7017	418.155	420.721	5.194	0.0973	0.5529
7019	418.166	421.098	5.200	0.0972	0.6291
7021	418.275	419.897	10.180	0.0998	0.3546
7023	418.277	420.191	10.178	0.0998	0.4152
7025	418.285	420.511	10.177	0.0997	0.4816
7027	418.286	420.847	10.173	0.0996	0.5531
7029	418.289	421.205	10.178	0.0996	0.6292
7031	418.343	419.902	20.267	0.1044	0.3545
7033	418.336	420.166	20.271	0.1043	0.4150
7035	418.342	420.475	20.266	0.1043	0.4815
7037	418.346	420.801	20.259	0.1042	0.5530
7039	418.350	421.148	20.260	0.1043	0.6292
7041	418.396	419.896	30.283	0.1083	0.3546
7043	418.403	420.166	30.280	0.1084	0.4152
7045	418.401	420.451	30.280	0.1084	0.4816
7047	418.404	420.764	30.283	0.1083	0.5530
7049	418.406	421.093	30.286	0.1084	0.6292
7051	418.442	419.873	40.318	0.1123	0.3545
7053	418.439	420.123	40.313	0.1122	0.4151
7055	418.442	420.406	40.307	0.1124	0.4816
7057	418.446	420.714	40.306	0.1122	0.5530
7059	418.446	421.030	40.301	0.1123	0.6292
8001	439.401	441.055	0.283	0.0922	0.3402
8003	439.414	441.365	0.287	0.0922	0.3983

8005	439.412	441.678	0.290	0.0921	0.4619
8007	439.412	442.024	0.293	0.0920	0.5304
8009	439.416	442.391	0.294	0.0919	0.6035
8011	439.451	441.068	5.095	0.0949	0.3402
8013	439.455	441.357	5.099	0.0949	0.3983
8015	439.455	441.669	5.100	0.0949	0.4619
8017	439.454	441.997	5.101	0.0948	0.5304
8019	439.455	442.360	5.103	0.0947	0.6035
8021	439.485	441.057	10.102	0.0976	0.3402
8023	439.490	441.338	10.103	0.0975	0.3983
8025	439.492	441.642	10.106	0.0974	0.4620
8027	439.493	441.972	10.106	0.0975	0.5305
8029	439.497	442.323	10.109	0.0974	0.6036
8031	439.534	441.016	20.423	0.1025	0.3402
8033	439.542	441.285	20.425	0.1024	0.3983
8035	439.539	441.572	20.427	0.1024	0.4620
8037	439.538	441.883	20.428	0.1023	0.5304
8039	439.540	442.217	20.427	0.1023	0.6035
8041	439.570	440.969	30.537	0.1068	0.3402
8043	439.571	441.221	30.538	0.1068	0.3983
8045	439.571	441.501	30.538	0.1068	0.4620
8047	439.572	441.803	30.532	0.1068	0.5306
8049	439.575	442.125	30.529	0.1068	0.6037
8051	439.599	440.964	40.385	0.1108	0.3402
8053	439.597	441.209	40.387	0.1108	0.3983
8055	439.594	441.479	40.387	0.1109	0.4620
8057	439.600	441.770	40.382	0.1107	0.5306
8059	439.597	442.079	40.377	0.1106	0.6038
9001	459.926	461.620	0.176	0.0894	0.3276
9003	459.929	461.857	0.180	0.0894	0.3835
9005	459.936	462.183	0.185	0.0894	0.4447
9007	459.937	462.512	0.188	0.0893	0.5106
9009	459.938	462.877	0.189	0.0892	0.5809
9011	459.977	461.576	5.141	0.0926	0.3276
9013	459.972	461.848	5.147	0.0925	0.3835
9015	459.981	462.160	5.151	0.0925	0.4447
9017	459.983	462.487	5.154	0.0925	0.5106
9019	459.982	462.840	5.157	0.0924	0.5809
9021	459.999	461.512	10.160	0.0951	0.3275
9023	460.004	461.789	10.158	0.0950	0.3835
9025	460.003	462.083	10.159	0.0949	0.4448
9027	460.006	462.405	10.165	0.0949	0.5106
9029	460.009	462.753	10.168	0.0949	0.5809
9031	460.042	461.486	20.580	0.1004	0.3276
9033	460.047	461.750	20.587	0.1004	0.3834
9035	460.048	462.033	20.587	0.1003	0.4447
9037	460.043	462.334	20.589	0.1003	0.5106
9039	460.042	462.656	20.592	0.1002	0.5810
9041	460.086	461.498	30.374	0.1050	0.3275
9043	460.087	461.749	30.376	0.1048	0.3835
9045	460.082	462.014	30.377	0.1048	0.4448
9047	460.078	462.302	30.378	0.1049	0.5107
9049	460.079	462.613	30.378	0.1047	0.5810
9051	460.094	461.416	40.317	0.1089	0.3275
9053	460.089	461.652	40.318	0.1090	0.3835
9055	460.082	461.903	40.317	0.1089	0.4448

9057	460.087	462.193	40.316	0.1089	0.5107
9059	460.084	462.490	40.318	0.1088	0.5811
10001	479.411	481.097	0.336	0.0871	0.3161
10003	479.412	481.381	0.340	0.0870	0.3700
10005	479.415	481.696	0.343	0.0870	0.4291
10007	479.415	482.031	0.345	0.0870	0.4926
10009	479.420	482.389	0.347	0.0870	0.5605
10011	479.438	481.018	5.174	0.0904	0.3159
10013	479.441	481.295	5.176	0.0904	0.3699
10015	479.438	481.591	5.178	0.0903	0.4290
10017	479.441	481.917	5.180	0.0903	0.4926
10019	479.437	482.255	5.182	0.0903	0.5604
10021	479.457	480.979	10.139	0.0936	0.3159
10023	479.460	481.249	10.141	0.0934	0.3699
10025	479.458	481.540	10.143	0.0934	0.4290
10027	479.458	481.849	10.144	0.0933	0.4926
10029	479.465	482.187	10.145	0.0933	0.5605
10031	479.480	480.776	20.316	0.0984	0.3159
10033	479.479	481.025	20.317	0.0983	0.3699
10035	479.479	481.307	20.320	0.0983	0.4290
10037	479.480	481.604	20.323	0.0983	0.4926
10039	479.477	481.922	20.325	0.0981	0.5605
10041	479.520	480.915	30.444	0.1032	0.3160
10043	479.521	481.159	30.446	0.1032	0.3700
10045	479.521	481.428	30.443	0.1031	0.4292
10047	479.517	481.709	30.430	0.1030	0.4930
10049	479.523	482.019	30.426	0.1030	0.5610
10051	479.537	480.848	40.385	0.1075	0.3161
10053	479.543	481.093	40.375	0.1075	0.3702
10055	479.537	481.339	40.372	0.1073	0.4294
10057	479.537	481.617	40.369	0.1073	0.4931
10059	479.533	481.903	40.373	0.1072	0.5610
11001	498.852	500.487	0.272	0.0847	0.3054
11003	498.859	500.779	0.272	0.0846	0.3575
11005	498.860	501.086	0.272	0.0846	0.4146
11007	498.868	501.425	0.273	0.0845	0.4761
11009	498.865	501.775	0.273	0.0845	0.5416
11011	498.891	500.429	5.205	0.0883	0.3053
11013	498.890	500.696	5.207	0.0883	0.3574
11015	498.891	500.993	5.209	0.0882	0.4146
11017	498.894	501.317	5.210	0.0882	0.4760
11019	498.892	501.649	5.210	0.0881	0.5416
11021	498.917	500.411	10.153	0.0913	0.3053
11023	498.922	500.676	10.156	0.0914	0.3575
11025	498.917	500.955	10.159	0.0914	0.4146
11027	498.920	501.269	10.159	0.0914	0.4760
11029	498.918	501.594	10.157	0.0914	0.5417
11031	498.959	500.316	20.481	0.0971	0.3053
11033	498.959	500.567	20.481	0.0972	0.3574
11035	498.952	500.827	20.483	0.0971	0.4146
11037	498.952	501.120	20.485	0.0971	0.4760
11039	498.956	501.437	20.487	0.0971	0.5416
11041	498.980	500.173	30.448	0.1016	0.3053
11043	498.983	500.414	30.450	0.1015	0.3575
11045	498.980	500.669	30.452	0.1016	0.4146
11047	498.976	500.951	30.451	0.1016	0.4761

11049	498.979	501.252	30.444	0.1013	0.5419
11051	498.975	500.341	30.450	0.1011	0.3055
11053	498.980	500.585	30.444	0.1014	0.3577
11055	498.979	500.846	30.440	0.1016	0.4149
11057	498.989	501.139	30.440	0.1014	0.4765
11059	498.982	501.429	30.445	0.1014	0.5420
11061	498.998	500.288	40.475	0.1061	0.3054
11063	498.996	500.510	40.477	0.1059	0.3576
11065	498.995	500.762	40.474	0.1061	0.4148
11067	498.992	501.029	40.465	0.1060	0.4764
11069	499.002	501.329	40.464	0.1059	0.5421

Table A3. Thermal conductivity Jet-A-4658 in the liquid phase.

Point ID	T_0 (K)	T_e (K)	P_e (MPa)	λ_e ($W \cdot m^{-1} K^{-1}$)	q ($W \cdot m^{-1}$)
1001	300.096	301.759	0.169	0.1119	0.3909
1003	300.100	302.080	0.173	0.1120	0.4654
1005	300.103	302.430	0.175	0.1120	0.5451
1007	300.102	302.800	0.177	0.1119	0.6322
1009	300.100	303.201	0.178	0.1118	0.7259
1011	300.131	301.771	5.661	0.1135	0.3913
1013	300.131	302.085	5.660	0.1137	0.4658
1015	300.130	302.421	5.669	0.1136	0.5453
1017	300.132	302.789	5.677	0.1135	0.6323
1019	300.131	303.186	5.683	0.1135	0.7260
1021	300.120	301.726	10.376	0.1151	0.3910
1023	300.121	302.035	10.377	0.1149	0.4654
1025	300.124	302.371	10.378	0.1150	0.5451
1027	300.120	302.734	10.378	0.1149	0.6322
1029	300.125	303.132	10.379	0.1148	0.7258
1031	300.144	301.699	20.338	0.1178	0.3911
1033	300.144	302.000	20.341	0.1177	0.4655
1035	300.144	302.325	20.345	0.1177	0.5450
1037	300.138	302.674	20.346	0.1177	0.6321
1039	300.140	303.062	20.345	0.1176	0.7258
1041	300.157	301.659	29.673	0.1202	0.3911
1043	300.153	301.950	29.503	0.1202	0.4655
1045	300.153	302.273	29.339	0.1200	0.5450
1047	300.154	302.629	29.142	0.1199	0.6327
1049	300.153	303.008	28.981	0.1200	0.7267
1051	300.151	301.688	30.288	0.1204	0.3916
1053	300.154	301.993	30.042	0.1202	0.4661
1055	300.149	302.307	29.829	0.1202	0.5455
1057	300.148	302.658	29.623	0.1201	0.6324
1059	300.145	303.033	29.424	0.1200	0.7260
2001	318.502	320.420	0.261	0.1097	0.4444
2003	318.500	320.745	0.253	0.1095	0.5205
2005	318.502	321.108	0.248	0.1095	0.6038
2007	318.501	321.498	0.248	0.1094	0.6932
2009	318.506	321.919	0.257	0.1094	0.7884
2011	318.517	320.396	5.594	0.1114	0.4441
2013	318.517	320.722	5.595	0.1112	0.5200

2015	318.519	321.081	5.594	0.1113	0.6032
2017	318.523	321.471	5.592	0.1112	0.6926
2019	318.518	321.876	5.573	0.1112	0.7884
2021	318.537	320.389	10.323	0.1129	0.4441
2023	318.535	320.709	10.324	0.1128	0.5200
2025	318.536	321.067	10.317	0.1128	0.6033
2027	318.536	321.447	10.301	0.1127	0.6929
2029	318.544	321.859	10.292	0.1127	0.7885
2031	318.557	320.350	20.726	0.1161	0.4441
2033	318.561	320.669	20.710	0.1161	0.5202
2035	318.557	321.009	20.696	0.1159	0.6036
2037	318.558	321.381	20.690	0.1159	0.6931
2039	318.558	321.778	20.685	0.1159	0.7886
2041	318.570	320.306	30.271	0.1187	0.4445
2043	318.577	320.621	30.268	0.1188	0.5205
2045	318.574	320.955	30.267	0.1187	0.6037
2047	318.567	321.309	30.274	0.1187	0.6930
2049	318.571	321.698	30.284	0.1186	0.7882
2051	318.585	320.312	39.924	0.1214	0.4446
2053	318.582	320.611	39.862	0.1213	0.5206
2055	318.580	320.941	39.802	0.1211	0.6038
2057	318.584	321.300	39.744	0.1211	0.6933
2059	318.581	321.678	39.692	0.1212	0.7887
3001	337.063	339.014	0.430	0.1070	0.4248
3003	337.079	339.362	0.446	0.1070	0.4973
3005	337.095	339.640	0.461	0.1070	0.5767
3007	337.117	340.054	0.474	0.1070	0.6621
3009	337.134	340.487	0.449	0.1069	0.7542
3011	337.462	339.323	0.216	0.1070	0.4249
3013	337.476	339.664	0.248	0.1070	0.4972
3015	337.492	340.035	0.280	0.1069	0.5763
3017	337.503	340.432	0.298	0.1068	0.6615
3019	337.520	340.862	0.315	0.1069	0.7526
3021	337.672	339.502	5.177	0.1089	0.4241
3023	337.686	339.839	5.191	0.1088	0.4965
3025	337.693	340.197	5.201	0.1088	0.5759
3027	337.710	340.596	5.214	0.1086	0.6612
3029	337.721	341.011	5.227	0.1086	0.7522
3031	337.815	339.635	10.394	0.1106	0.4242
3033	337.826	339.962	10.410	0.1106	0.4966
3035	337.833	340.316	10.427	0.1105	0.5759
3037	337.847	340.701	10.441	0.1104	0.6611
3039	337.859	341.112	10.453	0.1104	0.7521
3041	337.956	339.722	20.258	0.1139	0.4242
3043	337.969	340.044	20.271	0.1139	0.4966
3045	337.970	340.383	20.287	0.1138	0.5758
3047	337.982	340.755	20.303	0.1136	0.6610
3049	337.998	341.157	20.316	0.1137	0.7519
3051	338.080	339.801	30.330	0.1170	0.4241
3053	338.088	340.107	30.334	0.1170	0.4966
3055	338.102	340.453	30.346	0.1170	0.5758
3057	338.106	340.808	30.358	0.1168	0.6610
3059	338.114	341.191	30.373	0.1168	0.7519
3061	338.207	339.894	40.361	0.1200	0.4240
3063	338.219	340.199	40.382	0.1198	0.4963
3065	338.223	340.524	40.397	0.1199	0.5755

3067	338.230	340.876	40.410	0.1197	0.6607
3069	338.233	341.246	40.420	0.1197	0.7516
4001	358.387	360.194	0.259	0.1041	0.4043
4003	358.400	360.527	0.264	0.1040	0.4734
4005	358.412	360.887	0.253	0.1039	0.5494
4007	358.416	361.266	0.252	0.1038	0.6310
4009	358.430	361.680	0.259	0.1039	0.7179
4011	358.553	360.358	5.239	0.1061	0.4043
4013	358.563	360.628	5.250	0.1060	0.4732
4015	358.571	360.980	5.259	0.1060	0.5489
4017	358.577	361.353	5.257	0.1058	0.6304
4019	358.586	361.753	5.249	0.1058	0.7175
4021	358.679	360.458	10.300	0.1079	0.4042
4023	358.689	360.774	10.296	0.1079	0.4735
4025	358.695	361.119	10.295	0.1079	0.5493
4027	358.707	361.488	10.298	0.1078	0.6307
4029	358.712	361.830	10.310	0.1078	0.7173
4031	358.804	360.472	20.139	0.1115	0.4043
4033	358.810	360.776	20.145	0.1114	0.4734
4035	358.819	361.107	20.154	0.1115	0.5490
4037	358.827	361.463	20.168	0.1114	0.6301
4039	358.830	361.840	20.179	0.1114	0.7168
4041	358.923	360.572	30.297	0.1149	0.4040
4043	358.928	360.866	30.306	0.1150	0.4730
4045	358.932	361.185	30.313	0.1148	0.5486
4047	358.938	361.533	30.318	0.1147	0.6299
4049	358.945	361.904	30.302	0.1147	0.7171
4051	359.000	360.569	40.347	0.1181	0.4039
4053	359.007	360.857	40.354	0.1180	0.4730
4055	359.005	361.211	40.359	0.1180	0.5487
4057	359.014	361.553	40.364	0.1179	0.6300
4059	359.019	361.913	40.355	0.1179	0.7170
5001	377.692	379.446	0.229	0.1013	0.3878
5003	377.700	379.761	0.233	0.1013	0.4541
5005	377.707	380.107	0.248	0.1012	0.5265
5007	377.711	380.473	0.258	0.1011	0.6044
5009	377.716	380.867	0.266	0.1010	0.6876
5011	377.778	379.525	5.242	0.1034	0.3876
5013	377.786	379.837	5.230	0.1034	0.4541
5015	377.793	380.176	5.229	0.1033	0.5268
5017	377.799	380.540	5.230	0.1033	0.6049
5019	377.808	380.926	5.249	0.1033	0.6878
5021	377.863	379.557	10.147	0.1055	0.3876
5023	377.864	379.856	10.158	0.1054	0.4538
5025	377.871	380.189	10.166	0.1054	0.5264
5027	377.878	380.546	10.173	0.1053	0.6043
5029	377.882	380.925	10.170	0.1052	0.6877
5031	377.966	379.571	20.199	0.1094	0.3877
5033	377.969	379.861	20.212	0.1094	0.4539
5035	377.976	380.230	20.223	0.1093	0.5263
5037	377.980	380.572	20.229	0.1093	0.6043
5039	377.986	380.942	20.235	0.1092	0.6875
5041	378.047	379.657	30.249	0.1130	0.3875
5043	378.054	379.945	30.254	0.1129	0.4538
5045	378.051	380.246	30.259	0.1129	0.5263
5047	378.059	380.584	30.265	0.1128	0.6043

5049	378.062	380.940	30.262	0.1128	0.6877
5051	378.108	379.669	40.426	0.1164	0.3875
5053	378.107	379.941	40.430	0.1163	0.4538
5055	378.113	380.244	40.435	0.1163	0.5263
5057	378.116	380.569	40.438	0.1162	0.6043
5059	378.119	380.914	40.426	0.1162	0.6878
6001	397.892	399.625	0.179	0.0984	0.3716
6003	397.897	399.933	0.183	0.0984	0.4351
6005	397.899	400.268	0.185	0.0984	0.5047
6007	397.905	400.631	0.176	0.0983	0.5797
6009	397.908	401.012	0.177	0.0982	0.6596
6011	397.959	399.671	5.265	0.1009	0.3715
6013	397.965	399.974	5.261	0.1008	0.4352
6015	397.972	400.261	5.259	0.1007	0.5048
6017	397.975	400.615	5.261	0.1007	0.5796
6019	397.983	400.993	5.262	0.1006	0.6594
6021	398.036	399.691	10.282	0.1030	0.3716
6023	398.045	399.990	10.281	0.1030	0.4351
6025	398.047	400.307	10.283	0.1030	0.5047
6027	398.052	400.655	10.286	0.1030	0.5795
6029	398.062	401.032	10.291	0.1029	0.6593
6031	398.229	399.826	20.219	0.1072	0.3715
6033	398.229	400.107	20.221	0.1073	0.4350
6035	398.237	400.419	20.221	0.1070	0.5046
6037	398.236	400.750	20.224	0.1071	0.5794
6039	398.243	401.106	20.229	0.1070	0.6592
6041	398.290	399.833	30.311	0.1110	0.3715
6043	398.290	400.103	30.310	0.1110	0.4350
6045	398.297	400.408	30.312	0.1109	0.5046
6047	398.299	400.727	30.315	0.1109	0.5794
6049	398.296	401.065	30.314	0.1108	0.6592
6051	398.348	399.834	40.459	0.1146	0.3715
6053	398.352	400.102	40.459	0.1146	0.4350
6055	398.349	400.385	40.459	0.1145	0.5046
6057	398.353	400.701	40.459	0.1146	0.5794
6059	398.354	401.032	40.465	0.1145	0.6591
7001	418.962	420.670	0.329	0.0960	0.3563
7003	418.961	420.965	0.334	0.0959	0.4171
7005	418.962	421.286	0.335	0.0959	0.4838
7007	418.961	421.633	0.337	0.0958	0.5555
7009	418.963	422.007	0.338	0.0957	0.6320
7011	418.980	420.586	5.253	0.1001	0.3562
7013	418.986	420.935	5.257	0.0984	0.4171
7015	418.984	421.248	5.258	0.0984	0.4838
7017	418.981	421.586	5.252	0.0984	0.5556
7019	418.983	421.953	5.242	0.0982	0.6323
7021	419.002	420.619	10.394	0.1010	0.3563
7023	419.004	420.905	10.383	0.1009	0.4173
7025	419.008	421.218	10.382	0.1008	0.4841
7027	419.007	421.543	10.380	0.1008	0.5559
7029	419.008	421.901	10.378	0.1007	0.6325
7031	419.043	420.573	20.240	0.1053	0.3562
7033	419.043	420.844	20.243	0.1052	0.4171
7035	419.039	421.137	20.245	0.1051	0.4838
7037	419.041	421.459	20.246	0.1050	0.5555
7039	419.043	421.802	20.241	0.1049	0.6322

7041	419.062	420.509	30.369	0.1092	0.3562
7043	419.059	420.770	30.371	0.1092	0.4171
7045	419.061	421.057	30.370	0.1092	0.4838
7047	419.063	421.370	30.356	0.1091	0.5557
7049	419.059	421.696	30.352	0.1091	0.6324
7051	419.086	420.506	40.407	0.1128	0.3564
7053	419.085	420.758	40.406	0.1129	0.4174
7055	419.081	421.031	40.410	0.1129	0.4840
7057	419.085	421.334	40.416	0.1129	0.5556
7059	419.081	421.649	40.419	0.1128	0.6322
8001	439.283	440.964	0.387	0.0934	0.3425
8003	439.293	441.265	0.398	0.0933	0.4009
8005	439.293	441.586	0.406	0.0933	0.4650
8007	439.301	441.938	0.410	0.0933	0.5338
8009	439.313	442.319	0.403	0.0931	0.6076
8011	439.364	440.972	5.234	0.0962	0.3423
8013	439.370	441.265	5.232	0.0960	0.4009
8015	439.372	441.579	5.224	0.0961	0.4651
8017	439.386	441.924	5.225	0.0960	0.5341
8019	439.386	442.279	5.227	0.0959	0.6076
8021	439.437	441.020	10.276	0.0988	0.3425
8023	439.439	441.299	10.277	0.0987	0.4010
8025	439.446	441.604	10.282	0.0986	0.4650
8027	439.446	441.930	10.290	0.0986	0.5338
8029	439.452	442.284	10.294	0.0985	0.6073
8031	439.515	441.025	20.367	0.1035	0.3423
8033	439.522	441.299	20.371	0.1035	0.4008
8035	439.522	441.588	20.374	0.1034	0.4649
8037	439.522	441.903	20.375	0.1034	0.5338
8039	439.523	442.240	20.367	0.1033	0.6075
8041	439.576	441.017	30.385	0.1075	0.3425
8043	439.579	441.278	30.380	0.1077	0.4011
8045	439.578	441.555	30.380	0.1077	0.4652
8047	439.584	441.859	30.386	0.1075	0.5340
8049	439.579	442.175	30.396	0.1076	0.6074
8051	439.620	440.989	40.408	0.1117	0.3423
8053	439.616	441.229	40.412	0.1116	0.4008
8055	439.616	441.502	40.416	0.1116	0.4649
8057	439.616	441.790	40.418	0.1115	0.5338
8059	439.617	442.102	40.419	0.1115	0.6073
9001	459.247	460.894	0.411	0.0903	0.3299
9003	459.244	461.181	0.413	0.0904	0.3863
9005	459.249	461.498	0.415	0.0903	0.4480
9007	459.257	461.847	0.422	0.0902	0.5142
9009	459.256	462.208	0.428	0.0901	0.5850
9011	459.309	460.902	5.251	0.0933	0.3297
9013	459.314	461.190	5.254	0.0933	0.3860
9015	459.323	461.506	5.254	0.0932	0.4478
9017	459.326	461.838	5.246	0.0932	0.5144
9019	459.328	462.191	5.244	0.0931	0.5853
9021	459.365	460.887	10.221	0.0965	0.3297
9023	459.372	461.163	10.224	0.0964	0.3860
9025	459.374	461.463	10.227	0.0964	0.4477
9027	459.376	461.784	10.221	0.0963	0.5142
9029	459.383	462.133	10.218	0.0963	0.5852
9031	459.510	460.871	20.444	0.1015	0.3296

9033	459.515	461.138	20.446	0.1014	0.3859
9035	459.516	461.423	20.449	0.1014	0.4477
9037	459.520	461.734	20.449	0.1014	0.5141
9039	459.518	462.056	20.449	0.1013	0.5849
9041	459.550	460.915	30.365	0.1057	0.3298
9043	459.548	461.183	30.370	0.1058	0.3861
9045	459.550	461.455	30.373	0.1057	0.4478
9047	459.552	461.753	30.375	0.1057	0.5142
9049	459.553	462.064	30.377	0.1057	0.5850
9051	459.582	460.934	40.496	0.1100	0.3300
9053	459.579	461.169	40.502	0.1100	0.3863
9055	459.576	461.429	40.506	0.1099	0.4480
9057	459.580	461.714	40.511	0.1098	0.5143
9059	459.581	462.015	40.513	0.1098	0.5852
10001	479.309	480.930	0.226	0.0881	0.3182
10003	479.313	481.219	0.227	0.0880	0.3726
10005	479.319	481.535	0.234	0.0880	0.4320
10007	479.327	481.875	0.242	0.0880	0.4959
10009	479.331	482.237	0.248	0.0879	0.5641
10011	479.386	480.981	5.186	0.0914	0.3180
10015	479.395	481.566	5.193	0.0913	0.4320
10017	479.400	481.898	5.188	0.0912	0.4962
10019	479.404	482.251	5.184	0.0911	0.5647
10021	479.433	480.924	10.302	0.0944	0.3182
10023	479.435	481.193	10.308	0.0944	0.3725
10025	479.433	481.478	10.311	0.0943	0.4321
10027	479.441	481.801	10.314	0.0943	0.4961
10029	479.444	482.138	10.318	0.0943	0.5644
10031	479.489	480.767	20.363	0.0997	0.3181
10033	479.494	481.024	20.365	0.0997	0.3726
10035	479.486	481.291	20.369	0.0997	0.4321
10037	479.493	481.596	20.371	0.0997	0.4962
10039	479.497	481.918	20.373	0.0996	0.5645
10041	479.297	480.657	30.321	0.1043	0.3184
10043	479.281	480.862	30.301	0.1043	0.3729
10045	479.249	481.079	30.286	0.1043	0.4326
10047	479.243	481.352	30.274	0.1042	0.4967
10049	479.228	481.632	30.264	0.1042	0.5652
10051	479.242	480.566	40.454	0.1085	0.3184
10053	479.245	480.802	40.455	0.1085	0.3729
10055	479.248	481.059	40.456	0.1085	0.4325
10057	479.252	481.337	40.463	0.1084	0.4966
10059	479.256	481.636	40.468	0.1084	0.5650
11001	499.690	501.277	0.450	0.0858	0.3068
11003	499.693	501.560	0.450	0.0857	0.3593
11005	499.687	501.861	0.453	0.0856	0.4167
11007	499.696	502.203	0.456	0.0856	0.4783
11009	499.692	502.547	0.460	0.0856	0.5441
11011	499.737	501.289	5.240	0.0892	0.3068
11013	499.745	501.573	5.244	0.0891	0.3591
11015	499.749	501.873	5.250	0.0890	0.4165
11017	499.748	502.183	5.253	0.0890	0.4782
11019	499.756	502.535	5.257	0.0889	0.5440
11021	499.795	501.311	10.272	0.0922	0.3068
11023	499.793	501.566	10.280	0.0922	0.3591
11025	499.799	501.860	10.284	0.0922	0.4164

11027	499.803	502.171	10.287	0.0922	0.4781
11029	499.808	502.459	10.290	0.0921	0.5440
11031	499.857	501.081	20.483	0.0978	0.3066
11033	499.853	501.517	20.486	0.0977	0.3591
11035	499.860	501.798	20.486	0.0977	0.4166
11037	499.860	502.092	20.477	0.0977	0.4785
11039	499.866	502.408	20.474	0.0976	0.5445
11043	499.919	501.459	30.417	0.1028	0.3593
11045	499.918	501.717	30.421	0.1026	0.4166
11047	499.911	501.988	30.425	0.1026	0.4784
11049	499.919	502.296	30.428	0.1026	0.5443
11051	499.945	501.211	40.398	0.1069	0.3069
11053	499.947	501.442	40.397	0.1070	0.3593
11055	499.946	501.692	40.391	0.1070	0.4167
11057	499.945	501.961	40.381	0.1069	0.4785
11059	499.945	502.249	40.369	0.1069	0.5444

Table A4. Thermal conductivity for JP-8-3773 in the liquid phase.

Point ID	T_0 (K)	T_e (K)	P_e (MPa)	λ_e ($W \cdot m^{-1}K^{-1}$)	q ($W \cdot m^{-1}$)
1001	300.750	302.502	0.781	0.1157	0.3448
1002	300.748	302.502	0.781	0.1157	0.3448
1003	300.750	302.731	0.782	0.1158	0.3893
1004	300.748	302.727	0.782	0.1158	0.3893
1005	300.748	302.969	0.782	0.1157	0.4364
1006	300.749	302.971	0.783	0.1157	0.4364
1007	300.748	303.226	0.783	0.1155	0.4863
1008	300.749	303.225	0.783	0.1155	0.4862
1009	300.747	303.495	0.783	0.1154	0.5387
1010	300.751	303.497	0.783	0.1151	0.5387
1011	300.758	302.486	5.400	0.1173	0.3448
1012	300.747	302.475	5.400	0.1173	0.3448
1013	300.753	302.709	5.402	0.1173	0.3893
1014	300.754	302.708	5.403	0.1173	0.3893
1015	300.755	302.948	5.404	0.1173	0.4365
1016	300.752	302.945	5.405	0.1172	0.4364
1017	300.752	303.195	5.406	0.1172	0.4863
1018	300.751	303.196	5.406	0.1172	0.4863
1019	300.756	303.467	11.733	0.1171	0.5388
1020	300.755	303.465	11.736	0.1168	0.5388
1021	300.759	302.449	11.738	0.1187	0.3448
1022	300.750	302.444	11.740	0.1187	0.3448
1023	300.755	302.671	11.742	0.1187	0.3893
1024	300.755	302.670	11.743	0.1187	0.3893
1026	300.753	302.907	11.743	0.1181	0.4365
1027	300.756	303.159	11.742	0.1180	0.4862
1029	300.755	303.422	11.741	0.1187	0.5388

1030	300.752	303.416	11.740	0.1187	0.5388
1031	300.771	302.410	20.455	0.1218	0.3448
1032	300.771	302.409	20.455	0.1218	0.3448
1033	300.766	302.623	20.454	0.1218	0.3893
1034	300.769	302.623	20.454	0.1218	0.3893
1035	300.766	302.853	20.454	0.1219	0.4364
1036	300.770	302.855	20.455	0.1220	0.4364
1037	300.765	303.094	20.455	0.1219	0.4862
1038	300.771	303.099	20.456	0.1219	0.4863
1039	300.767	303.354	20.457	0.1218	0.5387
1041	300.785	302.393	30.829	0.1245	0.3448
1042	300.782	302.389	30.829	0.1245	0.3448
1043	300.784	302.606	30.829	0.1244	0.3893
1044	300.785	302.606	30.828	0.1244	0.3893
1045	300.781	302.830	30.830	0.1242	0.4364
1046	300.783	302.831	30.831	0.1237	0.4364
1047	300.785	303.076	30.834	0.1243	0.4862
1048	300.783	303.074	40.906	0.1243	0.4862
1049	300.784	303.326	40.909	0.1238	0.5387
1050	300.781	303.322	40.912	0.1239	0.5387
1051	300.789	302.364	40.912	0.1271	0.3448
1052	300.787	302.363	40.916	0.1271	0.3448
1053	300.791	302.577	40.918	0.1270	0.3893
1054	300.792	302.576	40.919	0.1270	0.3892
1055	300.783	302.793	40.921	0.1272	0.4364
1056	300.787	302.796	40.923	0.1272	0.4364
1057	300.788	303.031	40.923	0.1271	0.4862
1058	300.788	303.029	50.744	0.1271	0.4862
1059	300.785	303.274	50.744	0.1270	0.5387
1060	300.787	303.276	50.748	0.1264	0.5387
1061	300.796	302.359	50.750	0.1296	0.3447
1062	300.792	302.354	50.749	0.1296	0.3447
1063	300.794	302.572	50.750	0.1297	0.3891
1064	300.796	302.572	50.751	0.1297	0.3892
1065	300.793	302.787	60.438	0.1298	0.4363
1066	300.792	302.787	60.426	0.1299	0.4363
1067	300.795	303.020	60.413	0.1296	0.4861
1068	300.791	303.014	60.400	0.1295	0.4861
1069	300.794	303.262	60.389	0.1294	0.5386
1070	300.788	303.255	60.376	0.1293	0.5386
1071	300.798	302.319	60.366	0.1319	0.3447
1072	300.795	302.317	60.356	0.1319	0.3447
1073	300.797	302.522	60.346	0.1317	0.3892
1074	300.798	302.524	60.334	0.1317	0.3892
1075	300.795	302.734	0.781	0.1318	0.4363
1076	300.795	302.734	0.781	0.1317	0.4363
1077	300.798	302.963	0.782	0.1317	0.4861
1078	300.795	302.960	0.782	0.1317	0.4861

1079	300.796	303.199	0.782	0.1316	0.5386
1080	300.790	303.196	0.783	0.1314	0.5386
2003	355.094	357.010	0.783	0.1050	0.3506
2004	355.098	357.013	0.783	0.1049	0.3506
2005	355.100	357.256	0.783	0.1053	0.3930
2006	355.099	357.253	0.783	0.1053	0.3930
2007	355.102	357.508	5.400	0.1054	0.4379
2008	355.105	357.513	5.400	0.1054	0.4379
2009	355.107	357.778	5.402	0.1054	0.4851
2010	355.110	357.781	5.403	0.1053	0.4851
2011	355.146	356.812	5.404	0.1076	0.3105
2012	355.144	356.813	5.405	0.1076	0.3105
2015	355.150	357.276	5.406	0.1072	0.3930
2016	355.150	357.274	5.406	0.1072	0.3930
2017	355.147	357.520	11.733	0.1073	0.4379
2018	355.157	357.527	11.736	0.1073	0.4379
2019	355.149	357.780	11.738	0.1072	0.4851
2020	355.154	357.783	11.740	0.1071	0.4851
2021	355.183	356.825	11.742	0.1093	0.3105
2022	355.182	356.828	11.743	0.1087	0.3105
2023	355.186	357.051	11.743	0.1085	0.3505
2024	355.183	357.048	11.742	0.1086	0.3506
2025	355.188	357.283	11.741	0.1093	0.3930
2026	355.186	357.283	11.740	0.1092	0.3930
2027	355.191	357.529	20.455	0.1093	0.4378
2028	355.193	357.529	20.455	0.1092	0.4379
2029	355.188	357.784	20.454	0.1088	0.4851
2030	355.194	357.787	20.454	0.1087	0.4851
2031	355.242	356.830	20.454	0.1135	0.3105
2032	355.237	356.826	20.455	0.1135	0.3105
2033	355.241	357.040	20.455	0.1133	0.3505
2034	355.242	357.040	20.456	0.1132	0.3506
2035	355.244	357.265	20.457	0.1127	0.3930
2036	355.236	357.257	30.829	0.1128	0.3930
2037	355.245	357.501	30.829	0.1126	0.4378
2038	355.240	357.495	30.829	0.1125	0.4379
2039	355.244	357.749	30.828	0.1128	0.4851
2040	355.249	357.754	30.830	0.1129	0.4851
2043	355.278	357.015	30.831	0.1166	0.3505
2044	355.286	357.023	30.834	0.1166	0.3506
2045	355.278	357.228	40.906	0.1168	0.3930
2046	355.282	357.233	40.909	0.1167	0.3930
2047	355.285	357.466	40.912	0.1155	0.4378
2048	355.284	357.463	40.912	0.1158	0.4379
2049	355.282	357.706	40.916	0.1156	0.4851
2050	355.288	357.710	40.918	0.1156	0.4851
2051	355.307	356.806	40.919	0.1200	0.3105
2052	355.311	356.808	40.921	0.1199	0.3105

2053	355.304	357.001	40.923	0.1193	0.3505
2054	355.311	357.008	40.923	0.1193	0.3505
2055	355.307	357.216	50.744	0.1187	0.3930
2056	355.307	357.216	50.744	0.1192	0.3930
2057	355.311	357.443	50.748	0.1197	0.4378
2058	355.304	357.435	50.750	0.1198	0.4378
2059	355.308	357.675	50.749	0.1193	0.4851
2060	355.301	357.668	50.750	0.1192	0.4851
2063	355.318	356.963	50.751	0.1229	0.3505
2064	355.323	356.969	60.438	0.1229	0.3505
2065	355.322	357.174	60.426	0.1222	0.3930
2066	355.317	357.179	60.413	0.1222	0.3930
2067	355.321	357.401	60.400	0.1229	0.4378
2068	355.315	357.395	60.389	0.1226	0.4378
2069	355.319	357.628	60.376	0.1225	0.4851
2070	355.319	357.626	60.366	0.1225	0.4851
2072	355.331	356.765	60.356	0.1248	0.3104
2073	355.331	356.955	60.346	0.1247	0.3505
2074	355.334	356.954	60.334	0.1247	0.3505
2075	355.336	357.161	0.781	0.1249	0.3929
2076	355.327	357.152	0.781	0.1247	0.3929
2077	355.335	357.375	0.782	0.1254	0.4378
2078	355.328	357.364	0.782	0.1254	0.4378
2079	355.331	357.594	0.782	0.1261	0.4850
2080	355.330	357.590	0.783	0.1261	0.4851
3001	404.755	406.536	0.783	0.0967	0.3003
3003	404.757	406.775	0.783	0.0965	0.3391
3004	404.754	406.776	0.783	0.0964	0.3391
3005	404.759	407.027	0.783	0.0961	0.3801
3006	404.762	407.033	5.400	0.0957	0.3801
3007	404.760	407.294	5.400	0.0952	0.4235
3009	404.769	407.586	5.402	0.0961	0.4691
3010	404.764	407.581	5.403	0.0962	0.4692
3011	404.792	406.526	5.404	0.0993	0.3003
3012	404.795	406.528	5.405	0.0994	0.3003
3013	404.797	406.760	5.406	0.0986	0.3391
3014	404.791	406.754	5.406	0.0986	0.3391
3015	404.797	407.002	11.733	0.0992	0.3801
3016	404.792	406.995	11.736	0.0991	0.3801
3017	404.799	407.260	11.738	0.0990	0.4235
3019	404.792	407.525	11.740	0.0991	0.4692
3021	404.816	406.498	11.742	0.1011	0.3003
3022	404.810	406.493	11.743	0.1011	0.3003
3027	404.808	407.210	11.743	0.1007	0.4235
3028	404.811	407.213	11.742	0.1000	0.4235
3030	404.809	407.474	11.741	0.1000	0.4692
3031	404.814	406.514	11.740	0.1011	0.3003
3032	404.815	406.515	20.455	0.1012	0.3004

3035	404.815	406.980	20.455	0.1006	0.3801
3036	404.810	406.958	20.454	0.1001	0.3801
3037	404.814	407.234	20.454	0.1005	0.4235
3038	404.813	407.233	20.454	0.1001	0.4235
3039	404.815	407.500	20.455	0.1002	0.4692
3040	404.816	407.499	20.455	0.0999	0.4692
3041	404.840	406.453	20.456	0.1061	0.3004
3042	404.842	406.458	20.457	0.1061	0.3003
3043	404.837	406.671	30.829	0.1062	0.3391
3044	404.837	406.665	30.829	0.1060	0.3391
3047	404.835	407.136	30.829	0.1056	0.4235
3048	404.836	407.137	30.828	0.1055	0.4236
3049	404.835	407.390	30.830	0.1058	0.4692
3050	404.833	407.387	30.831	0.1058	0.4692
3053	404.853	406.616	30.834	0.1099	0.3391
3054	404.851	406.616	40.906	0.1100	0.3392
3055	404.851	406.834	40.909	0.1101	0.3802
3056	404.852	406.835	40.912	0.1100	0.3802
3057	404.851	407.067	40.912	0.1100	0.4235
3058	404.850	407.061	40.916	0.1100	0.4235
3059	404.852	407.309	40.918	0.1099	0.4693
3060	404.849	407.306	40.919	0.1100	0.4693
3061	404.861	406.367	40.921	0.1139	0.3004
3062	404.854	406.356	40.923	0.1139	0.3004
3063	404.866	406.571	40.923	0.1139	0.3391
3064	404.857	406.562	50.744	0.1139	0.3391
3065	404.861	406.777	50.744	0.1138	0.3802
3066	404.859	406.772	50.748	0.1137	0.3802
3067	404.854	406.993	50.750	0.1137	0.4235
3068	404.862	407.001	50.749	0.1138	0.4236
3069	404.857	407.231	50.750	0.1137	0.4692
3070	404.859	407.232	50.751	0.1137	0.4692
3071	404.870	406.332	60.438	0.1174	0.3003
3072	404.865	406.359	60.426	0.1174	0.3003
3073	404.868	406.558	60.413	0.1174	0.3390
3074	404.862	406.550	60.400	0.1173	0.3390
3075	404.864	406.757	60.389	0.1173	0.3801
3076	404.865	406.759	60.376	0.1173	0.3801
3077	404.861	406.971	60.366	0.1172	0.4235
3078	404.863	406.973	60.356	0.1172	0.4234
3079	404.865	407.204	60.346	0.1172	0.4692
3080	404.860	407.199	60.334	0.1172	0.4692
3081	404.874	406.290	0.781	0.1206	0.3003
3082	404.866	406.284	0.781	0.1205	0.3003
3083	404.870	406.476	0.782	0.1205	0.3391
3084	404.873	406.524	0.782	0.1204	0.3390
3085	404.868	406.723	0.782	0.1203	0.3801
3086	404.863	406.718	0.783	0.1203	0.3800

3087	404.864	406.928	0.783	0.1203	0.4234
3088	404.869	406.932	0.783	0.1203	0.4235
3089	404.867	407.156	0.783	0.1202	0.4691
3090	404.864	407.152	0.783	0.1202	0.4691
3091	404.736	406.460	5.400	0.1024	0.3002
3092	404.740	406.425	5.400	0.1029	0.3002
3093	404.740	406.645	5.402	0.1030	0.3389
3094	404.745	406.654	5.403	0.1030	0.3389
3095	404.748	406.888	5.404	0.1027	0.3799
3096	404.742	406.881	5.405	0.1024	0.3799
3097	404.744	407.134	5.406	0.1028	0.4233
3098	404.750	407.140	5.406	0.1027	0.4233
3099	404.745	407.394	11.733	0.1028	0.4690
3100	404.758	407.411	11.736	0.1029	0.4690
4001	451.962	453.817	11.738	0.0877	0.2878
4002	451.965	453.825	11.740	0.0873	0.2878
4003	451.964	454.068	11.742	0.0879	0.3249
4004	451.968	454.072	11.743	0.0871	0.3249
4005	451.970	454.336	11.743	0.0883	0.3642
4006	451.972	454.340	11.742	0.0880	0.3642
4007	451.972	454.613	11.741	0.0882	0.4058
4008	451.973	454.614	11.740	0.0884	0.4058
4009	451.980	454.908	20.455	0.0879	0.4496
4010	451.980	454.904	20.455	0.0881	0.4496
4011	451.988	453.763	20.454	0.0908	0.2878
4012	451.995	453.770	20.454	0.0914	0.2878
4013	451.991	454.001	20.454	0.0913	0.3249
4014	451.993	454.002	20.455	0.0913	0.3249
4015	451.994	454.250	20.455	0.0919	0.3642
4016	451.993	454.249	20.456	0.0919	0.3642
4017	451.991	454.507	20.457	0.0913	0.4058
4018	451.990	454.507	30.829	0.0915	0.4058
4021	452.021	453.726	30.829	0.0957	0.2878
4022	452.016	453.719	30.829	0.0956	0.2878
4023	452.021	453.949	30.828	0.0958	0.3249
4024	452.021	453.950	30.830	0.0958	0.3249
4025	452.026	454.196	30.831	0.0957	0.3642
4027	452.022	454.451	30.834	0.0949	0.4058
4028	452.027	454.459	40.906	0.0948	0.4058
4029	452.021	454.720	40.909	0.0948	0.4496
4030	452.024	454.715	40.912	0.0945	0.4496
4031	452.055	453.727	40.912	0.0990	0.2877
4033	452.051	453.934	40.916	0.0998	0.3249
4034	452.047	453.927	40.918	0.0998	0.3248
4035	452.046	454.157	40.919	0.0989	0.3642
4036	452.052	454.164	40.921	0.0997	0.3642
4037	452.056	454.410	40.923	0.0998	0.4057
4038	452.054	454.408	40.923	0.0998	0.4058

4039	452.049	454.662	50.744	0.0997	0.4495
4040	452.053	454.670	50.744	0.0988	0.4495
4041	452.078	453.644	50.748	0.1042	0.2878
4042	452.077	453.640	50.750	0.1042	0.2878
4043	452.074	453.853	50.749	0.1034	0.3249
4044	452.073	453.848	50.750	0.1034	0.3249
4045	452.078	454.075	50.751	0.1036	0.3642
4046	452.071	454.070	60.438	0.1036	0.3642
4047	452.073	454.305	60.426	0.1041	0.4058
4048	452.075	454.307	60.413	0.1042	0.4058
4051	452.096	453.603	60.400	0.1075	0.2877
4052	452.088	453.595	60.389	0.1076	0.2878
4053	452.097	453.806	60.376	0.1069	0.3249
4054	452.092	453.798	60.366	0.1069	0.3249
4055	452.096	454.020	60.356	0.1070	0.3642
4056	452.093	454.016	60.346	0.1071	0.3642
4057	452.093	454.243	60.334	0.1069	0.4058
4058	452.093	454.242	0.781	0.1069	0.4057
4059	452.087	454.470	0.781	0.1068	0.4496
4061	452.108	453.542	0.782	0.1122	0.2877
4062	452.110	453.547	0.782	0.1121	0.2877
4063	452.110	453.738	0.782	0.1120	0.3249
4064	452.110	453.740	0.783	0.1119	0.3249
4070	452.104	454.386	0.783	0.1114	0.4496
4071	452.103	453.592	0.783	0.1121	0.2877
4072	452.099	453.587	0.783	0.1121	0.2877
4073	452.092	453.773	0.783	0.1122	0.3248
4074	452.104	453.784	5.400	0.1122	0.3248
4075	452.103	453.986	5.400	0.1121	0.3641
4076	452.100	453.988	5.402	0.1120	0.3641
4077	452.100	454.206	5.403	0.1111	0.4057
4078	452.100	454.203	5.404	0.1113	0.4057
4079	452.100	454.433	5.405	0.1119	0.4495
4080	452.098	454.436	5.406	0.1117	0.4495
4081	452.113	453.518	5.406	0.1153	0.2877
4082	452.108	453.512	11.733	0.1156	0.2877
4083	452.113	453.707	11.736	0.1154	0.3248
4084	452.109	453.702	11.738	0.1151	0.3248
4085	452.107	453.899	11.740	0.1154	0.3642
4086	452.108	453.899	11.742	0.1156	0.3642
4087	452.109	454.119	11.743	0.1146	0.4057
4088	452.110	454.118	11.743	0.1148	0.4057
4089	452.106	454.333	11.742	0.1155	0.4495
4090	452.107	454.336	11.741	0.1155	0.4495
4091	452.073	453.601	11.740	0.1117	0.2876
4092	452.070	453.598	20.455	0.1116	0.2876
4093	452.076	453.803	20.455	0.1114	0.3248
4094	452.073	453.803	20.454	0.1117	0.3247

4095	452.073	453.975	20.454	0.1120	0.3641
4096	452.076	453.978	20.454	0.1121	0.3641
4097	452.071	454.191	20.455	0.1120	0.4057
4098	452.076	454.196	20.455	0.1119	0.4056
4099	452.075	454.425	20.456	0.1119	0.4494
4100	452.071	454.422	20.457	0.1117	0.4495
4101	452.048	453.618	30.829	0.1071	0.2877
4102	452.050	453.620	30.829	0.1069	0.2876
4103	452.052	453.801	30.829	0.1075	0.3248
4104	452.053	453.801	30.828	0.1072	0.3248
4105	452.050	454.012	30.830	0.1079	0.3641
4106	452.053	454.016	30.831	0.1078	0.3641
4107	452.050	454.240	30.834	0.1073	0.4056
4108	452.056	454.248	40.906	0.1069	0.4056
4109	452.051	454.481	40.909	0.1074	0.4494
4110	452.051	454.480	40.912	0.1072	0.4494
5003	495.464	497.561	40.912	0.0826	0.3002
5004	495.466	497.567	40.916	0.0818	0.3002
5006	495.473	497.832	40.918	0.0817	0.3366
5007	495.475	498.107	40.919	0.0818	0.3749
5008	495.472	498.106	40.921	0.0819	0.3750
5009	495.478	498.397	40.923	0.0820	0.4154
5010	495.484	498.402	40.923	0.0820	0.4154
5011	495.490	497.336	50.744	0.0818	0.2659
5015	495.494	497.847	50.744	0.0817	0.3366
5016	495.494	497.848	50.748	0.0816	0.3366
5019	495.497	498.403	50.750	0.0824	0.4154
5020	495.502	498.408	50.749	0.0821	0.4154
5021	495.527	497.280	50.750	0.0863	0.2659
5022	495.529	497.280	50.751	0.0863	0.2659
5023	495.529	497.510	60.438	0.0862	0.3002
5024	495.525	497.504	60.426	0.0862	0.3002
5026	495.530	497.768	60.413	0.0857	0.3366
5027	495.527	498.035	60.400	0.0852	0.3750
5028	495.525	498.015	60.389	0.0859	0.3750
5033	495.543	497.452	60.376	0.0904	0.3002
5034	495.546	497.454	60.366	0.0903	0.3002
5035	495.545	497.686	60.356	0.0899	0.3366
5036	495.546	497.684	60.346	0.0896	0.3366
5037	495.541	497.929	60.334	0.0894	0.3750
5038	495.542	497.927	0.781	0.0893	0.3750
5039	495.548	498.194	0.781	0.0900	0.4154
5041	495.556	497.131	0.782	0.0946	0.2659
5042	495.557	497.131	0.782	0.0944	0.2659
5043	495.561	497.373	0.782	0.0946	0.3002
5044	495.558	497.368	0.783	0.0946	0.3002
5045	495.556	497.593	0.783	0.0948	0.3366
5046	495.552	497.586	0.783	0.0939	0.3366

5047	495.554	497.822	0.783	0.0941	0.3750
5048	495.552	497.824	0.783	0.0941	0.3749
5049	495.554	498.074	5.400	0.0938	0.4155
5050	495.548	498.071	5.400	0.0937	0.4154
5051	495.558	497.083	5.402	0.0983	0.2659
5052	495.561	497.084	5.403	0.0982	0.2659
5053	495.559	497.284	5.404	0.0986	0.3002
5054	495.559	497.282	5.405	0.0985	0.3002
5056	495.554	497.491	5.406	0.0981	0.3366
5057	495.554	497.720	5.406	0.0993	0.3750
5058	495.552	497.719	11.733	0.0992	0.3750
5059	495.554	497.955	11.736	0.0993	0.4154
5060	495.558	497.961	11.738	0.0990	0.4154
5061	495.575	497.010	11.740	0.1028	0.2659
5062	495.573	497.008	11.742	0.1019	0.2659
5064	495.572	497.200	11.743	0.1026	0.3002
5065	495.572	497.410	11.743	0.1021	0.3366
5066	495.567	497.407	11.742	0.1031	0.3366
5067	495.565	497.620	11.741	0.1016	0.3750
5068	495.571	497.627	11.740	0.1023	0.3750
5069	495.568	497.857	20.455	0.1025	0.4155
5070	495.571	497.861	20.455	0.1017	0.4155
5071	495.582	496.997	20.454	0.1077	0.2659
5072	495.584	497.000	20.454	0.1077	0.2659
5073	495.579	497.182	20.454	0.1079	0.3002
5074	495.583	497.182	20.455	0.1078	0.3002
5075	495.576	497.374	20.455	0.1083	0.3365
5076	495.574	497.375	20.456	0.1074	0.3365
5078	495.577	497.590	20.457	0.1064	0.3749
5079	495.579	497.814	30.829	0.1065	0.4154
5080	495.579	497.806	30.829	0.1066	0.4154
5091	495.621	497.036	30.829	0.1110	0.2657
5092	495.619	497.032	30.828	0.1111	0.2658
5093	495.626	497.222	30.830	0.1109	0.3001
5094	495.622	497.217	30.831	0.1106	0.3001
5095	495.621	497.406	30.834	0.1101	0.3364
5096	495.619	497.407	40.906	0.1104	0.3364
5097	495.617	497.607	40.909	0.1109	0.3748
5098	495.621	497.611	40.912	0.1109	0.3748
5099	495.621	497.831	40.912	0.1097	0.4152
5100	495.622	497.832	40.916	0.1101	0.4152
6001	547.296	549.127	40.918	0.0764	0.2427
6002	547.305	549.139	40.919	0.0763	0.2427
6003	547.301	549.371	40.921	0.0763	0.2740
6004	547.304	549.376	40.923	0.0762	0.2740
6005	547.318	549.641	40.923	0.0759	0.3072
6006	547.313	549.639	50.744	0.0762	0.3072
6007	547.317	549.908	50.744	0.0755	0.3423

6008	547.320	549.917	50.748	0.0753	0.3422
6009	547.322	550.197	50.750	0.0756	0.3792
6010	547.329	550.207	50.749	0.0757	0.3792
6013	547.357	549.306	50.750	0.0796	0.2740
6014	547.356	549.301	50.751	0.0806	0.2740
6015	547.352	549.539	60.438	0.0805	0.3072
6016	547.356	549.549	60.426	0.0799	0.3072
6017	547.357	549.802	60.413	0.0802	0.3422
6018	547.358	549.802	60.400	0.0799	0.3422
6019	547.365	550.078	60.389	0.0802	0.3791
6020	547.359	550.076	60.376	0.0800	0.3792
6021	547.374	548.996	60.366	0.0838	0.2427
6022	547.372	548.992	60.356	0.0838	0.2427
6023	547.367	549.210	60.346	0.0833	0.2740
6024	547.371	549.214	60.334	0.0837	0.2740
6025	547.372	549.437	0.781	0.0833	0.3072
6026	547.374	549.437	0.781	0.0829	0.3072
6027	547.372	549.682	0.782	0.0837	0.3422
6028	547.371	549.681	0.782	0.0835	0.3422
6029	547.377	549.942	0.782	0.0840	0.3792
6030	547.378	549.943	0.783	0.0839	0.3792
6031	547.403	548.960	0.783	0.0887	0.2427
6032	547.388	548.952	0.783	0.0883	0.2428
6033	547.399	549.163	0.783	0.0885	0.2741
6034	547.400	549.164	0.783	0.0889	0.2740
6035	547.397	549.373	5.400	0.0895	0.3072
6036	547.395	549.379	5.400	0.0896	0.3072
6037	547.393	549.607	5.402	0.0882	0.3423
6039	547.394	549.861	5.403	0.0883	0.3793
6040	547.393	549.845	5.404	0.0882	0.3792
6042	547.405	548.875	5.405	0.0947	0.2428
6045	547.401	549.274	5.406	0.0943	0.3073
6046	547.402	549.268	5.406	0.0945	0.3073
6047	547.400	549.483	11.733	0.0948	0.3424
6048	547.406	549.490	11.736	0.0946	0.3424
6049	547.404	549.717	11.738	0.0948	0.3793
6050	547.398	549.712	11.740	0.0943	0.3793
6051	547.418	548.769	11.742	0.0985	0.2428
6052	547.427	548.776	11.743	0.0997	0.2428
6053	547.421	548.955	11.743	0.0990	0.2741
6054	547.425	548.956	11.742	0.0989	0.2742
6055	547.427	549.206	11.741	0.0994	0.3073
6056	547.425	549.200	11.740	0.0995	0.3073
6057	547.424	549.408	20.455	0.1000	0.3423
6058	547.426	549.411	20.455	0.0990	0.3424
6059	547.431	549.634	20.454	0.0997	0.3793
6060	547.426	549.634	20.454	0.0982	0.3793
6061	547.459	548.770	20.454	0.1044	0.2428

6062	547.453	548.761	20.455	0.1043	0.2428
6063	547.452	548.939	20.455	0.1042	0.2741
6064	547.456	548.941	20.456	0.1035	0.2741
6065	547.460	549.132	20.457	0.1043	0.3073
6066	547.456	549.132	30.829	0.1037	0.3073
6067	547.458	549.333	30.829	0.1028	0.3424
6071	547.481	548.778	30.829	0.1080	0.2428
6072	547.485	548.783	30.828	0.1079	0.2428
6073	547.483	548.947	30.830	0.1079	0.2741
6074	547.489	548.957	30.831	0.1080	0.2741
6075	547.488	549.132	30.834	0.1060	0.3073
6076	547.489	549.138	40.906	0.1076	0.3073
6077	547.489	549.324	40.909	0.1076	0.3424
6078	547.487	549.323	40.912	0.1079	0.3424
6079	547.484	549.520	40.912	0.1078	0.3794
6080	547.489	549.529	40.916	0.1078	0.3793

Table A5. Thermal conductivity of liquid S-8.

Point ID	T_0 (K)	T_e (K)	P_e (MPa)	ρ_e (mol·L^{-1})	λ_e (W·m^{-1}K^{-1})	q (W·m^{-1})
1013	301.957	303.640	0.095	4.245	0.1169	0.3730
1015	301.929	303.922	0.095	4.244	0.1176	0.4439
1017	301.909	304.236	0.095	4.243	0.1179	0.5199
1019	301.885	304.575	0.095	4.241	0.1176	0.6032
1021	301.671	303.087	0.510	4.250	0.1168	0.3085
1023	301.662	303.369	0.502	4.248	0.1170	0.3734
1025	301.655	303.686	0.498	4.247	0.1169	0.4445
1027	301.648	304.022	0.497	4.245	0.1175	0.5205
1029	301.643	304.388	0.501	4.244	0.1171	0.6035
1031	301.441	302.846	0.342	4.250	0.1166	0.3086
1033	301.437	303.137	0.333	4.249	0.1170	0.3736
1035	301.434	303.459	0.325	4.247	0.1173	0.4447
1037	301.434	303.803	0.319	4.246	0.1167	0.5207
1039	301.430	304.180	0.312	4.244	0.1176	0.6040
1041	301.547	302.957	5.249	4.271	0.1201	0.3086
1043	301.562	303.222	5.266	4.270	0.1189	0.3734
1045	301.584	303.574	5.278	4.269	0.1190	0.4445
1047	301.605	303.947	5.292	4.267	0.1188	0.5205
1049	301.620	304.346	5.305	4.266	0.1184	0.6037
1051	301.743	303.175	10.283	4.291	0.1199	0.3085
1053	301.750	303.478	10.286	4.290	0.1204	0.3734
1055	301.754	303.807	10.286	4.289	0.1210	0.4444
1057	301.764	304.156	10.287	4.287	0.1211	0.5204
1059	301.764	304.530	10.289	4.286	0.1203	0.6037

1061	301.816	303.449	20.266	4.330	0.1244	0.3732
1063	301.819	303.767	20.259	4.328	0.1234	0.4443
1065	301.826	304.107	20.258	4.327	0.1242	0.5203
1067	301.832	304.474	20.258	4.326	0.1241	0.6035
1069	301.833	304.867	20.260	4.324	0.1236	0.6929
1071	301.975	303.572	30.348	4.366	0.1281	0.3730
1073	301.998	303.909	30.369	4.365	0.1274	0.4440
1075	302.019	304.260	30.390	4.363	0.1274	0.5199
1077	302.043	304.647	30.412	4.362	0.1269	0.6030
1079	302.067	305.070	30.434	4.360	0.1267	0.6924
1081	302.364	303.977	40.266	4.398	0.1294	0.3729
1083	302.369	304.280	40.265	4.397	0.1290	0.4439
1085	302.370	304.606	40.265	4.395	0.1295	0.5198
1087	302.365	304.952	40.269	4.394	0.1300	0.6028
1089	302.361	305.320	40.275	4.393	0.1301	0.6921
1091	302.342	303.768	50.044	4.429	0.1329	0.3725
1093	302.330	304.045	50.033	4.428	0.1314	0.4434
1095	302.322	304.348	50.023	4.427	0.1332	0.5192
1097	302.311	304.821	50.010	4.426	0.1327	0.6025
1099	302.297	305.173	49.995	4.424	0.1330	0.6918
1101	302.144	303.689	58.820	4.456	0.1354	0.3731
1103	302.130	303.956	58.602	4.454	0.1346	0.4441
1105	302.109	304.240	58.405	4.453	0.1350	0.5200
1107	302.095	304.560	58.216	4.451	0.1353	0.6031
1109	302.082	304.905	58.039	4.449	0.1341	0.6924
1111	302.126	303.623	65.938	4.476	0.1376	0.3730
1113	302.141	303.944	64.626	4.471	0.1368	0.4439
1115	302.151	304.278	63.559	4.467	0.1353	0.5198
1117	302.168	304.650	62.667	4.464	0.1353	0.6029
1119	302.178	305.028	61.911	4.460	0.1365	0.6923
2001	321.327	322.975	0.135	4.162	0.1145	0.3556
2003	321.330	323.297	0.136	4.161	0.1145	0.4233
2005	321.324	323.627	0.133	4.160	0.1138	0.4957
2007	321.319	323.941	0.129	4.158	0.1150	0.5749
2009	321.312	324.328	0.123	4.157	0.1140	0.6601
2011	320.975	322.406	5.148	4.190	0.1162	0.3556
2013	320.960	322.692	5.124	4.189	0.1160	0.4234
2015	320.951	323.222	5.105	4.186	0.1162	0.4963
2017	320.945	323.572	5.094	4.185	0.1161	0.5757
2019	320.947	323.960	5.091	4.183	0.1157	0.6610
2021	321.084	322.709	10.277	4.213	0.1175	0.3560
2023	321.103	323.045	10.289	4.211	0.1180	0.4238
2025	321.123	323.400	10.300	4.210	0.1178	0.4963
2027	321.144	323.783	10.316	4.209	0.1171	0.5756
2029	321.162	324.191	10.334	4.207	0.1187	0.6608
2031	320.956	322.481	19.958	4.256	0.1208	0.3562

2033	320.952	322.769	19.953	4.255	0.1216	0.4240
2035	320.954	323.090	19.953	4.253	0.1212	0.4964
2037	320.968	323.454	19.959	4.252	0.1214	0.5758
2039	320.973	323.831	19.971	4.251	0.1210	0.6610
2041	321.196	322.736	30.236	4.296	0.1253	0.3560
2043	321.219	323.061	30.248	4.294	0.1245	0.4238
2045	321.235	323.400	30.258	4.293	0.1247	0.4963
2047	321.251	323.764	30.269	4.292	0.1247	0.5757
2049	321.268	324.159	30.280	4.291	0.1251	0.6610
2051	321.207	322.736	40.378	4.333	0.1285	0.3561
2053	321.185	322.993	40.359	4.332	0.1283	0.4239
2055	321.167	323.271	40.341	4.331	0.1281	0.4964
2057	321.151	323.585	40.332	4.329	0.1274	0.5756
2059	321.131	323.912	40.323	4.328	0.1283	0.6608
2061	321.286	322.764	50.582	4.367	0.1315	0.3560
2063	321.309	323.076	50.601	4.366	0.1311	0.4237
2065	321.328	323.407	50.620	4.365	0.1313	0.4961
2067	321.345	323.764	50.636	4.364	0.1303	0.5754
2069	321.359	324.139	50.652	4.363	0.1314	0.6607
2071	321.419	322.936	60.482	4.398	0.1338	0.3559
2073	321.406	323.197	60.463	4.397	0.1337	0.4236
2075	321.392	323.474	60.441	4.396	0.1343	0.4960
2077	321.371	323.768	60.420	4.395	0.1340	0.5754
2079	321.357	324.091	60.395	4.394	0.1346	0.6606
2081	321.163	322.519	69.044	4.425	0.1360	0.3562
2083	321.159	322.785	69.016	4.424	0.1375	0.4239
2085	321.160	323.069	68.990	4.423	0.1364	0.4964
2087	321.167	323.392	68.969	4.422	0.1360	0.5758
2089	321.179	323.753	68.947	4.421	0.1358	0.6611
3001	337.824	339.476	0.188	4.092	0.1106	0.3422
3003	337.828	339.786	0.193	4.091	0.1116	0.4074
3005	337.834	340.125	0.197	4.089	0.1117	0.4771
3007	337.838	340.487	0.202	4.088	0.1117	0.5533
3009	337.843	340.874	0.205	4.086	0.1118	0.6353
3011	337.913	339.475	5.412	4.121	0.1139	0.3422
3013	337.917	339.778	5.415	4.120	0.1138	0.4073
3015	337.917	340.102	5.418	4.118	0.1139	0.4769
3017	337.922	340.460	5.421	4.117	0.1141	0.5532
3019	337.925	340.842	5.424	4.115	0.1136	0.6352
3021	337.965	339.518	10.140	4.145	0.1156	0.3421
3023	337.969	339.817	10.141	4.144	0.1157	0.4072
3025	337.970	340.136	10.128	4.142	0.1161	0.4770
3027	337.977	340.490	10.124	4.141	0.1159	0.5534
3029	337.979	340.866	10.122	4.139	0.1162	0.6355
3031	338.036	339.548	20.415	4.193	0.1197	0.3423
3033	338.037	339.836	20.412	4.192	0.1199	0.4075

3035	338.039	340.147	20.410	4.191	0.1201	0.4772
3037	338.040	340.490	20.409	4.190	0.1199	0.5535
3039	338.043	340.854	20.408	4.189	0.1194	0.6356
3041	338.095	339.574	30.197	4.235	0.1233	0.3423
3043	338.098	339.859	30.204	4.234	0.1236	0.4074
3045	338.102	340.163	30.213	4.233	0.1237	0.4770
3047	338.098	340.487	30.222	4.232	0.1231	0.5531
3049	338.100	340.844	30.228	4.231	0.1237	0.6351
3051	338.131	339.566	40.187	4.274	0.1267	0.3423
3053	338.138	339.848	40.184	4.273	0.1274	0.4075
3055	338.138	340.141	40.182	4.272	0.1269	0.4772
3057	338.142	340.468	40.180	4.271	0.1268	0.5535
3059	338.137	340.812	40.181	4.270	0.1268	0.6355
3061	338.173	339.564	50.546	4.312	0.1299	0.3423
3063	338.173	339.834	50.541	4.311	0.1298	0.4075
3065	338.176	340.125	50.536	4.310	0.1299	0.4771
3067	338.180	340.447	50.534	4.309	0.1295	0.5535
3069	338.177	340.783	50.531	4.308	0.1290	0.6355
3072	338.203	339.554	60.331	4.345	0.1335	0.3420
3074	338.208	339.823	60.331	4.344	0.1333	0.4071
3076	338.202	340.100	60.328	4.343	0.1328	0.4768
3078	338.203	340.412	60.309	4.342	0.1329	0.5532
3080	338.207	340.751	60.296	4.341	0.1329	0.6354
3082	338.226	339.537	69.455	4.374	0.1352	0.3424
3084	338.231	339.848	69.449	4.373	0.1355	0.4075
3086	338.229	340.130	69.449	4.372	0.1360	0.4771
3088	338.232	340.432	69.448	4.371	0.1350	0.5533
3090	338.229	340.756	69.447	4.370	0.1353	0.6351
4001	357.955	359.827	0.147	4.004	0.1084	0.3896
4003	357.975	360.169	0.159	4.003	0.1080	0.4562
4005	357.987	360.540	0.168	4.001	0.1079	0.5291
4007	357.999	360.932	0.178	4.000	0.1084	0.6076
4009	358.015	361.359	0.191	3.998	0.1075	0.6912
4011	358.334	360.181	0.397	4.004	0.1083	0.3891
4013	358.346	360.515	0.406	4.003	0.1089	0.4556
4015	358.358	360.885	0.412	4.001	0.1083	0.5285
4017	358.373	361.279	0.417	4.000	0.1082	0.6069
4019	358.388	361.697	0.429	3.998	0.1078	0.6904
4021	358.506	360.379	5.123	4.033	0.1103	0.3891
4023	358.516	360.707	5.130	4.032	0.1102	0.4556
4025	358.528	360.968	5.137	4.031	0.1105	0.5283
4027	358.538	361.351	5.144	4.029	0.1104	0.6067
4029	358.549	361.756	5.156	4.028	0.1104	0.6902
4031	358.653	360.455	10.216	4.062	0.1128	0.3889
4033	358.664	360.782	10.222	4.061	0.1128	0.4554
4035	358.669	361.128	10.228	4.060	0.1122	0.5282

4037	358.681	361.505	10.216	4.058	0.1126	0.6069
4039	358.690	361.902	10.217	4.057	0.1124	0.6906
4041	358.788	360.533	19.951	4.113	0.1167	0.3892
4043	358.797	360.846	19.952	4.112	0.1166	0.4557
4045	358.812	361.190	19.963	4.111	0.1168	0.5285
4047	358.812	361.543	19.973	4.110	0.1171	0.6067
4049	358.828	361.934	19.987	4.108	0.1163	0.6902
4051	358.909	360.580	30.512	4.163	0.1210	0.3889
4053	358.913	360.877	30.520	4.162	0.1208	0.4553
4055	358.923	361.206	30.519	4.161	0.1208	0.5282
4057	358.925	361.552	30.509	4.159	0.1214	0.6068
4059	358.928	361.924	30.512	4.158	0.1208	0.6904
4061	359.024	360.680	40.478	4.205	0.1249	0.3892
4063	359.028	360.971	40.480	4.204	0.1239	0.4557
4065	359.034	361.285	40.484	4.203	0.1247	0.5286
4067	359.038	361.630	40.497	4.202	0.1244	0.6067
4069	359.038	361.987	40.511	4.201	0.1244	0.6901
4071	359.104	360.680	50.282	4.243	0.1276	0.3891
4073	359.105	361.014	50.282	4.242	0.1277	0.4557
4075	359.107	361.322	50.283	4.241	0.1278	0.5286
4077	359.110	361.650	50.292	4.240	0.1272	0.6068
4079	359.116	362.007	50.303	4.239	0.1272	0.6903
4081	359.187	360.744	60.423	4.280	0.1312	0.3890
4083	359.190	361.021	60.432	4.279	0.1312	0.4554
4085	359.192	361.324	60.444	4.278	0.1311	0.5282
4087	359.190	361.643	60.450	4.278	0.1300	0.6064
4089	359.195	361.988	60.457	4.276	0.1316	0.6899
4091	359.234	360.768	68.584	4.308	0.1338	0.3891
4093	359.237	361.040	68.585	4.307	0.1337	0.4556
4095	359.240	361.339	68.587	4.306	0.1331	0.5283
4097	359.253	361.666	68.592	4.305	0.1336	0.6064
4099	359.253	362.000	68.591	4.304	0.1339	0.6899
5001	377.752	379.509	8.533	3.976	0.1089	0.3737
5003	377.766	379.832	8.545	3.975	0.1096	0.4376
5005	377.775	380.174	8.554	3.974	0.1091	0.5075
5007	377.788	380.549	8.539	3.972	0.1088	0.5832
5009	377.801	380.946	8.535	3.970	0.1084	0.6637
5011	377.851	379.684	0.270	3.919	0.1048	0.3736
5013	377.860	380.004	0.253	3.917	0.1045	0.4379
5015	377.872	380.368	0.256	3.916	0.1048	0.5080
5017	377.886	380.704	0.259	3.914	0.1046	0.5832
5019	377.893	381.104	0.265	3.913	0.1044	0.6635
5021	377.992	379.748	5.185	3.953	0.1072	0.3735
5023	378.004	380.074	5.191	3.952	0.1077	0.4374
5025	378.011	380.418	5.178	3.950	0.1075	0.5077
5027	378.023	380.795	5.179	3.949	0.1068	0.5830

5029	378.035	381.195	5.181	3.947	0.1064	0.6633
5031	378.135	379.869	10.373	3.986	0.1097	0.3734
5033	378.143	380.177	10.379	3.985	0.1096	0.4373
5035	378.152	380.519	10.384	3.984	0.1101	0.5072
5037	378.163	380.890	10.379	3.982	0.1096	0.5826
5039	378.179	381.282	10.373	3.981	0.1102	0.6631
5041	378.268	379.931	20.142	4.043	0.1146	0.3733
5043	378.275	380.230	20.150	4.042	0.1144	0.4371
5045	378.285	380.561	20.156	4.041	0.1139	0.5070
5047	378.296	380.916	20.156	4.039	0.1139	0.5823
5049	378.298	381.286	20.141	4.038	0.1140	0.6629
5051	378.383	379.974	30.345	4.095	0.1183	0.3733
5053	378.389	380.261	30.353	4.094	0.1179	0.4371
5055	378.398	380.582	30.360	4.093	0.1188	0.5070
5057	378.401	380.920	30.367	4.092	0.1185	0.5821
5059	378.408	381.278	30.373	4.091	0.1184	0.6623
5061	378.503	380.072	40.331	4.141	0.1226	0.3733
5063	378.499	380.343	40.338	4.140	0.1225	0.4371
5065	378.513	380.659	40.343	4.139	0.1215	0.5070
5067	378.514	380.983	40.339	4.138	0.1222	0.5822
5069	378.525	381.344	40.323	4.137	0.1225	0.6628
5071	378.590	380.128	50.227	4.182	0.1260	0.3733
5073	378.587	380.392	50.231	4.182	0.1260	0.4371
5075	378.594	380.699	50.237	4.181	0.1261	0.5070
5077	378.596	381.020	50.242	4.180	0.1261	0.5821
5079	378.601	381.358	50.246	4.179	0.1263	0.6623
5081	378.658	380.162	60.412	4.222	0.1295	0.3733
5083	378.657	380.425	60.420	4.221	0.1289	0.4371
5085	378.664	380.720	60.425	4.220	0.1295	0.5070
5087	378.668	381.032	60.429	4.219	0.1298	0.5821
5089	378.672	381.362	60.432	4.218	0.1291	0.6623
5091	378.716	380.191	67.328	4.247	0.1307	0.3735
5093	378.714	380.450	67.139	4.246	0.1307	0.4373
5095	378.717	380.745	66.955	4.244	0.1309	0.5070
5097	378.719	381.050	66.766	4.242	0.1309	0.5822
5099	378.722	381.379	66.576	4.241	0.1310	0.6624
6001	399.395	401.184	0.108	3.823	0.1016	0.3570
6003	399.392	401.486	0.108	3.821	0.1006	0.4181
6005	399.389	401.817	0.114	3.820	0.1009	0.4847
6007	399.391	402.177	0.119	3.818	0.1015	0.5565
6009	399.391	402.561	0.120	3.817	0.1010	0.6332
6011	399.665	401.413	0.268	3.823	0.1013	0.3566
6013	399.668	401.726	0.268	3.822	0.1008	0.4176
6015	399.669	402.067	0.253	3.820	0.1010	0.4847
6017	399.667	402.424	0.248	3.818	0.1007	0.5566
6019	399.675	402.822	0.245	3.817	0.1008	0.6333

6021	399.683	401.387	5.081	3.862	0.1044	0.3566
6023	399.687	401.693	5.068	3.861	0.1040	0.4178
6025	399.682	402.013	5.063	3.860	0.1040	0.4847
6027	399.683	402.418	5.062	3.858	0.1037	0.5566
6029	399.683	402.799	5.070	3.856	0.1039	0.6331
6031	399.702	401.407	10.182	3.900	0.1064	0.3568
6033	399.701	401.699	10.181	3.899	0.1068	0.4178
6035	399.699	402.019	10.184	3.897	0.1065	0.4846
6037	399.698	402.366	10.190	3.896	0.1065	0.5563
6039	399.694	402.731	10.194	3.895	0.1067	0.6329
6041	399.732	401.353	20.145	3.965	0.1113	0.3567
6043	399.730	401.633	20.150	3.964	0.1112	0.4177
6045	399.725	401.936	20.155	3.963	0.1112	0.4844
6047	399.726	402.273	20.158	3.961	0.1117	0.5562
6049	399.729	402.631	20.160	3.960	0.1111	0.6328
6051	399.751	401.284	30.065	4.021	0.1159	0.3568
6053	399.749	401.557	30.075	4.020	0.1154	0.4177
6055	399.746	401.858	30.080	4.019	0.1160	0.4844
6057	399.750	402.187	30.082	4.018	0.1153	0.5562
6059	399.745	402.524	30.086	4.017	0.1159	0.6328
6063	399.767	401.581	40.311	4.071	0.1211	0.4178
6065	399.763	401.870	40.315	4.071	0.1199	0.4846
6067	399.762	402.184	40.317	4.070	0.1205	0.5564
6069	399.760	402.516	40.319	4.068	0.1201	0.6330
6071	399.777	401.254	49.938	4.116	0.1243	0.3570
6073	399.779	401.518	49.869	4.115	0.1241	0.4180
6075	399.776	401.795	49.805	4.114	0.1240	0.4848
6077	399.775	402.106	49.748	4.113	0.1239	0.5565
6079	399.773	402.432	49.693	4.112	0.1239	0.6331
6081	399.793	401.354	55.002	4.138	0.1248	0.3569
6083	399.783	401.653	53.060	4.129	0.1238	0.4180
6085	399.777	401.905	51.965	4.123	0.1238	0.4848
6087	399.775	402.218	51.227	4.119	0.1239	0.5567
6089	399.769	402.551	50.637	4.115	0.1235	0.6336
7001	418.662	420.400	0.102	3.736	0.0980	0.3437
7003	418.670	420.719	0.101	3.734	0.0983	0.4025
7005	418.675	421.059	0.102	3.733	0.0980	0.4669
7007	418.673	421.414	0.104	3.731	0.0978	0.5360
7009	418.679	421.803	0.106	3.729	0.0976	0.6097
7011	418.723	420.439	5.140	3.782	0.1018	0.3437
7013	418.725	420.740	5.143	3.781	0.1010	0.4025
7015	418.731	421.074	5.146	3.780	0.1013	0.4668
7017	418.729	421.421	5.151	3.778	0.1008	0.5359
7019	418.738	421.801	5.158	3.777	0.1007	0.6096
7021	418.811	420.469	10.555	3.827	0.1039	0.3436
7023	418.822	420.771	10.554	3.825	0.1037	0.4024

7025	418.831	421.100	10.554	3.824	0.1037	0.4668
7027	418.831	421.439	10.555	3.823	0.1036	0.5360
7029	418.839	421.814	10.559	3.821	0.1036	0.6098
7031	418.918	420.525	20.239	3.895	0.1094	0.3436
7033	418.922	420.806	20.235	3.894	0.1093	0.4025
7035	418.926	421.116	20.234	3.893	0.1090	0.4669
7037	418.933	421.456	20.237	3.892	0.1088	0.5360
7039	418.936	421.808	20.243	3.891	0.1087	0.6098
7041	418.999	420.554	30.475	3.958	0.1139	0.3437
7043	419.010	420.833	30.474	3.957	0.1134	0.4025
7045	419.009	421.128	30.477	3.956	0.1136	0.4669
7047	419.012	421.444	30.482	3.955	0.1135	0.5359
7049	419.014	421.786	30.489	3.954	0.1129	0.6097
7051	419.079	420.583	40.435	4.012	0.1179	0.3436
7053	419.081	420.849	40.442	4.011	0.1178	0.4023
7055	419.084	421.137	40.448	4.010	0.1170	0.4666
7057	419.086	421.451	40.452	4.009	0.1174	0.5357
7059	419.092	421.790	40.456	4.008	0.1171	0.6095
7061	419.136	420.591	49.169	4.054	0.1220	0.3435
7063	419.142	420.856	48.957	4.053	0.1215	0.4022
7065	419.138	421.136	48.747	4.051	0.1209	0.4665
7067	419.143	421.446	48.536	4.049	0.1200	0.5357
7069	419.145	421.767	48.316	4.047	0.1205	0.6098
8001	439.886	441.678	0.247	3.638	0.0949	0.3305
8003	439.890	441.940	0.248	3.637	0.0948	0.3869
8005	439.893	442.271	0.249	3.635	0.0950	0.4488
8007	439.895	442.630	0.253	3.634	0.0945	0.5153
8009	439.905	442.968	0.257	3.632	0.0943	0.5862
8011	439.983	441.663	5.101	3.690	0.0978	0.3302
8013	439.988	441.957	5.106	3.689	0.0976	0.3866
8015	439.988	442.275	5.111	3.688	0.0981	0.4484
8017	439.993	442.627	5.114	3.686	0.0978	0.5149
8019	439.998	442.998	5.117	3.685	0.0980	0.5858
8021	440.042	441.693	10.160	3.738	0.1007	0.3303
8023	440.042	441.979	10.164	3.737	0.1014	0.3867
8025	440.047	442.295	10.168	3.735	0.1011	0.4485
8027	440.050	442.631	10.174	3.734	0.1010	0.5149
8029	440.056	442.997	10.178	3.733	0.1010	0.5858
8031	440.105	441.633	20.377	3.820	0.1073	0.3303
8033	440.100	441.901	20.375	3.819	0.1065	0.3868
8035	440.104	442.198	20.371	3.818	0.1066	0.4487
8037	440.107	442.522	20.371	3.816	0.1063	0.5152
8039	440.111	442.868	20.376	3.815	0.1066	0.5861
8041	440.153	441.664	30.286	3.886	0.1116	0.3304
8043	440.148	441.920	30.286	3.885	0.1116	0.3869
8045	440.154	442.210	30.290	3.884	0.1118	0.4487

8047	440.149	442.511	30.295	3.883	0.1119	0.5151
8049	440.149	442.835	30.301	3.882	0.1119	0.5860
8051	440.185	441.620	40.345	3.945	0.1156	0.3304
8053	440.187	441.875	40.332	3.944	0.1162	0.3869
8055	440.190	442.152	40.321	3.944	0.1159	0.4487
8057	440.186	442.446	40.315	3.943	0.1157	0.5151
8059	440.182	442.757	40.307	3.942	0.1160	0.5860
8061	440.195	441.649	41.920	3.954	0.1166	0.3303
8063	440.185	441.897	41.449	3.951	0.1161	0.3868
8065	440.179	442.172	41.049	3.947	0.1168	0.4486
8067	440.177	442.471	40.704	3.945	0.1159	0.5150
8069	440.175	442.789	40.401	3.942	0.1159	0.5859
9001	460.245	461.930	0.191	3.539	0.0917	0.3185
9003	460.235	462.212	0.192	3.538	0.0915	0.3728
9005	460.228	462.532	0.193	3.536	0.0917	0.4323
9007	460.218	462.861	0.194	3.535	0.0914	0.4963
9009	460.216	463.227	0.194	3.533	0.0914	0.5646
9011	460.218	461.822	5.456	3.605	0.0952	0.3182
9013	460.220	462.105	5.458	3.604	0.0956	0.3726
9015	460.220	462.416	5.462	3.603	0.0959	0.4322
9017	460.217	462.748	5.463	3.601	0.0955	0.4963
9019	460.219	463.107	5.460	3.600	0.0953	0.5647
9021	460.289	461.908	10.329	3.657	0.0991	0.3183
9023	460.295	462.193	10.334	3.656	0.0988	0.3727
9025	460.297	462.496	10.338	3.655	0.0987	0.4322
9027	460.298	462.827	10.341	3.653	0.0989	0.4963
9029	460.302	463.179	10.344	3.652	0.0984	0.5647
9031	460.365	461.853	20.311	3.746	0.1053	0.3182
9033	460.368	462.123	20.315	3.745	0.1043	0.3726
9035	460.372	462.421	20.317	3.744	0.1038	0.4321
9037	460.370	462.728	20.312	3.743	0.1047	0.4963
9039	460.384	463.074	20.305	3.741	0.1044	0.5649
9041	460.426	461.837	30.198	3.819	0.1095	0.3182
9043	460.422	462.092	30.202	3.818	0.1094	0.3726
9045	460.425	462.374	30.204	3.817	0.1099	0.4322
9047	460.424	462.669	30.201	3.816	0.1097	0.4963
9049	460.427	462.996	30.193	3.815	0.1098	0.5649
9055	460.479	462.392	39.784	3.878	0.1141	0.4324
9057	460.484	462.687	39.721	3.876	0.1139	0.4966
9059	460.485	462.993	39.661	3.875	0.1141	0.5650
9061	460.535	461.966	42.387	3.894	0.1158	0.3184
9063	460.531	462.217	41.417	3.888	0.1146	0.3729
9065	460.530	462.503	40.644	3.882	0.1144	0.4325
9067	460.525	462.792	40.011	3.878	0.1141	0.4966
9069	460.522	463.106	39.488	3.874	0.1145	0.5650
10001	480.862	482.558	0.238	3.435	0.0890	0.3068

10003	480.867	482.860	0.237	3.433	0.0889	0.3593
10005	480.871	483.185	0.238	3.432	0.0885	0.4167
10007	480.877	483.536	0.237	3.430	0.0887	0.4785
10009	480.884	483.913	0.238	3.428	0.0886	0.5444
10011	480.929	482.553	5.166	3.508	0.0925	0.3069
10013	480.929	482.830	5.169	3.507	0.0929	0.3593
10015	480.932	483.146	5.175	3.505	0.0926	0.4167
10017	480.932	483.468	5.178	3.504	0.0928	0.4784
10019	480.935	483.830	5.181	3.502	0.0925	0.5443
10021	480.979	482.557	10.227	3.570	0.0962	0.3070
10023	480.976	482.826	10.228	3.569	0.0957	0.3594
10025	480.978	483.127	10.229	3.568	0.0964	0.4169
10027	480.978	483.446	10.233	3.566	0.0960	0.4786
10029	480.980	483.787	10.239	3.565	0.0964	0.5445
10042	481.072	482.521	20.214	3.670	0.1023	0.3197
10044	481.072	482.776	20.215	3.669	0.1021	0.3744
10046	481.073	483.049	20.216	3.668	0.1022	0.4343
10048	481.070	483.337	20.219	3.667	0.1022	0.4986
10050	481.076	483.661	20.222	3.666	0.1020	0.5672
10052	481.134	482.424	30.227	3.751	0.1078	0.3197
10054	481.129	482.655	30.227	3.750	0.1077	0.3744
10056	481.130	482.916	30.222	3.749	0.1079	0.4344
10058	481.131	483.194	30.220	3.748	0.1077	0.4987
10060	481.125	483.534	30.218	3.747	0.1075	0.5676
10062	481.147	482.429	38.228	3.806	0.1116	0.3199
10064	481.146	482.659	37.952	3.803	0.1114	0.3745
10066	481.136	482.901	37.705	3.801	0.1113	0.4344
10068	481.130	483.169	37.478	3.799	0.1111	0.4988
10070	481.125	483.452	37.265	3.796	0.1110	0.5676
11001	501.375	503.024	0.450	3.328	0.0858	0.3080
11003	501.377	503.253	0.451	3.327	0.0857	0.3607
11005	501.380	503.568	0.453	3.325	0.0857	0.4183
11007	501.387	503.900	0.451	3.323	0.0857	0.4804
11009	501.387	504.255	0.450	3.321	0.0855	0.5466
11011	501.401	502.944	5.134	3.412	0.0899	0.3079
11013	501.399	503.212	5.135	3.410	0.0898	0.3607
11015	501.400	503.506	5.135	3.409	0.0898	0.4183
11017	501.399	503.819	5.136	3.408	0.0897	0.4803
11019	501.401	504.162	5.137	3.406	0.0897	0.5465
11021	501.412	502.906	10.181	3.483	0.0936	0.3079
11023	501.412	503.165	10.182	3.482	0.0936	0.3607
11025	501.408	503.446	10.183	3.481	0.0935	0.4183
11027	501.406	503.750	10.183	3.480	0.0934	0.4803
11029	501.407	504.076	10.183	3.478	0.0934	0.5465
11031	501.406	502.853	15.115	3.542	0.0970	0.3080
11033	501.401	503.103	15.115	3.541	0.0969	0.3607

11035	501.409	503.383	15.116	3.540	0.0969	0.4183
11037	501.400	503.671	15.117	3.539	0.0968	0.4803
11039	501.405	503.988	15.118	3.538	0.0968	0.5465
11041	501.410	502.814	20.195	3.595	0.1001	0.3081
11043	501.410	503.060	20.197	3.594	0.1000	0.3607
11045	501.405	503.317	20.199	3.593	0.1000	0.4183
11047	501.401	503.600	20.199	3.592	0.1000	0.4803
11049	501.399	503.898	20.199	3.591	0.0999	0.5465
11051	501.398	502.754	25.203	3.642	0.1030	0.3080
11053	501.401	502.993	25.200	3.641	0.1029	0.3608
11055	501.402	503.252	25.199	3.640	0.1028	0.4185
11057	501.395	503.526	25.198	3.639	0.1027	0.4805
11059	501.391	503.824	25.199	3.638	0.1028	0.5466
11061	501.381	502.704	30.260	3.684	0.1057	0.3080
11063	501.380	502.934	30.256	3.683	0.1057	0.3608
11065	501.375	503.183	30.255	3.682	0.1057	0.4185
11067	501.375	503.456	30.253	3.681	0.1055	0.4805
11069	501.375	503.745	30.254	3.681	0.1056	0.5466
11071	501.376	502.588	35.386	3.724	0.1083	0.3079
11073	501.375	502.812	35.385	3.723	0.1082	0.3606
11075	501.370	503.056	35.384	3.722	0.1083	0.4183
11077	501.370	503.327	35.376	3.721	0.1081	0.4804
11079	501.367	503.609	35.372	3.720	0.1084	0.5466
11081	501.373	502.620	39.367	3.752	0.1103	0.3079
11083	501.372	502.848	39.213	3.750	0.1100	0.3607
11085	501.376	503.100	39.068	3.748	0.1101	0.4184
11087	501.375	503.356	38.930	3.746	0.1101	0.4804
11089	501.371	503.639	38.799	3.745	0.1101	0.5465